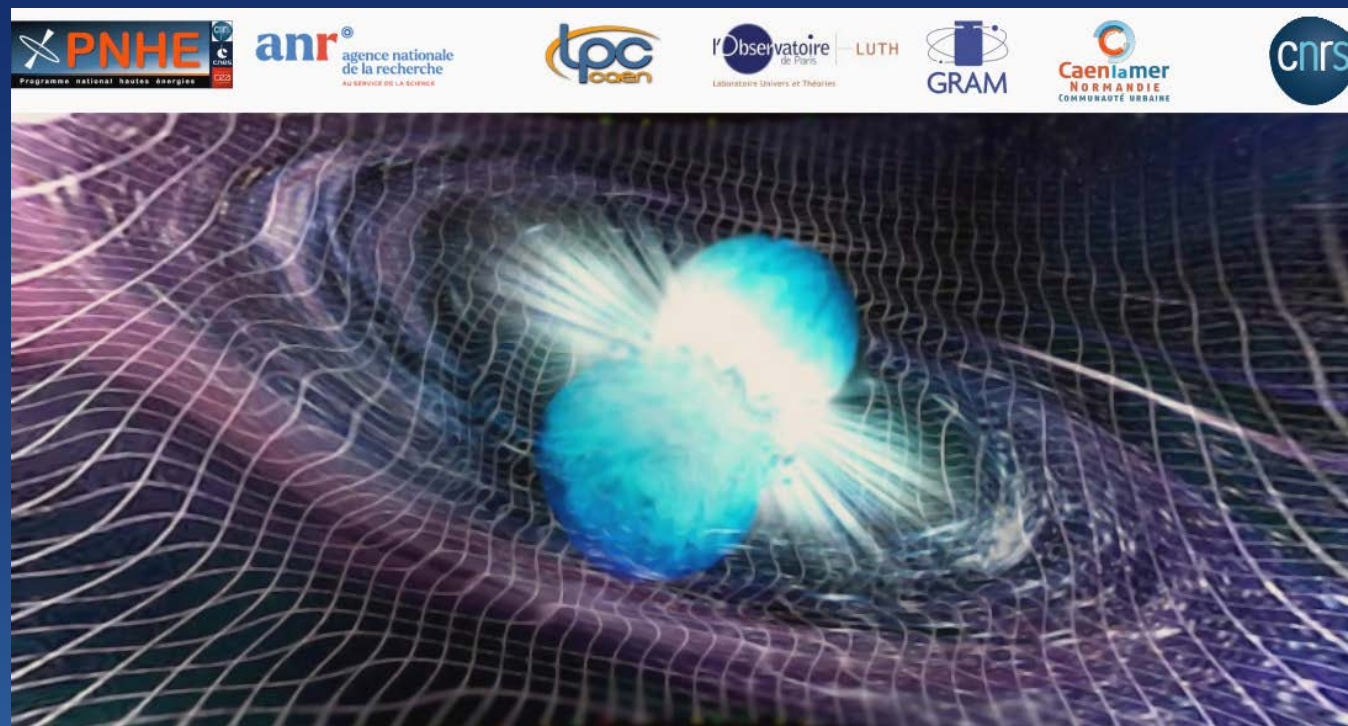


# Ultra-dense matter in Neutron Stars and Supernovae

Fiorella Burgio  
INFN Sezione di Catania, Italy



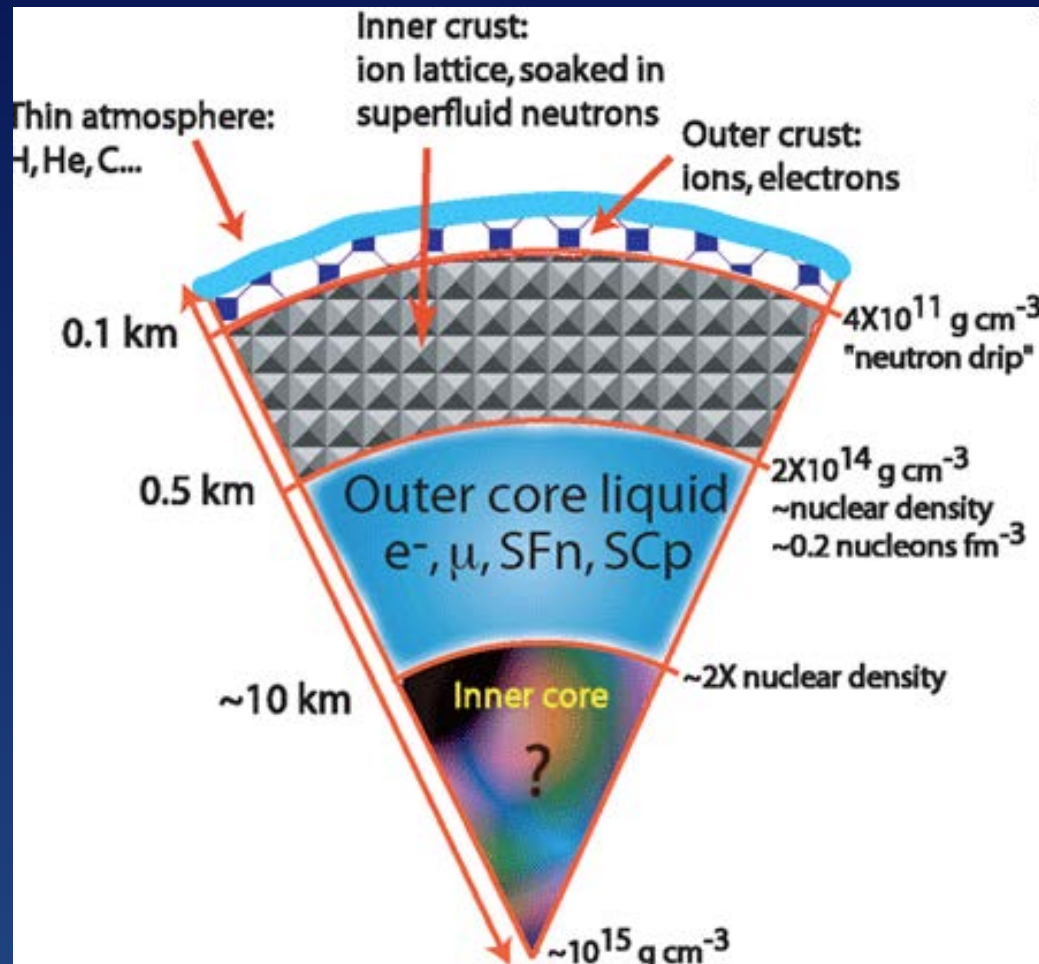
Thematic School GWsNS-2023 :  
“Gravitational Waves from Neutron Stars”  
Centre de Colloqui Paul Langevin, Aussois, 5-9 June, 2023

# Preliminary notes

1. “Nuclear Methods and the Nuclear Equation of State”, edited by M. Baldo, International Review of Nuclear Physics 8, (1999), World Scientific.
2. “Neutron Stars I”, Equation of State and Structure, P. Haensel, A. Potekhin, D. Yakovlev, 2007, Springer.
3. “Equations of State for Supernovae and compact stars”, M. Oertel, M. Hempel, T. Klähn, & S. Typel, Review of Modern Physics, 89, (2017), 015007.
4. “Neutron Stars and the Nuclear Equation of State”, G.F. Burgio, H.-J. Schulze, I. Vidaña & J.-B. Wei, Progress in Particle & Nuclear Physics, 120 (2021) 103879.

Further references will be given during the lecture.

# Schematic view of a neutron star



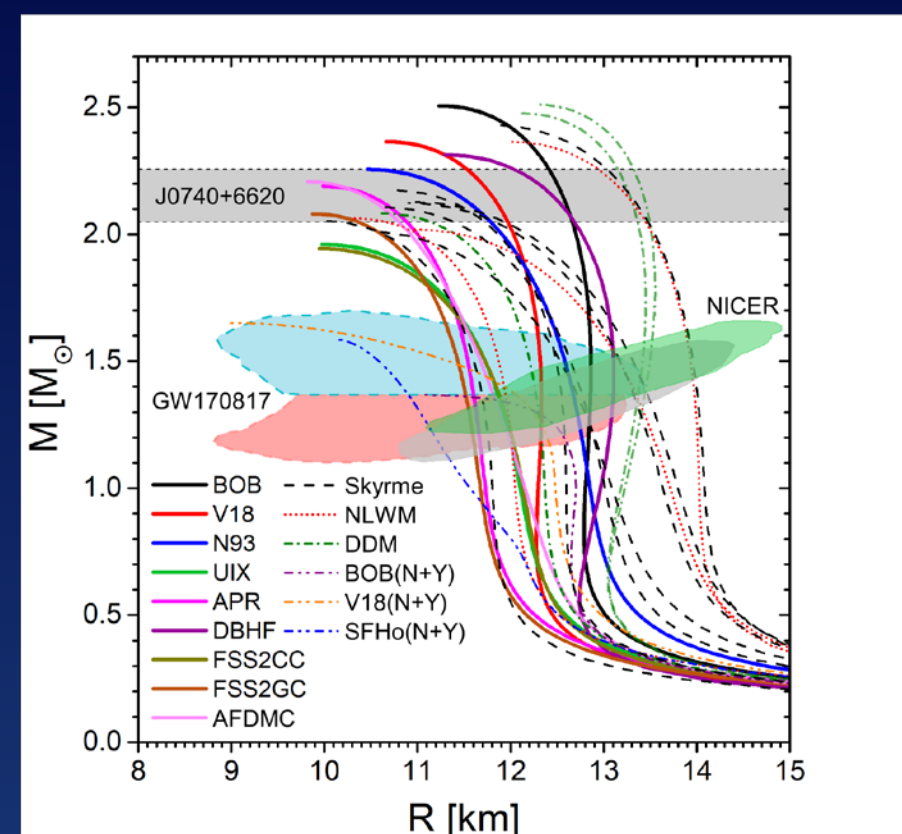
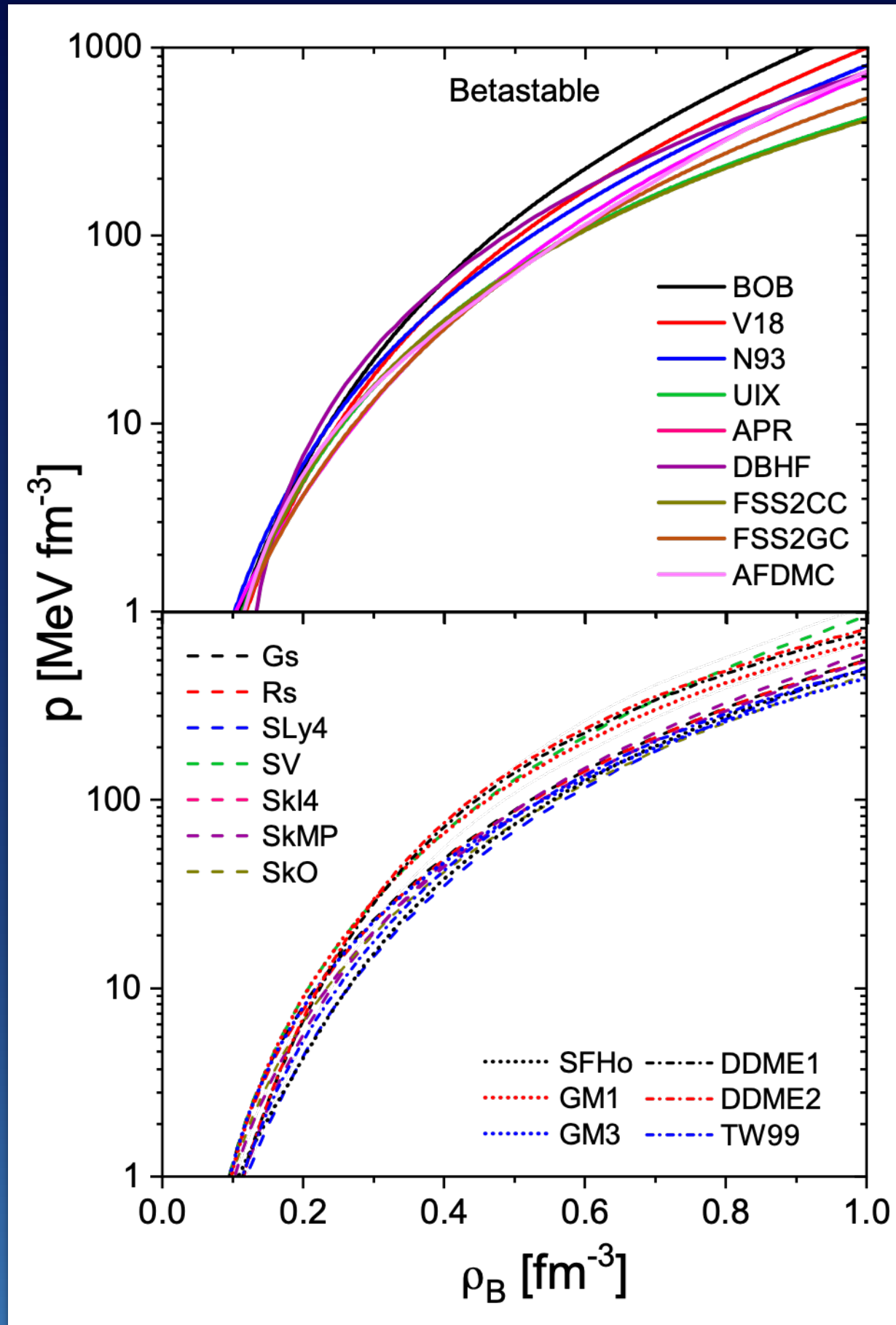
**Outer crust.** Nuclei immersed in an electron gas.

**Inner crust.** Electrons beta-captured by nuclei  $\rightarrow$  neutron-rich  $\rightarrow$  drip point. Gas of free neutrons. Nuclei melt down and nuclear matter sets in starting from drip point up to about half the saturation density.

**Outer core.** Asymmetric nuclear matter above saturation. Mainly composed by neutrons, protons, and leptons. Exact composition dependent on the nuclear matter Equation of State (EoS).

**Inner core.** The most unknown region. "Exotic matter". Hyperons? Kaons? Quarks?

- ✦ EoS in the crust known reasonably well
- ✦ EoS in the outer core not very certain
- ✦ EoS in the inner core : a mystery



## What do we need ?

Exact theory to deal with

- (a) Strong interactions of particles of different species
- (b) Many-body effects in dense matter

## What do we have ?

Many drastically different theoretical models!



# Equation of State @T=0

$$P=P(\epsilon) \text{ or } P=P(n)$$

- \* Input needed to close the equation of hydrostatic equilibrium and the one of mass conservation for describing compact star configurations.
- \* In nuclear physics, additional forms of the EOS in terms of the binding energy per particle  $E_b$  as a function of baryon number density  $n_B$ :

$$\frac{E_b}{A} = \frac{E_b}{A}(n_B) = \frac{\epsilon}{n_B} - m_N$$

- \* Easy transformation into the one for the pressure  $P$  by using thermodynamic relations:

$$P = n_B^2 \frac{d(E_b/A)}{dn_B}$$

- \* Slope of the energy per particle as a function of  $n_B$  directly proportional to the pressure.
- \* Minimum in the energy per particle  $\longrightarrow$  vanishing pressure  $\longrightarrow$  stable equilibrated matter.



# Tolman-Oppenheimer-Volkoff equations



We consider static spherically symmetric stars.

$$\frac{dP}{dr} = -\frac{Gm(r)\epsilon(r)}{r^2} \left(1 + \frac{P}{\epsilon(r)c^2}\right) \left(1 + \frac{4\pi r^3 P}{m(r)c^2}\right) \left(1 - \frac{2Gm(r)}{rc^2}\right)^{-1}$$

$$\frac{dm(r)}{dr} = 4\pi r^2 \epsilon(r)$$

First term on r.h.s. : Newtonian term from hydrostatic equilibrium, with  $\epsilon(r)$  the mass density.

$$\frac{dP}{dr} = -\frac{Gm(r)\epsilon(r)}{r^2}$$

Three correction terms from GR.

- Coupling of gravity to the energy density  $\epsilon(r)$  and the pressure  $P(r)$  of matter.
- Modification of the mass function  $m(r)$  due to the pressure.
- Modification of the radius.



The equation of state is needed to close the system of equations.

$$P = P(\epsilon)$$

# Solving the TOV equations

The TOV eqs. are first--order differential equations, which have to be integrated with the following boundary conditions:

$$M(r=0) = 0, \quad P(r=R) = P_{\text{surf}}$$

Usually one takes  $P_{\text{surf}} = 0$  or  $P_{\text{surf}} = P(\rho_{\text{Fe}})$ , with  $\rho_{\text{Fe}} = 7.86 \text{ g/cm}^3$  being the density of solid  $^{56}\text{Fe}$ . This defines the surface of the star, and specifies the radius  $R$ .

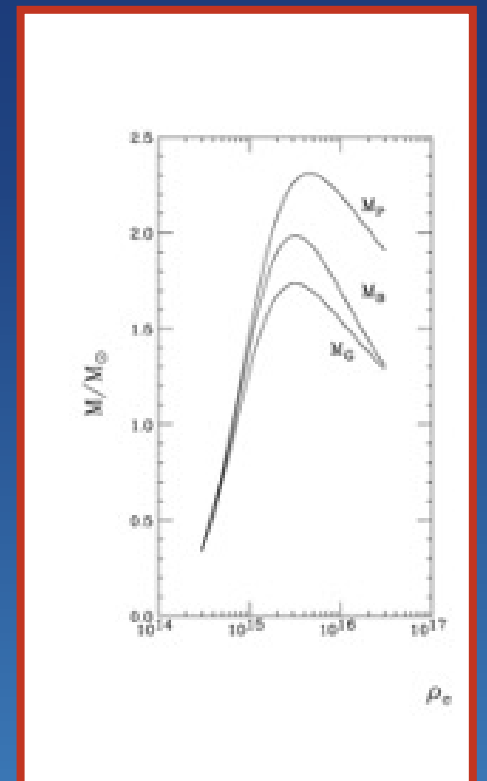
The TOV eqs. are integrated for a given value of the central density  $\rho_c$  (or equivalently of the central pressure  $P_c$ ), and the solution  $M(r; \rho_c)$ ,  $P(r; \rho_c)$  depends parametrically on  $\rho_c$ .

## The TOV mass

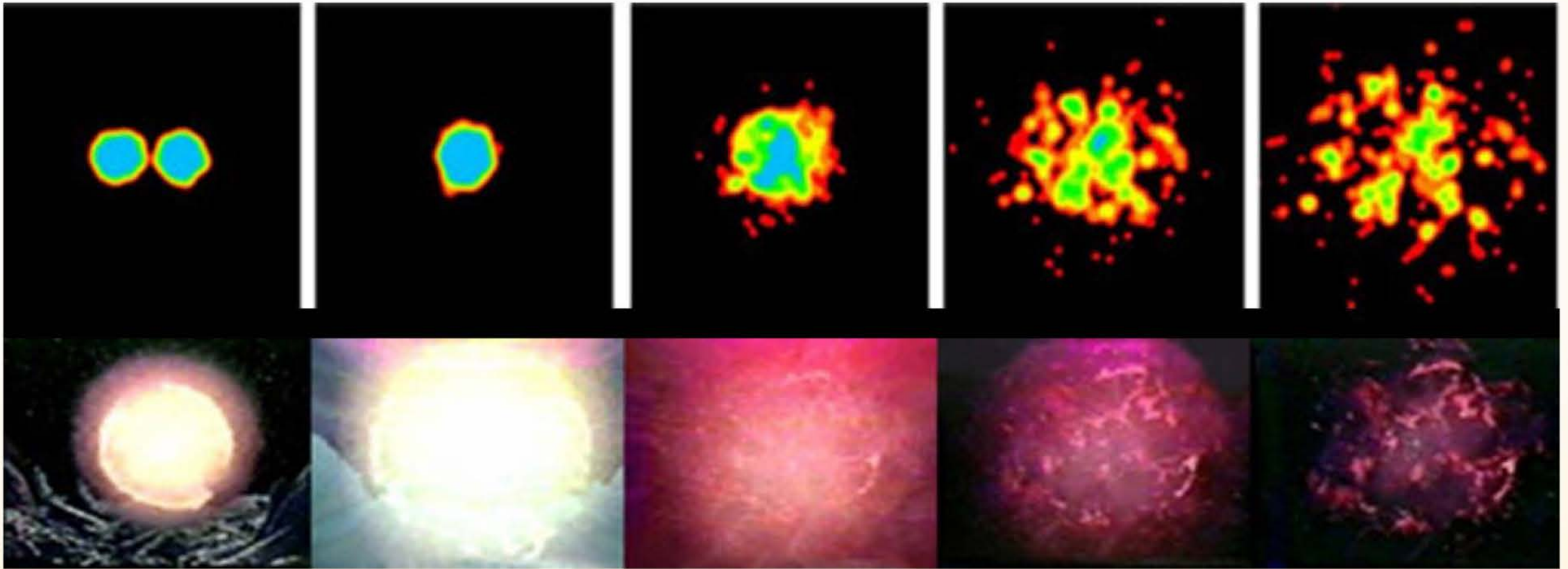
There is a maximum value  $M_{\text{ov}}$  of the gravitational mass of a neutron star that a given EOS can support. Similarity with Chandrasekhar mass for WD.

The existence of a finite value for the maximum mass of a neutron star implies that configurations with  $M_G$  greater than  $M_{\text{ov}}$  will collapse to a black hole.

Stable configurations can be obtained only when  $dM_G/d\rho_c > 0$ . This condition is necessary but not sufficient for stability. Hence, configurations on the decreasing branch of the function  $M_G(\rho_c)$  are unstable, and on the rising branch are stable. The stable branch terminates in the point where  $dM_G/d\rho_c = 0$ . This point sets the maximum value for the gravitational mass of a stable neutron star.



# Relevance of the EoS



1. Heavy ion collisions (small  $N/Z$ , high  $T$ )
2. Supernovae and Neutron Stars  
(high  $N/Z$ , high (small)  $T$  in SN (NS))
3. Binary NS merger and GW emission  
(high density, high  $N/Z$  and  $T$ )

Quite different physical conditions  
in each case !

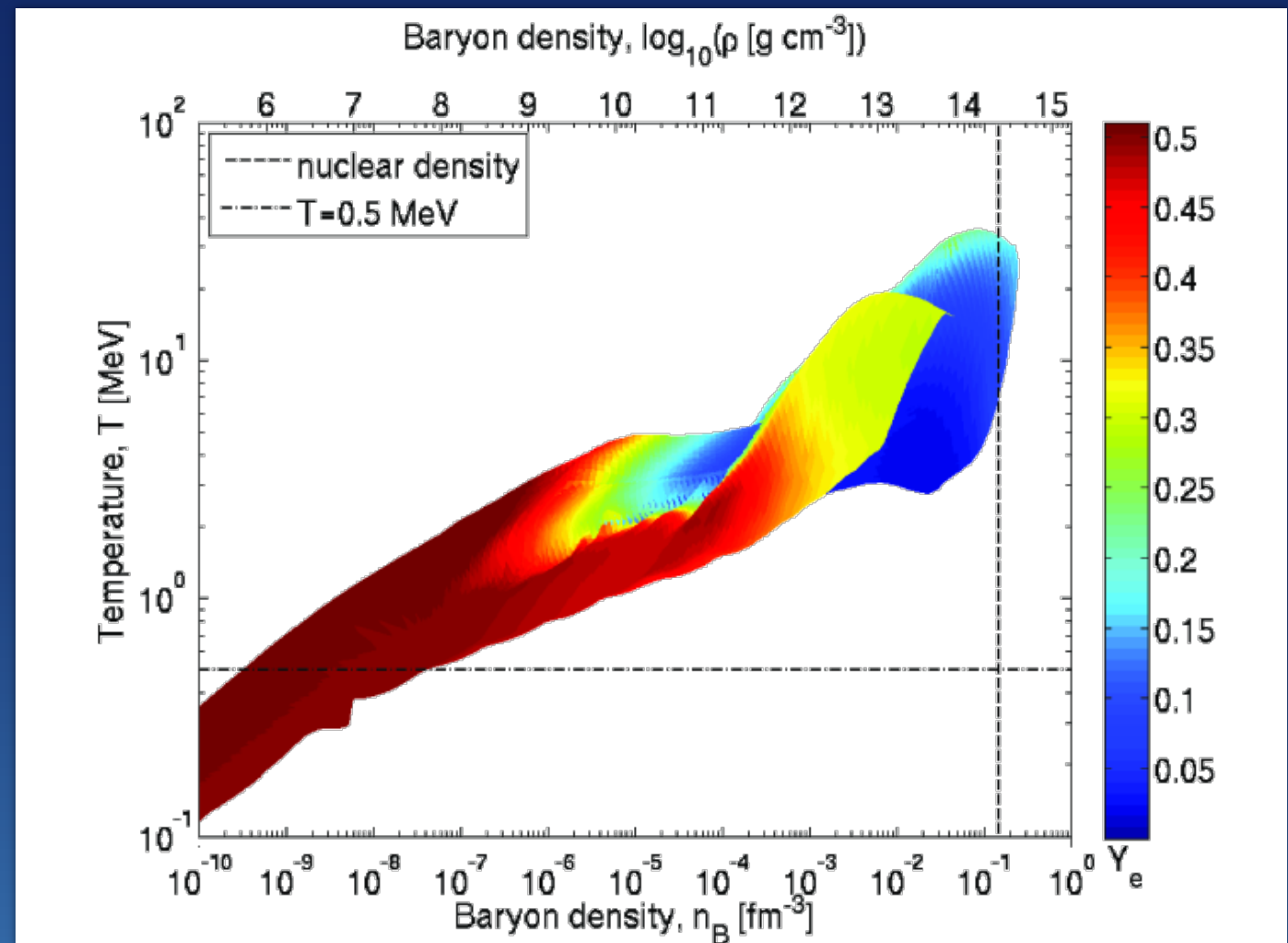
**A nuclear matter  
theory must be able  
to treat all these  
physical situations.**

# The construction of the EoS

## A challenging task

- \* Wide range of temperature, density and isospin asymmetry reached in astrophysical scenarios.
- \* Role of the hadronic interaction and its complexity
- \* Complicated solution of the nuclear many-body problem

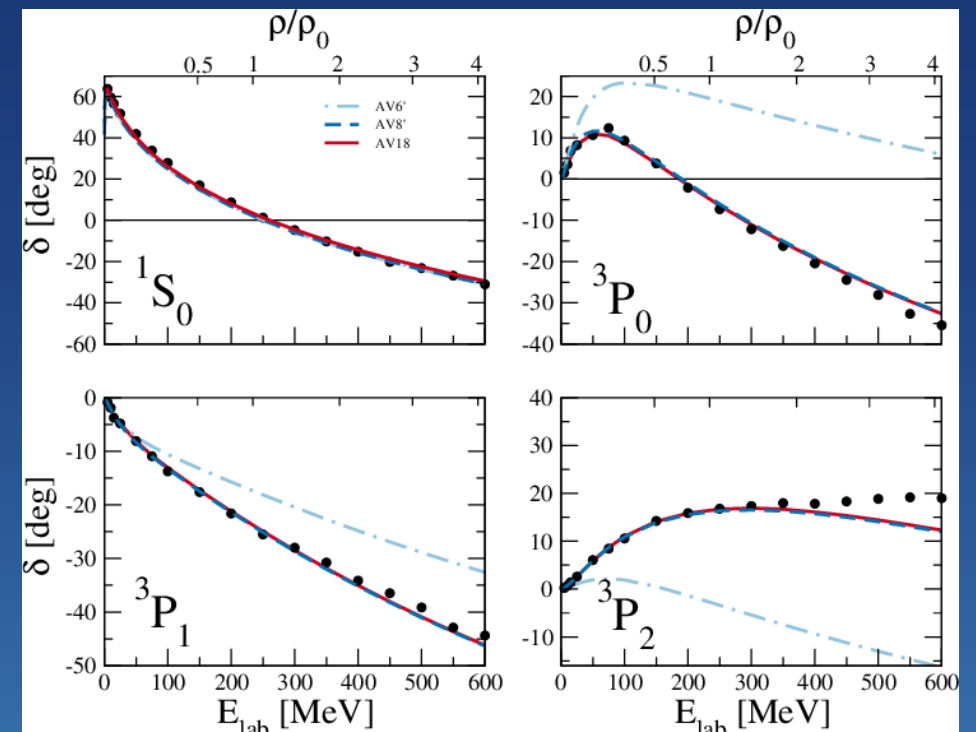
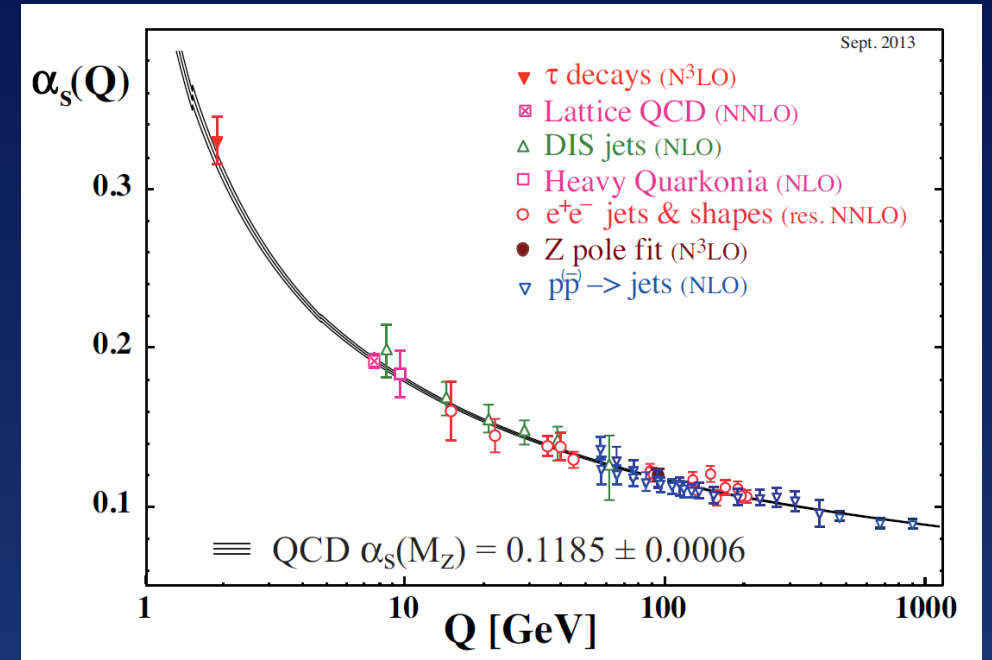
Fischer et al., 2021



*Temperature and density reached during a standard core-collapse supernova simulation at 100 ms post bounce.*

# Overview of the strong interaction in dense matter

- ✦ Hadronic Hamiltonian can, in principle, be derived from the underlying quark-gluon dynamics in QCD.
- ✦ However, because of the sign problem raised by the non-perturbative character of QCD at low and intermediate energies ( $\alpha_s$  behaviour) one is far from a quantitative understanding of the baryon-baryon interaction from the QCD point of view.
- ✦ Solution : to adopt simplified models where the hadronic degrees of freedom are the relevant ones.
- ✦ Use of phenomenological models of the hadronic interaction : meson exchange models and potential models.
- ✦ Fit of the nucleon-nucleon phase shifts.

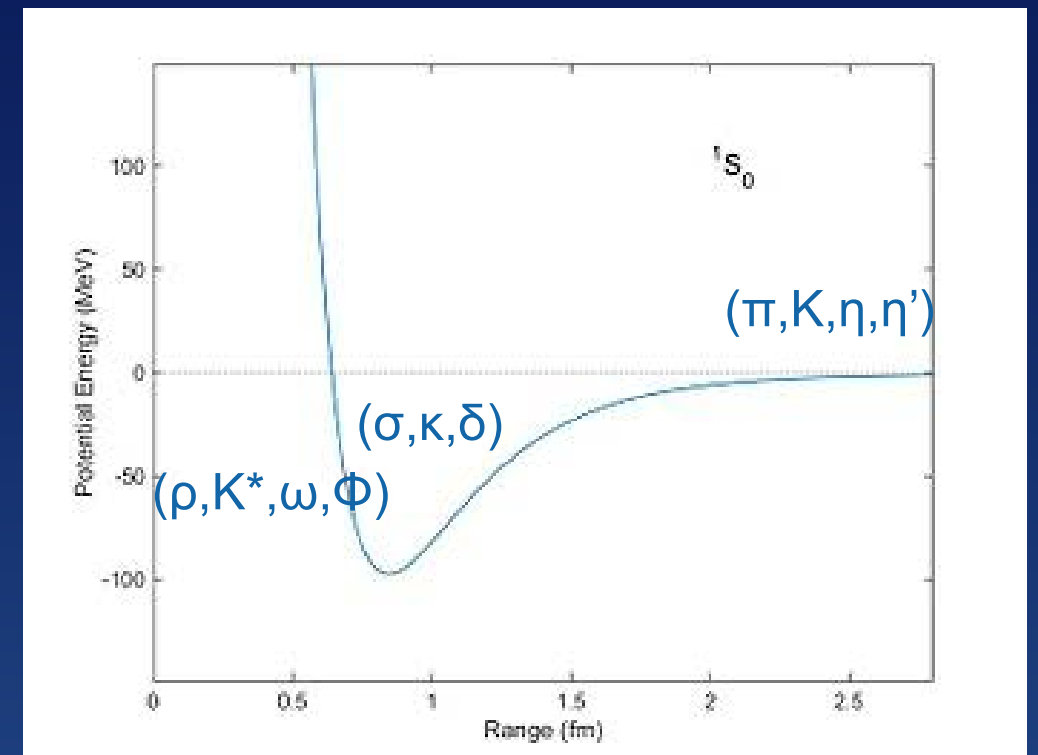


Workman et al., PRC94, 065203 (2016)

# Meson-exchange models

Based on the Yukawa theory : baryon-baryon interaction is mediated by the exchange of mesons.

- At large distance, attractive interaction mediated by pseudoscalar mesons ( $\pi, K, \eta, \eta'$ )
- At intermediate distance, a stronger attraction is present, at least once an average is made over the different channels. Scalar mesons ( $\sigma, \kappa, \delta$ )
- At short distance,  $r < 0.5$  fm, a strong repulsive core is present. Vector mesons : ( $\rho, K^*, \omega, \Phi$ ).



Very refined models are constructed for the NN interactions. Tested using thousands of experimental data on NN scattering cross sections supplemented with experimental properties on deuteron. Paris, Bonn, Nijmegen.

CAVEAT ! At short distance, serious divergency problems in many-body calculations. Standard perturbation theory not applicable !

YN and YY meson exchange potentials : Nijmegen, Juelich.

Machleidt et al., Phys. Rep. 149, 1 (1987)  
Nagels et al., PRD 17, 768 (1978)

# Potential models



## A modern NN potential : Argonne v18

A non-relativistic NN potential can be expressed in terms of a set of operators acting on the spin ( $\sigma$ ) and isospin ( $\tau$ ) variables of the two nucleons, as well as on the relative angular momentum ( $L$ ), the total spin operators  $\mathbf{S}$ , and  $\mathbf{r}$  the relative coordinate.

The form of the operators is dictated by **symmetry requirements** : translational and rotational invariance, charge independence of the nuclear forces, parity and time-reversal symmetry.

1	<i>central</i>
$\sigma_1 \cdot \sigma_2$	<i>spin - spin</i>
$(\sigma_1 \cdot \sigma_2)(\tau_1 \cdot \tau_2)$	<i>spin - isospin</i>
$\frac{3(\sigma_1 \cdot \mathbf{r})(\sigma_2 \cdot \mathbf{r})}{r^3} - (\sigma_1 \cdot \sigma_2)$	<i>tensor</i>
$(\frac{3(\sigma_1 \cdot \mathbf{r})(\sigma_2 \cdot \mathbf{r})}{r^3} - (\sigma_1 \cdot \sigma_2))(\tau_1 \cdot \tau_2)$	<i>tensor - isospin</i>
$\mathbf{1} \cdot \mathbf{S}$	<i>spin - orbit</i>
$\mathbf{l}^2$	<i>ang. mom. square</i>

In operatorial form the Argonne v18 NN potential is expressed by :

$$v_{18} = \sum_{p=1,18} v_p(r_{ij}) O_{ij}^p$$

$$O_{ij}^p = \left[ 1, \sigma_i \cdot \sigma_j, \overset{\text{tensor force}}{S_{ij}}, L \cdot S, L^2, \overset{\text{isotensor force}}{L^2(\sigma_i \cdot \sigma_j)}, (L \cdot S)^2 \right] \otimes [1, \tau_i \cdot \tau_j],$$

$$[1, \sigma_i \cdot \sigma_j, S_{ij}] \otimes T_{ij}, \text{ and } (\tau_i + \tau_j)$$

Wiringa et al.,  
PRC51, 38 (1995)

The first fourteen terms express charge independence (corresponding to  $V_{nn}=V_{np}=V_{pp}$ ). The four additional operators are small and break the charge independence.

In coordinate representation each term is multiplied by a form factor  $v_p$  which is in general a non-local potential and describes the possible velocity dependence of the NN potential.

## Several NN potentials available in literature

Fit to pp data Reid('68), Nijmegen ('78), Paris ('80)

Fit to np data Urbana v14 ('81), Argonne v14 ('84), Bonn ('87)

Potential models which have been fit only to the np data often give a poor description of the pp data, and viceversa

Fit to both np and pp data : only a limited set of forces remain

1. Argonne  $v_{18}$  (strictly local in each channel, Wiringa 1995)
2. CD Bonn potential (OBE, Machleidt 2001)
3. IS potential (non-local modifications of  $v_{18}$ , Doleschall 2004)

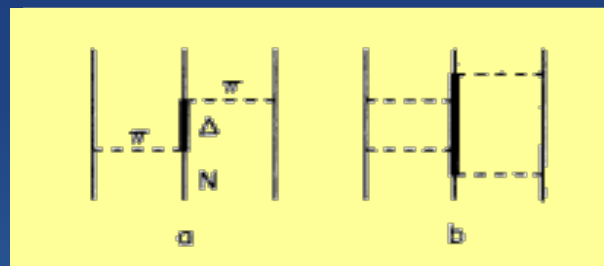
# Three-body forces

Two-body hadronic interactions yield only a part of the hadronic Hamiltonian of dense matter. At densities typical of NS core, interactions involving three and more hadrons might be important. Our experimental knowledge of three-body interaction is restricted to nucleons. The three-nucleon (NNN) force is necessary to reproduce properties of  $^3\text{H}$  and  $^3\text{He}$ , and to obtain correct parameters of symmetric nuclear matter at saturation.

- No complete theory available yet.
- Compare phenomenological and microscopic approaches.

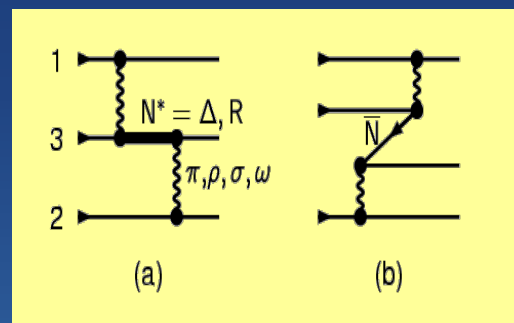
## ✓ Urbana IX model

Carlson et al., NP A401,(1983) 59

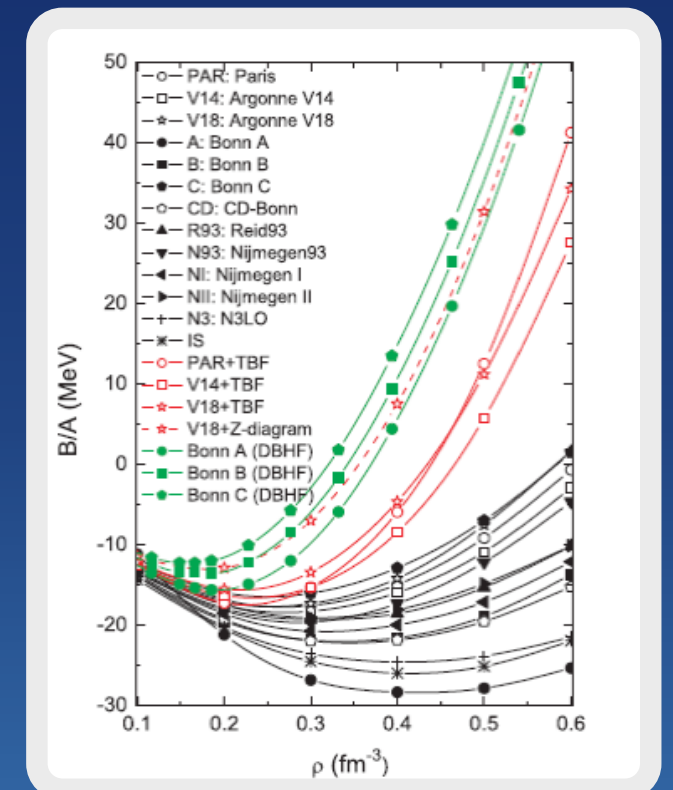


## ✓ Microscopic model

P. Grange' et al, PR C40, (1989) 1040

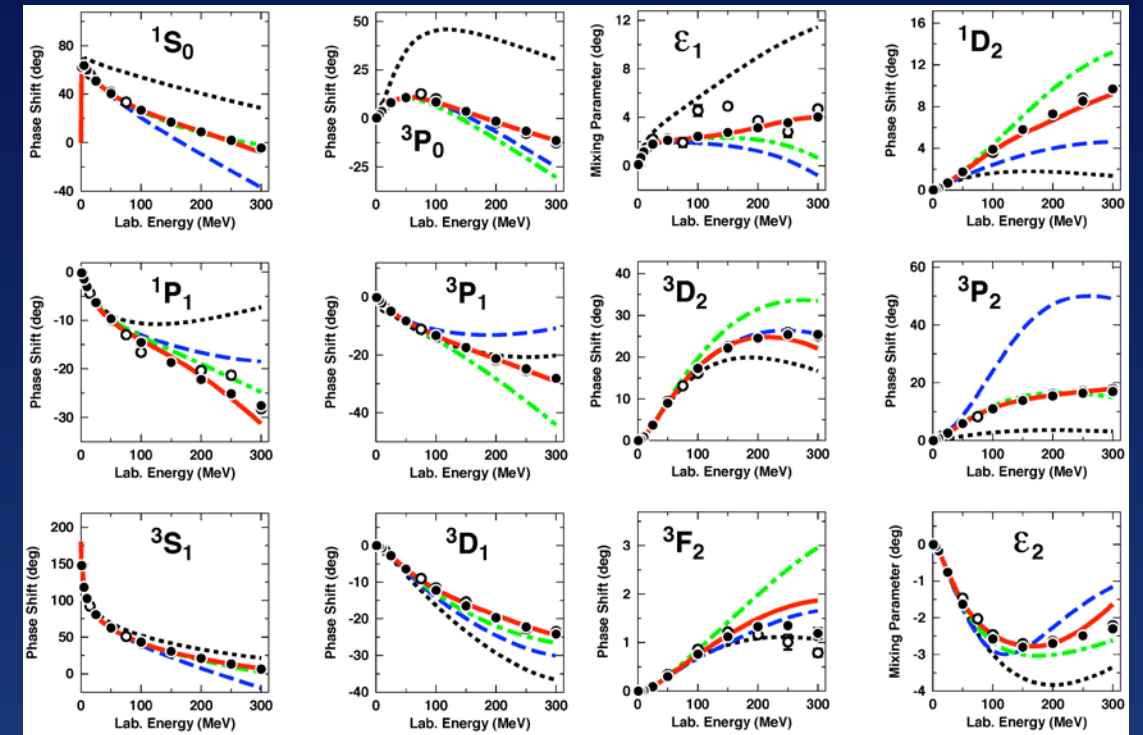
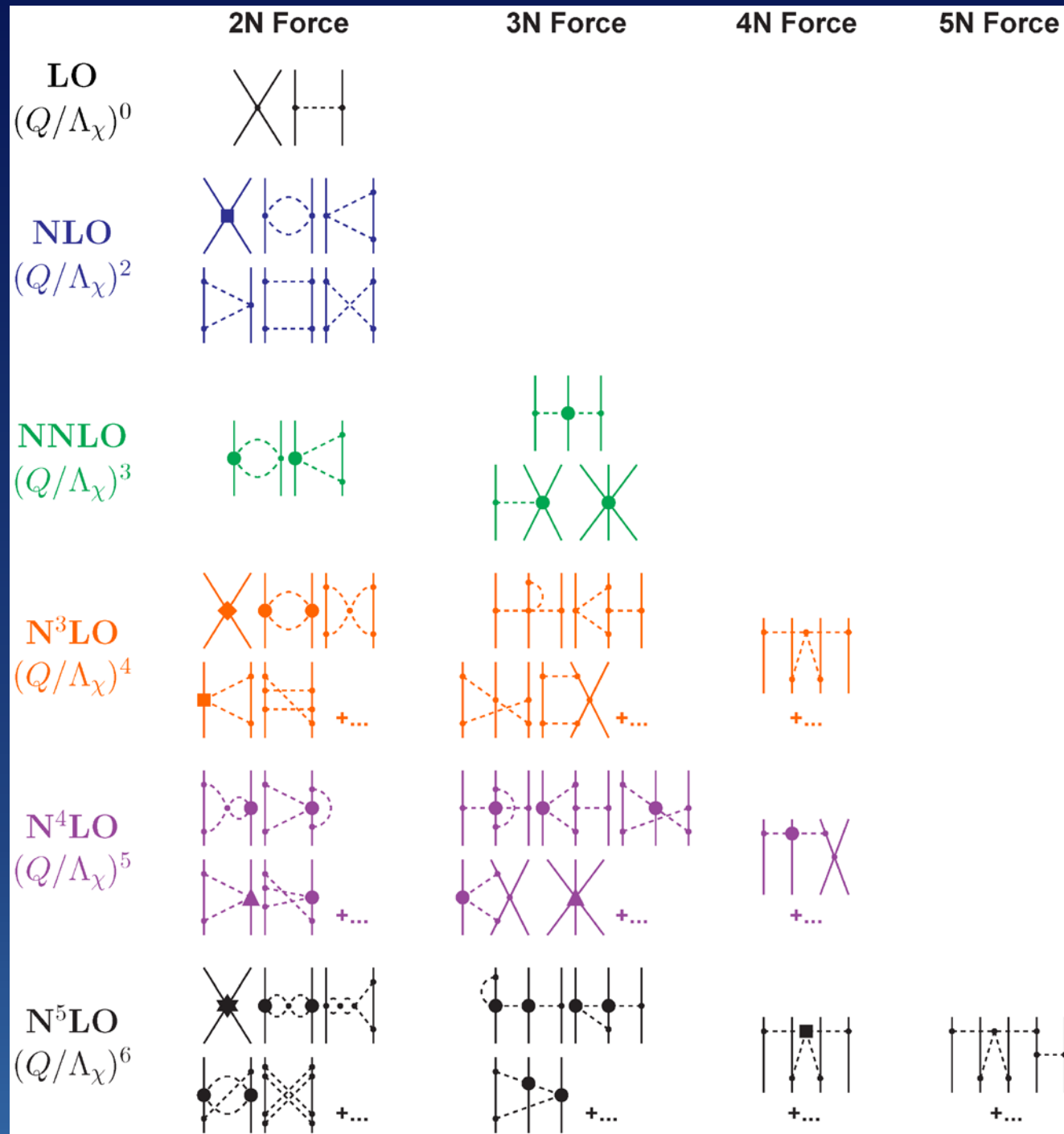


- TBF needed to improve saturation point.
- Dependence on NN potential.
- Uncertain high-density behaviour due to unknown TBF.



Z.H. Li, U. Lombardo, H.-J. Schulze, W. Zuo, PRC 74, 047304 (2006)

# Chiral perturbation expansion (ChPE)



- Starting point : quark and gluons as relevant degrees of freedom. Bridge between the low-energy hadron physics phenomena with the underlying QCD structure of the baryons.
- Weinberg (1990-91) : EFT based on the QCD broken symmetries.
- ChPE used to construct NN interactions of reasonably good quality in reproducing the two-body data.
- Various contributions to the potential systematically calculated order by order. Calculation of two-nucleon and many-nucleon forces in a consistent manner.

**CAVEAT ! ChPE valid for not too large momenta (i.e.density) of nuclear matter. Safe maximum density around the saturation value.**

Weinberg, PLB 251, 288 (1990); NPB 363, 3 (1991)

Entem & Machleidt, PRC 68, 041001(R) (2003)

Epelbaum et al., NPA 747, 363 (2005)

# Renormalization group (RG) method

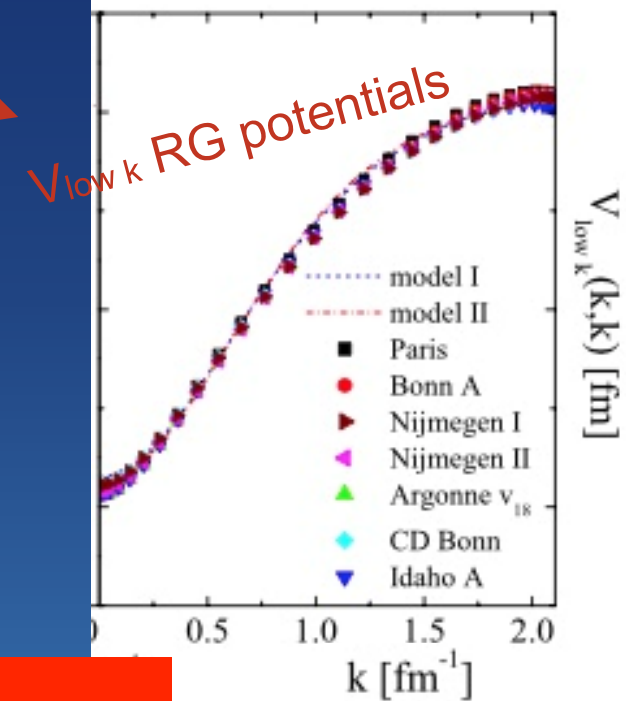
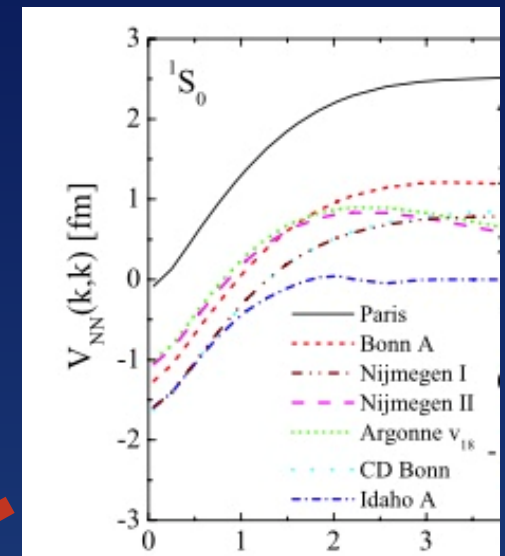
- ◆ The short-range hard core of the NN interaction  $V$  makes any perturbation expansion in terms of  $V$  meaningless
- ◆ **How to soften it ?** Integrating out all the momenta  $q$  larger than a certain cut-off  $\Lambda$   $\rightarrow$  effective interaction  $V_{\text{low } k}$  equivalent to the original one for momenta  $q < \Lambda$

- ◆ Result  $>$  a modified Lippmann-Schwinger equation with a cut-off dependent effective potential  $V_{\text{low } k}$

$$T(k', k; E_k) = V_{\text{low } k}(k', k) + \frac{2}{\pi} P \int_0^{\Lambda} dq q^2 \frac{V_{\text{low } k}(k', q) T(q, k; E_k)}{k^2 - q^2 + i\eta}$$

- ◆ Imposing  $dT(k', k; E_k)/d\Lambda=0$ , one gets an exact RG flow equation for  $V_{\text{low } k}$

$$\frac{dV_{\text{low } k}(k', k)}{d\Lambda} = \frac{2 V_{\text{low } k}(k', k) T(\Lambda, k, \Lambda^2)}{\pi (1 - k^2/\Lambda^2)}$$



Cut-off  $\Lambda$  taken at  $q \approx 2.1 \text{ fm}^{-1}$  (300 MeV lab. data)  
RG potential : softer, phase shift equivalent and energy independent !

cont.

- ◆ Softer potential : can be used in nuclear structure calculations and perturbation expansions.
- ◆ Method applied also to the hyperon-nucleon case. The results seem to indicate a similar convergence to a “universal” softer low-momentum hyperon-nucleon interaction.



## Baryon-baryon interactions from Lattice QCD

- ❖ Construction of a baryon–baryon interaction based on lattice QCD.
- ❖ Extremely expensive from the numerical point of view.
- ❖ Current simulations can be performed only with large quark masses.
- ❖ Two different collaborations and strategies : HALQCD & NPLQCD.
  - \* HALQCD investigation of the properties of nuclei and the EoS of nuclear matter. Binding energy per nucleon with a uniform mass-number  $A$  dependence, consistent with the Bethe–Weizsäcker mass formula, but bound at a quark mass corresponding to a pion mass of 469 MeV.
  - \* NPLQcd : in the strangeness sector determination of the binding energies of light hypernuclei. Results for NN, NY and YY interactions.

# Solving the nuclear many-body problem

# Two different philosophies toward the construction of the nuclear EoS :

## Phenomenological vs. ab initio approaches

### Phenomenological approaches

Based on effective density-dependent NN force with parameters fitted to reproduce nuclear observables and compact stars observables.

- **Non-relativistic models:** Skyrme and Gogny
- **Relativistic mean-field models (RMF)**

For clusterized matter

- **SN approximation models :** Liquid Drop models, Thomas-Fermi models, Self-consistent mean field models.
- **NSE models.** NSE, virial EoS.

### Ab initio approaches

Based on two- and three-nucleon realistic interaction which reproduces scattering data and deuteron properties. The EoS is found by solving the complicated many-body problem.

- **Diagrammatic:** (Dirac)-Brueckner-Hartree-Fock, SCGF
- **Variational :** APR, FHNC, LOCV, CBF.
- **Quantum Monte Carlo :** VMC, GFMC, AFDMC.
- **Chiral approaches :**  $\chi$ EFT.

**more in :** Neutron stars and the nuclear equation of state,  
F.B., HJ Schulze, I. Vidana, JB Wei, PPNP 120 (2021) 103879,

# Ab-initio approaches

# Diagrammatic technique (I): The (Dirac)-Brueckner theory of nuclear matter

The (Dirac)-Brueckner-Hartree-Fock theory is based on the Goldstone expansion, which is a perturbation series for the ground-state energy of a many-body system. The theory amounts to ordinary perturbation theory expressed in a tractable form.

Consider a system of  $A$  identical nucleons whose Hamiltonian is the sum of the kinetic energies of all the particles plus the sum of the two-body interactions

$$H = \sum_{i=1}^A \frac{\hbar^2}{2m} k_i^2 + \sum_{i<j=1}^A v_{ij} = H_0 + H_1$$

The above equation splits  $H$  into two parts. The unperturbed Hamiltonian  $H_0$  is the sum of the kinetic energy  $T$  and a one-body potential operator  $U$ .

$$H_0 = \sum_{i=1}^A \left( \frac{\hbar^2}{2m} k_i^2 + U_i \right)$$

The perturbation is what is left over.

$$H_1 = \sum_{i<j=1}^A v_{ij} - \sum_{i=1}^A U_i$$

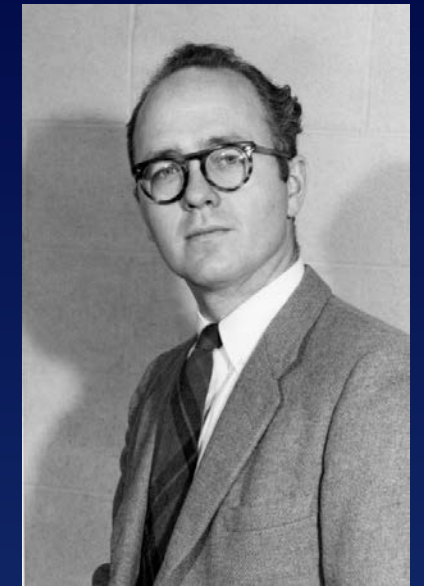
# CAVEATS !

- ★ The introduction of the single-particle potential  $U$  (auxiliary potential) is intended to make numerical calculation easier. Since the total Hamiltonian does not involve  $U$ , the final result should in principle be independent of  $U$ . However, the energy is to be calculated as an expansion in powers of  $H_1$ , and the expansion will converge more rapidly for some choices of  $U$  than for others. Thus we must try to choose  $U$  in such a way that the energy expansion converges rapidly enough to be useful for practical calculations.
- ★ Ordinary perturbation theory cannot be used in its commonly used form for nuclear calculations because the strong short-range repulsion in the NN potential makes all the matrix elements very large, and the series cannot converge.

The strong short-range repulsion causes a similar difficulty in the problem of NN scattering. If one calculates the scattering matrix  $T$  to first order in  $V$  (Born approximation), then one obtains a large and inaccurate result. But if one calculates to all orders in  $V$  (two-particle Schroedinger eq.), then one obtains the correct result.

$$T = V + V \frac{1}{H_0 - E + i\epsilon} T ; \quad H = H_0 + V$$
$$G_0 = (H_0 - E + i\epsilon)^{-1}$$
$$T = V + VG_0V + VG_0VG_0V + \dots$$

# The Bethe-Goldstone equation



K. Brueckner

The procedure followed for nuclear matter is analogous to the treatment of NN scattering. All terms in the expansion of the Hamiltonian are rearranged in such a way that each matrix element of  $V$  is replaced by an infinite series which takes account the two-body interaction to all orders of the potential.

The quantity that replaces the two-body potential  $V$  is called the reaction matrix  $G$ ; and calculating the reaction matrix is equivalent to solving a Schrodinger equation which describes the scattering of two particles in the presence of all the others. The  $G$ -matrix is well-behaved even for a singular two-body force, all terms in this new perturbation series are finite and of reasonable size.

Stopping the perturbative series at first order (keep the two-body correlations only), one gets the Brueckner-Hartree-Fock approximation for the binding energy.

$$G(\rho; \omega) = V + \sum_{k_a, k_b} V \frac{|k_a k_b\rangle Q \langle k_a k_b|}{\omega - e(k_a) - e(k_b)} G(\rho; \omega)$$

$\omega$  = starting energy  
 single-particle energy

$$e(k; \rho) = \frac{k^2}{2m} + U(k; \rho)$$

$$U(k; \rho) = \text{Re} \sum_{k' \leq k_F} \langle k k' | G(\rho; \omega) | k k' \rangle_a$$

$$\frac{E}{A}(\rho) = \frac{3}{5} \frac{k_F^2}{2m} + \frac{1}{2\rho} \sum_{k, k' \leq k_F} \langle k k' | G[\rho; \omega] | k k' \rangle_a$$

## The perturbative expansion is convergent !

# The relativistic BHF

- Introducing the in-medium relativistic G-matrix.
- Nuclear mean field in terms of scalar and vector components
- Use of spinor formalism, equivalent to introduce a special TBF, the Z-diagram, nucleon-anti nucleon pair which gives a repulsive contribution.
- Stiffer EoS than the non-relativistic case.
- Superluminal EoS at large density.

## The variational method in its practical form

Pandharipande & Wiringa, 1979; Lagaris & Pandharipande, 1981

The variational method is based on the Ritz's principle, according to which the expectation value of the Hamiltonian is stationary with respect to variations about the eigenvectors

$$\delta \frac{\langle \Psi | H | \Psi \rangle}{\langle \Psi | \Psi \rangle} = 0 \quad \text{for an arbitrary variation } \delta \Psi \text{ of } \Psi$$

In the variational method one assumes that the ground state wave function  $\Psi$  can be written in the following form, being  $\Phi$  the unperturbed ground state wave function, properly antisymmetrized, and the product runs over all possible distinct pairs of particles.

$$\Psi(r_1, r_2, \dots) = \prod_{i < j} f(r_{ij}) \Phi(r_1, r_2, \dots)$$

The correlation factor  $f(r_{ij})$  is determined by the variational principle, i.e. by assuming that the mean value of the Hamiltonian has a stationary point.

This is a functional equation for the correlation function  $f$ , which can be expanded in the same spin-isospin, spin-orbit and tensor operators appearing in the NN interaction.

$$\frac{\delta \langle \Psi | H | \Psi \rangle}{\delta f \langle \Psi | \Psi \rangle} = 0$$

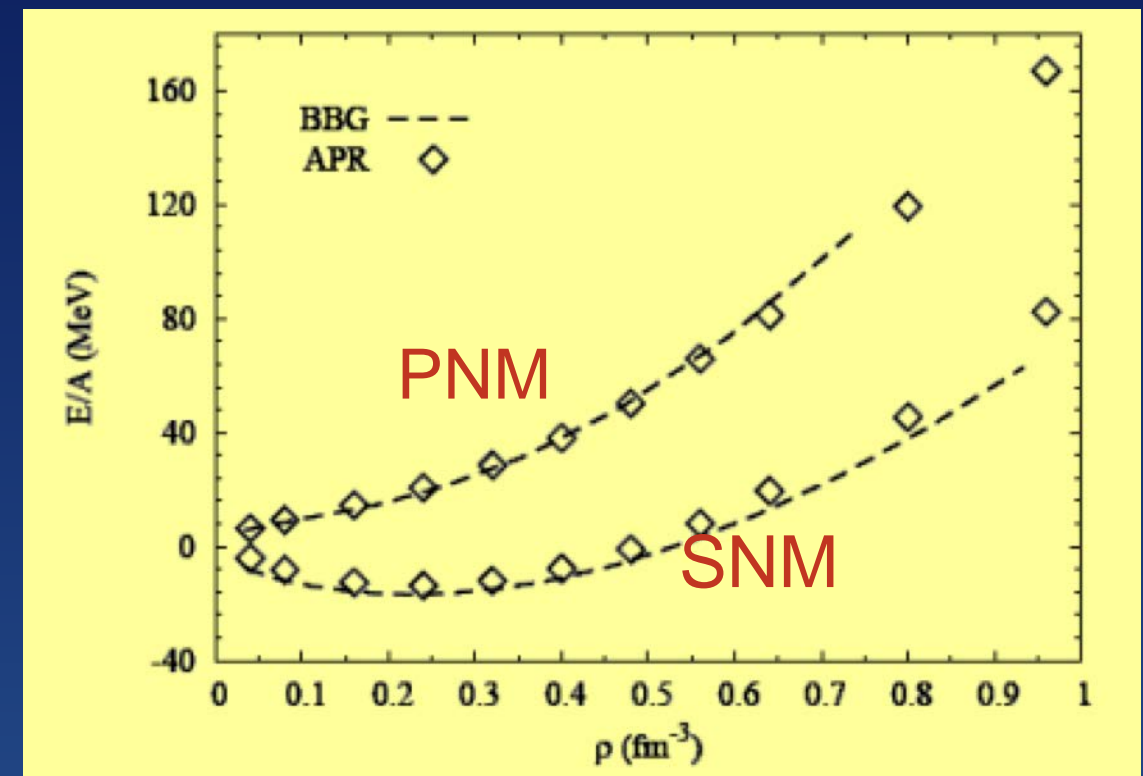
The best known and most used variational nuclear matter EoS is the one by Akmal, Pandharipande, Ravenhall (APR EOS, PRC 58, 1804 (1998))

# Dependence on the many-body scheme: BHF vs. APR

## Main differences :

a) In BHF the kinetic energy contribution is kept at its unperturbed value at all orders of the expansion, while all correlations are embodied in the interaction energy part. In the variational, both kinetic and interaction parts are directly modified by the correlation factors.

b) In BHF the s.p. potential is introduced in the expansion and improves the rate of convergence. In the variational, no single particle potential is introduced.



At two-body level, both methods give quite similar results.

# Diagrammatic technique II : Self-consistent Green's functions (SCGF)

- ✓ Elegant method based on the Martin-Schwinger hierarchy of Green's Functions
- ✓ More complete treatment of the NN correlations.

EoS of nuclear matter :

$$\frac{E}{N}(\rho, T) = \frac{v}{\rho} \int \frac{d^3k}{(2\pi)^3} \int_{-\infty}^{\infty} \frac{d\omega}{2\pi} \frac{1}{2} \left( \frac{\hbar^2 k^2}{2m} + \omega \right) A(k, \omega) f(\omega).$$

Spectral function :

$$A(k, \omega) = \frac{-2\text{Im}\Sigma(k, \omega)}{[\omega - \frac{\hbar^2 k^2}{2m} - \text{Re}\Sigma(k, \omega)]^2 + [\text{Im}\Sigma(k, \omega)]^2}$$

Self-energy

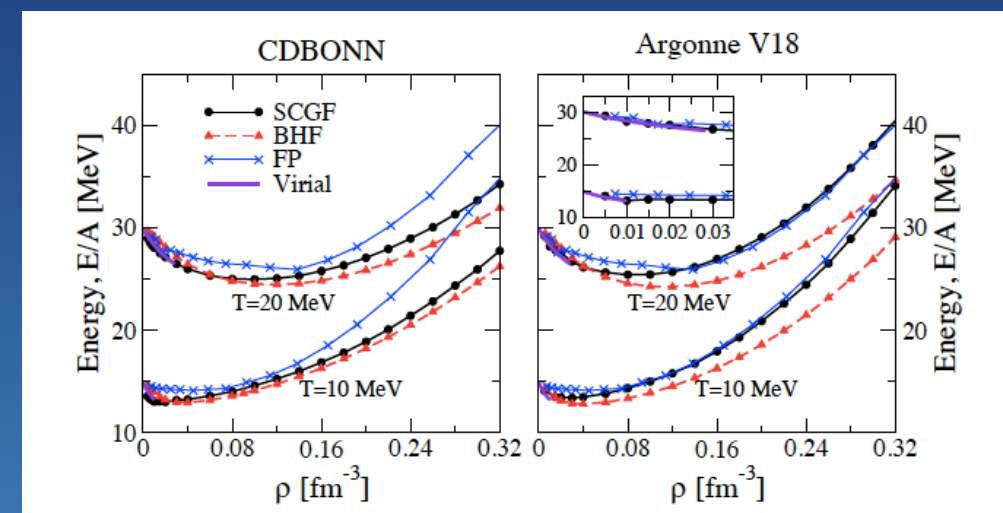
Results for hot neutron matter :

More in :

Ramos, Polls & Dickhoff, Nucl. Phys. A **503**, 1 (1989)

Muether & Dickhoff, Phys. Rev. C **72**, 054313 (2005)

Somà & Bož'ek, Phys. Rev. C **78**, 054003 (2008)



Rios, Polls, & Vidana, PRC79  
(2009)

$$\min \left\{ \frac{\langle \Psi | \hat{H} | \Psi \rangle}{\langle \Psi | \Psi \rangle} \right\} \geq E$$

# Quantum Monte Carlo methods

VMC, GFMC, AFDMC : MC sampling of a probability density

- **Variational MC** : variational method for the approximation of the g.s. A specific class of trial wave functions is considered, and using Monte Carlo quadrature to evaluate the multidimensional integrals, the energy with respect to changes in a set of variational parameters is minimized.
- **GFMC** : best when an accurate trial wave function (VM) is available, Very accurate for light nuclei, but increasingly more difficult for larger systems (Exponential growth of the computing time). The largest nuclear GFMC calculations are for the  $^{12}\text{C}$  nucleus, and for systems of 16 neutrons.
- **AFDMC** : extended GFMC to include a diffusion in the spin and isospin states of the individual nucleons. More efficient in treating homogeneous neutron matter It does require the use of simpler trial wave functions -> not yet quite flexible in the treating complex nuclear Hamiltonians.

**Advantages** : finite nuclei - virtually exact, BUT only local NN potentials

All non-relativistic many-body methods fail to reproduce the correct saturation point.

Three-body forces need to be included.

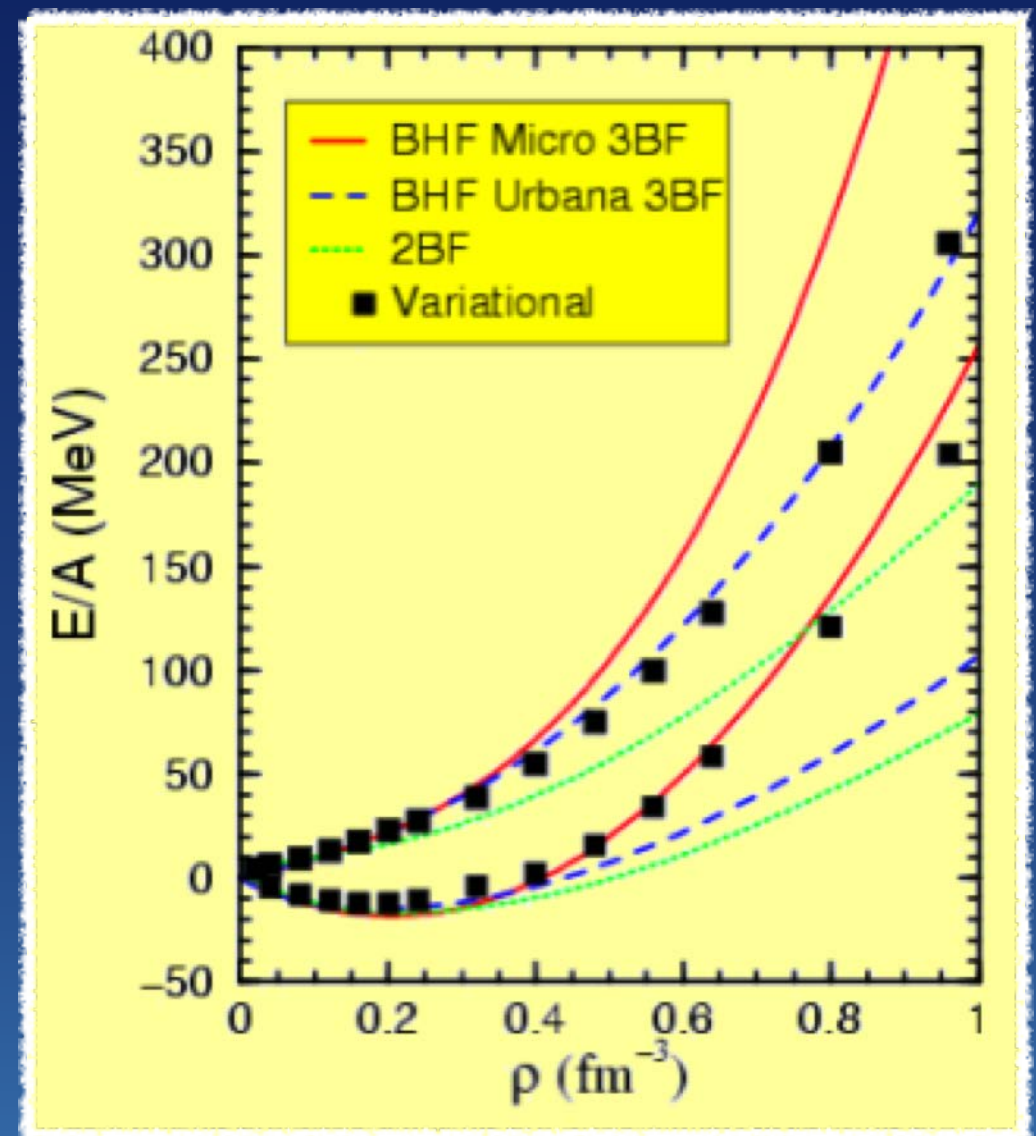
They must allow to reproduce “reasonably well” also the data on three and four nucleon systems.

They must be consistent with the two-body force adopted . Only partially explored !



# Including TBF's and comparing up to high density

- TBF's parameters fitted either to NM saturation point or to finite nuclei g.s.
- TBF's are different in either methods.
- Good agreement in SNM up to  $0.4 \text{ fm}^{-3}$
- Large discrepancy at the high density typical of a NS core.



# Phenomenological approaches

## Mean-field models with Skyrme and Gogny interactions

- ✦ Use effective interactions : simpler structure than realistic interactions used in ab initio approaches.
- ✦ Dependence on a number of parameters (10-15) fitted to different properties of several nuclei and nuclear matter properties.
- ✦ Typical representatives : Skyrme and Gogny forces in non-relativistic calculations and meson-exchange forces in relativistic mean-field models.
- ✦ Caveat : extrapolation to exotic conditions has to be considered with caution
- ✦ Phenomenological approaches are the most widely used methods to construct EoSs for astrophysical applications.

## Skyrme : Effective zero-range density dependent interaction

$$\begin{aligned}\hat{V}_{12}^{(\text{Skyrme})} = & t_0(1 + x_0\hat{P}_\sigma)\delta(\mathbf{r}_{12}) \\ & + \frac{t_1}{2}(1 + x_1\hat{P}_\sigma) \left[ \hat{\mathbf{k}}^\dagger\delta(\mathbf{r}_{12}) + \delta(\mathbf{r}_{12})\hat{\mathbf{k}}^2 \right] \\ & + t_2(1 + x_2\hat{P}_\sigma)\hat{\mathbf{k}}^\dagger \cdot \delta(\mathbf{r}_{12})\hat{\mathbf{k}} \\ & + \frac{1}{6}t_3(1 + x_3\hat{P}_\sigma)\delta(\mathbf{r}_{12})\varrho^\alpha(\mathbf{R}_{12}) \\ & + iW_0(\hat{\sigma}_1 + \hat{\sigma}_2) \cdot \hat{\mathbf{k}}^\dagger\delta(\mathbf{r}_{12})\hat{\mathbf{k}}\end{aligned}$$

Free parameters :  $t_i, x_i, \alpha, W_0$ .

The energy density is calculated in the HF approximation, thus yielding a simple EDF for nuclear matter expressed as fractional powers of the number densities.

Many parametrizations do exist !

## Gogny : Effective finite-range density dependent interaction

$$\begin{aligned}\hat{V}_{12}^{(\text{Gogny})} = & \sum_{j=1,2} \exp\left(-\frac{\mathbf{r}_{12}^2}{\mu_j^2}\right) \\ & \times \left( W_j + B_j\hat{P}_\sigma - H_j\hat{P}_\tau - M_j\hat{P}_\sigma\hat{P}_\tau \right) \\ & + t_3(1 + x_0\hat{P}_\sigma)\delta(\mathbf{r}_{12})\varrho^\alpha(\mathbf{R}_{12}) \\ & + iW_{ls}(\hat{\sigma}_1 + \hat{\sigma}_2) \cdot \hat{\mathbf{k}}^\dagger\delta(\mathbf{r}_{12})\hat{\mathbf{k}}\end{aligned}$$

Less number of parameters wrt Skyrme.

Numerically more complicated because of the **finite-range** terms.

# Relativistic mean-field models

Starting point : **effective Lagrangian density** in which the baryon-baryon interaction is given in terms of meson exchange

$$\mathcal{L} = \mathcal{L}_{\text{nuc}} + \mathcal{L}_{\text{mes}} + \mathcal{L}_{\text{int}}$$

$$\mathcal{L}_{\text{nuc}} = \sum_{i=n,p} \bar{\psi}_i (\gamma_\mu i \partial^\mu - m_i) \psi_i \quad \mathcal{L}_{\text{int}} = - \sum_{i=n,p} \bar{\psi}_i [\gamma_\mu (g_\omega \omega^\mu + \vec{\tau} \cdot g_\rho \rho^\mu) + g_\sigma \sigma] \psi_i$$

$$\begin{aligned} \mathcal{L}_{\text{mes}} = & \frac{1}{2} (\partial_\mu \sigma \partial^\mu \sigma - m_\sigma^2 \sigma^2) \\ & - \frac{1}{4} G_{\mu\nu} G^{\mu\nu} + \frac{1}{2} m_\omega^2 \omega_\mu \omega^\mu \\ & - \frac{1}{4} \vec{H}_{\mu\nu} \cdot \vec{H}^{\mu\nu} + \frac{1}{2} m_\rho^2 \vec{\rho}_\mu \cdot \vec{\rho}^\mu \end{aligned}$$

$$G_{\mu\nu} = \partial_\mu \omega_\nu - \partial_\nu \omega_\mu \text{ and } \vec{H}_{\mu\nu} = \partial_\mu \vec{\rho}_\nu - \partial_\nu \vec{\rho}_\mu.$$

Applying the mean field approximation, i.e. replacing the meson fields  $\sigma, \omega, \rho$  by their expectation values and the baryon currents by their ground state expectations generated by the presence of mean meson fields, the EoS can be obtained

➤ Energy density

$$\begin{aligned} \varepsilon = & \frac{1}{3} b m_N (g_{\sigma N} \langle \sigma \rangle)^3 + \frac{1}{4} c m_N (g_{\sigma N} \langle \sigma \rangle)^4 + \frac{1}{2} m_\sigma^2 \langle \sigma \rangle^2 + \frac{1}{2} m_\omega^2 \langle \omega_0 \rangle^2 + \frac{1}{2} m_\rho^2 \langle \rho_{03} \rangle^2 \\ & + \sum_B \frac{2J_B + 1}{2\pi^2} \int_0^{k_{FB}} \sqrt{k^2 + (m_B + g_{\sigma B} \langle \sigma \rangle)^2} k^2 dk + \sum_\lambda \frac{1}{\pi^2} \int_0^{k_{F\lambda}} \sqrt{k^2 + m_\lambda^2} k^2 dk \end{aligned}$$

➤ Pressure

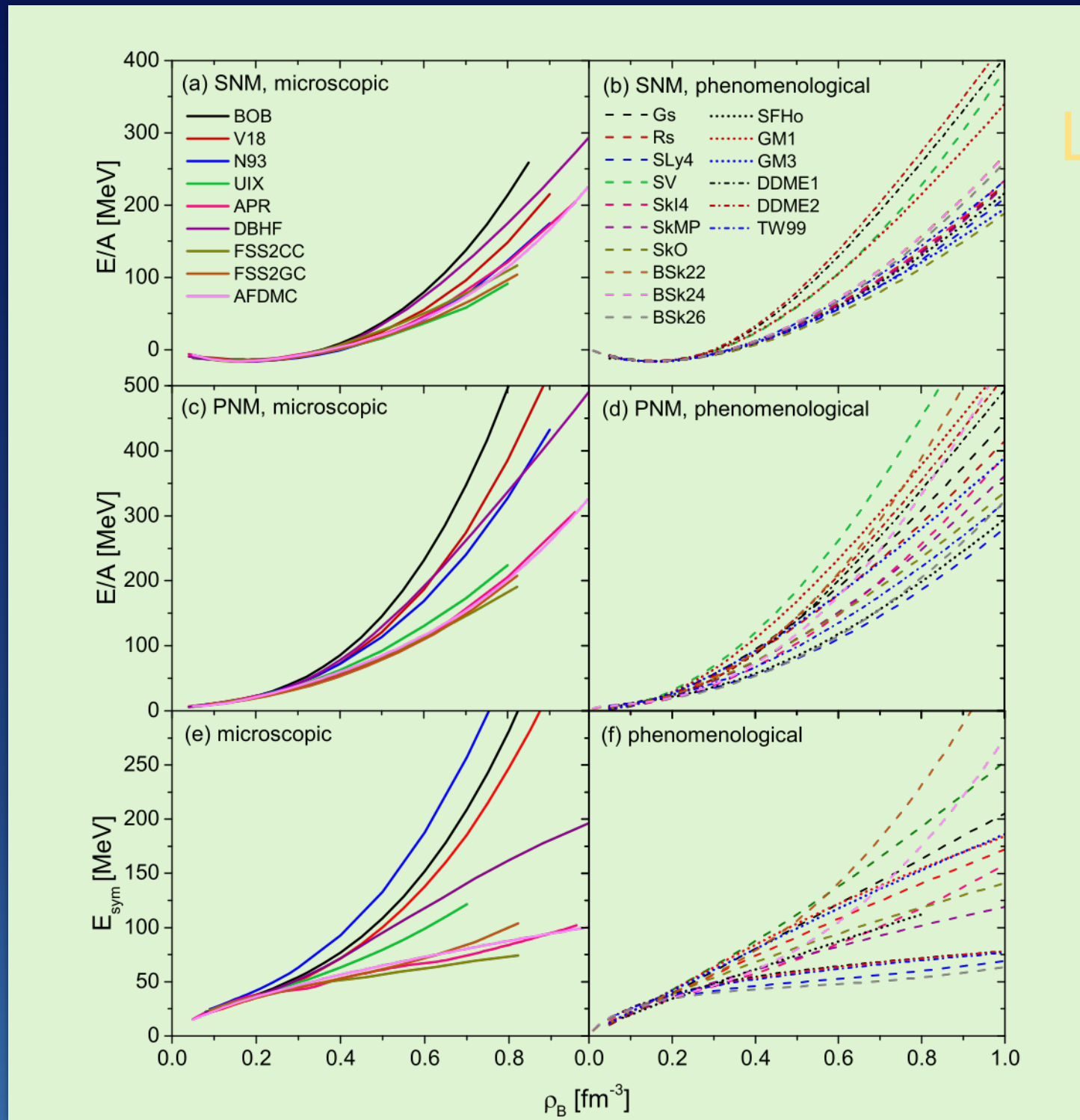
$$\begin{aligned} p = & -\frac{1}{3} b m_N (g_{\sigma N} \langle \sigma \rangle)^3 - \frac{1}{4} c m_N (g_{\sigma N} \langle \sigma \rangle)^4 - \frac{1}{2} m_\sigma^2 \langle \sigma \rangle^2 + \frac{1}{2} m_\omega^2 \langle \omega_0 \rangle^2 + \frac{1}{2} m_\rho^2 \langle \rho_{03} \rangle^2 \\ & + \frac{1}{3} \sum_B \frac{2J_B + 1}{2\pi^2} \int_0^{k_{FB}} \frac{k^4 dk}{\sqrt{k^2 + (m_B + g_{\sigma B} \langle \sigma \rangle)^2}} + \frac{1}{3} \sum_\lambda \frac{1}{\pi^2} \int_0^{k_{F\lambda}} \frac{k^4 dk}{\sqrt{k^2 + m_\lambda^2}} \end{aligned}$$

$$B = n, p, \Lambda, \Sigma^-, \Sigma^0, \Sigma^+, \Xi^-, \Xi^0$$

Nucleon coupling constants :  $g_{\sigma N}$ ,  $g_{\omega N}$ ,  $g_{\rho N}$ ,  $b$  and  $c$  are fixed by the nuclear matter properties at saturation (density, binding energy, compressibility, symmetry energy, effective mass).

Hyperon coupling constants :  $g_{\sigma Y}$ ,  $g_{\omega Y}$ ,  $g_{\rho Y}$  constrained by  $\Lambda$  binding energy in nuclear matter, hypernuclei properties and NS maximum observed mass.

# Comparing ab-initio and phenomenological approaches : Binding and Symmetry energy

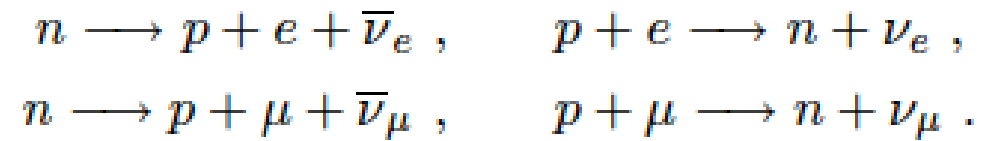


Large variations over  
the  
density range

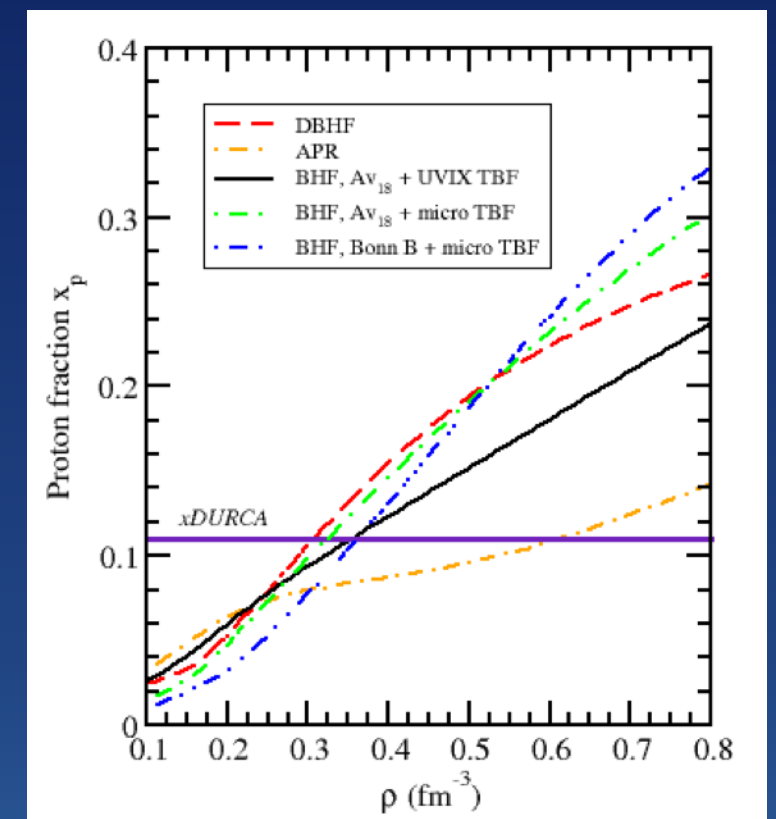
Symmetry energy

$$E_{sym}(\rho) = E_{PNM}(\rho) - E_{SNM}(\rho)$$

# Direct URCA processes in NS

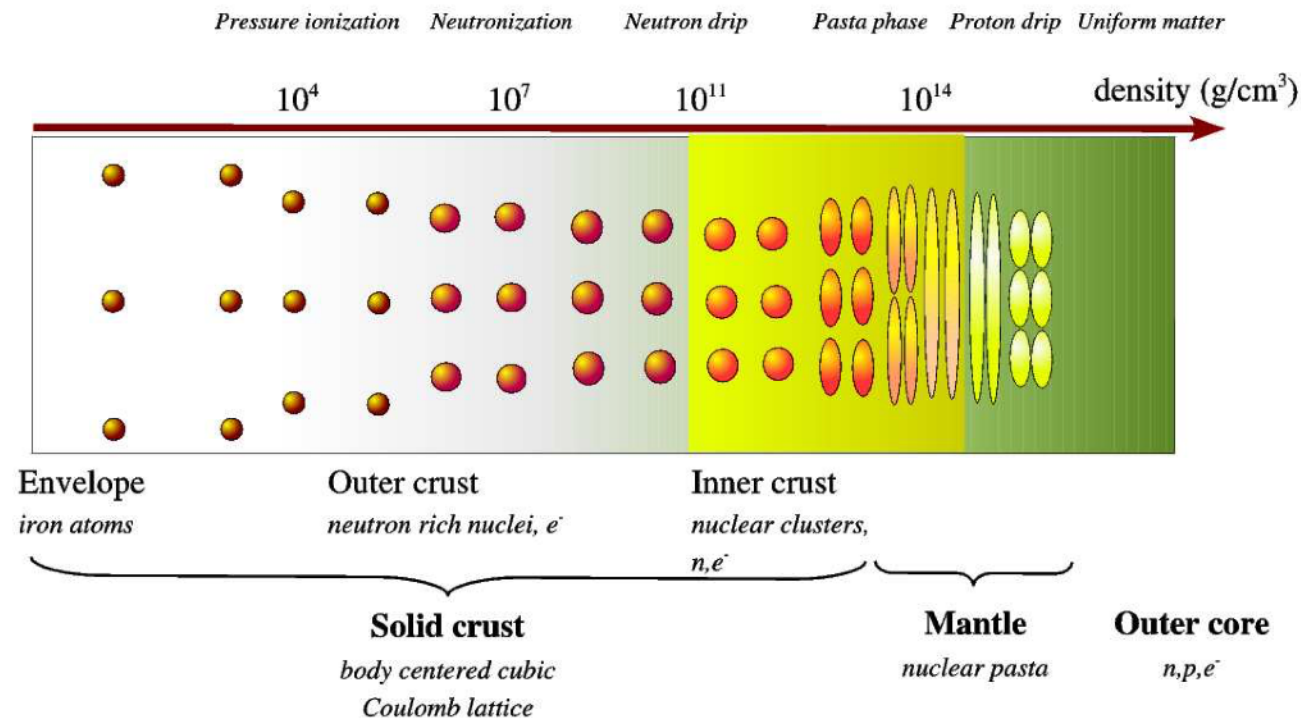


- They are allowed only at a rather high density at which the proton fraction  $x_D > 0.11-0.14$  (Lattimer et al. 1991).
- If Direct URCA operate, then a non-superfluid NS core cools to  $10^9$  K in a minute, and to  $10^8$  K in a year. If they are not allowed, the time scales will be one year and  $10^5$  years respectively.
- The symmetry energy is crucial for determining the proton fraction.



INSERT A FEW SLIDES ABOUT METAMODELS

# From clustered to homogeneous matter : the crust-core transition



Chamel&Haensel, *Living Reviews in Relativity* 11 (2008), 10

The crust exhibits various phases but with  $e$ ,  $p$ ,  $n$  only: its properties can be fully determined by known atomic and nuclear physics.

Even though the crust of a NS represents about 1% of the stellar mass and 10% of the radius, the crust is crucial because it is related to many astrophysical phenomena, e.g.

- *pulsar glitches (sudden spin-ups)*
- *nucleosynthesis in NS mergers*
- *gravitational wave emission*

# EoS of clustered and non-uniform matter

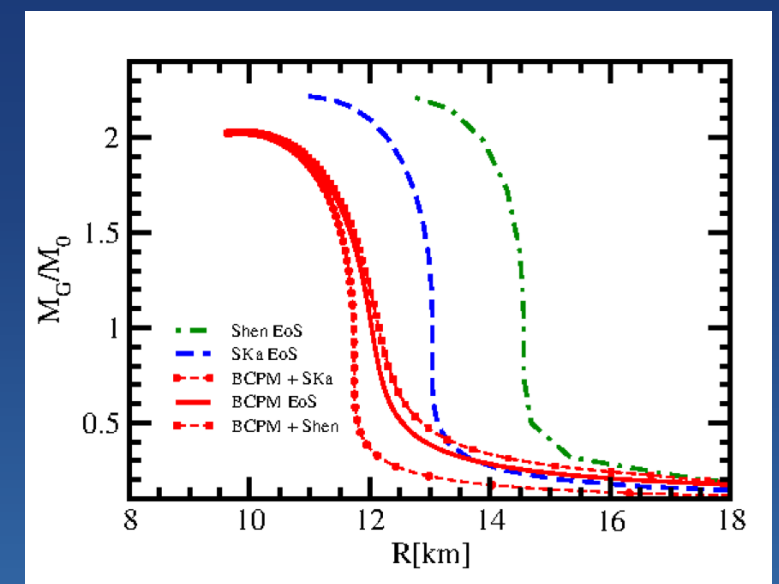
Insert slides about SNA and NSE models

# Towards a unified description from the crust to the core

- ★ Common prescription : treating the core and the crust of the star with different nuclear models. This non-unified treatment of the equation of state leads to errors on on the modeling of mass, radius, and moment of inertia, of a cold neutron star.
- ★ Need to develop a unified theory which is able to describe the overall structure of Neutron Stars, from the outer crust to the inner core.
- ★ There are a few EoS devised to describe the whole NS within a unified theoretical framework.

- ✓ **Lattimer-Swesty** (CLDM, EoS from Skyrme effective force).
- ✓ **Shen** (Thomas-Fermi scheme and RMF model).
- ✓ **Douchin-Haensel** (CLDM, SLy4 force fitted to microscopic neutron matter calculations).
- ✓ **BSk** (ETFSI, Skyrme force fitted to known masses of nuclei and microscopic neutron matter calculations with different stiffness).
- ✓ **BCPM** (Energy Density Functional designed from BHF computations, used in the Thomas-Fermi approximation for the inner crust).

Baldo et al., 1308.2304



Strong effect for the radius of canonical mass star

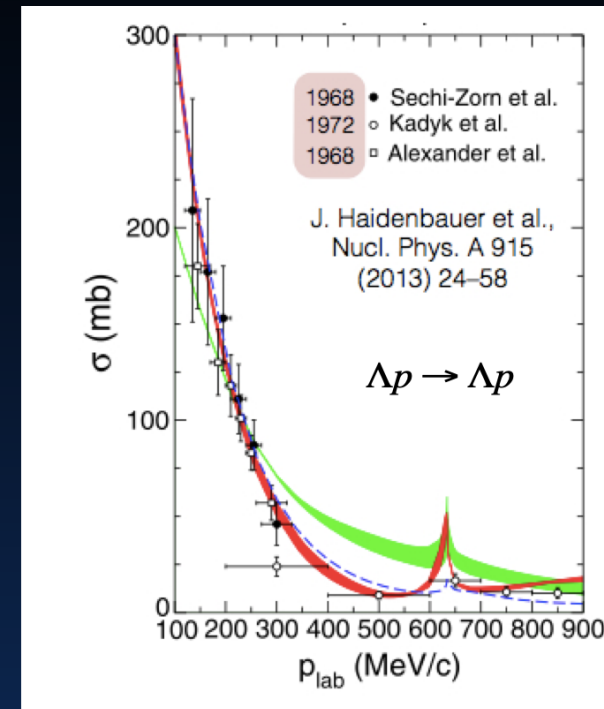
## Hyperons in dense matter

What do we know to include hyperons in the EoS ?  
Unfortunately much less than in the nucleonic sector, in order to put stringent constraints in the NY and YY interaction.

The experimental situation for the  $\Lambda$  hyperon regards single particle energies of hypernuclei from spectroscopy. It shows a binding energy of the  $\Lambda$  in bulk matter is determined to be 30 MeV, so the  $\Lambda$  feels an attractive potential in bulk nuclear matter of

$$U_{\Lambda}(n = n_0) = U_{\Lambda,0} = -30 \text{ MeV}$$

at saturation density  $n_0$ . A refined fit to the single-particle energies reveals that there is a nontrivial density dependence of the  $\Lambda$  potential as a function of the baryon number density.



- Very few YN scattering data due to short lifetime of hyperons & low intensity beam fluxes
  - ~ 35 data points, all from the 1960s
  - 10 new data points, from KEK-PS E251 collaboration (2000)
- No YY scattering data exists

(cf. > 4000 NN data for  $E_{\text{lab}} < 350 \text{ MeV}$ )

For hyperons heavier than the  $\Lambda$  the situation is much less certain.

For  $\Sigma$  hyperons, it is established now that the  $\Sigma$  potential in nuclear matter is strongly repulsive with a likely value of  $U = 30 \pm 20 \text{ MeV}$ .

For the  $\Xi$  hyperons, there are a few old emulsion data suggesting bound  $\Xi$  hypernuclear states, which hint at an attractive potential which in nuclear matter is much less attractive compared to the  $\Lambda$ , likely to be about half of it, that is,  $U \approx -15 \text{ MeV}$ .

Nothing is known experimentally about  $\Omega$  hypernuclei.

# Hyperons in Neutron Stars

Hyperons in NS considered by many authors since the pioneering work of Ambartsumyan & Saakyan (1960)



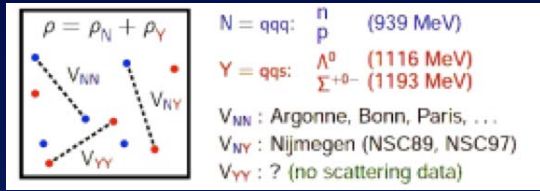
## Phenomenological approaches

- ✧ **Relativistic Mean Field Models:** Glendenning 1985; Knorren et al. 1995; Shaffner-Bielich & Mishustin 1996, Bonano & Sedrakian 2012, ...
- ✧ **Non-relativistic potential model:** Balberg & Gal 1997
- ✧ **Quark-meson coupling model:** Pal et al. 1999, ...
- ✧ **Chiral Effective Lagrangians:** Hanauske et al., 2000
- ✧ **Density dependent hadron field models:** Hofmann, Keil & Lenske 2001

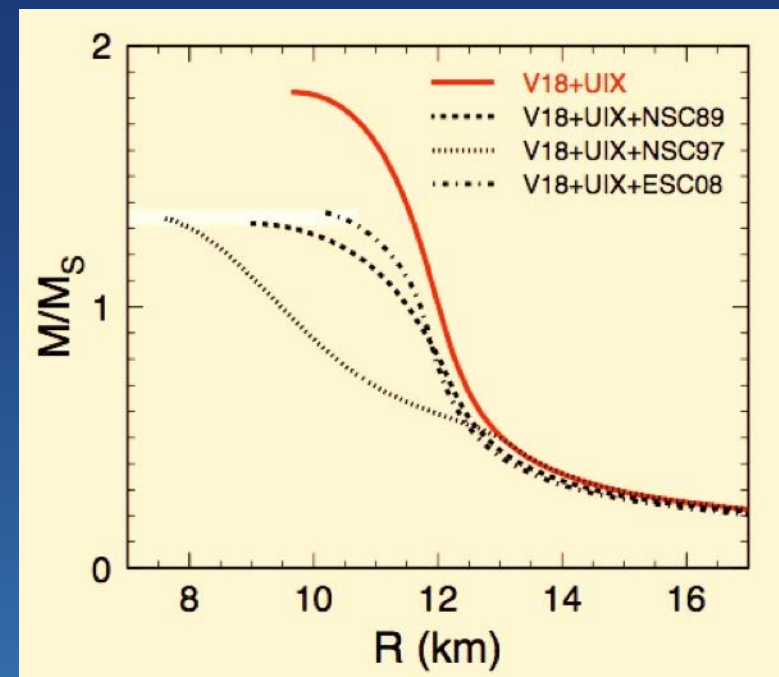
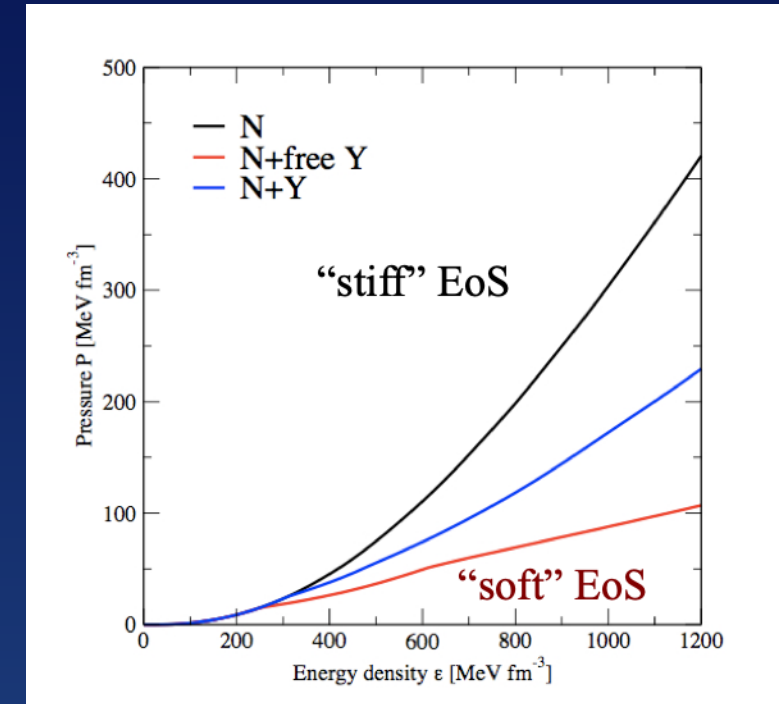
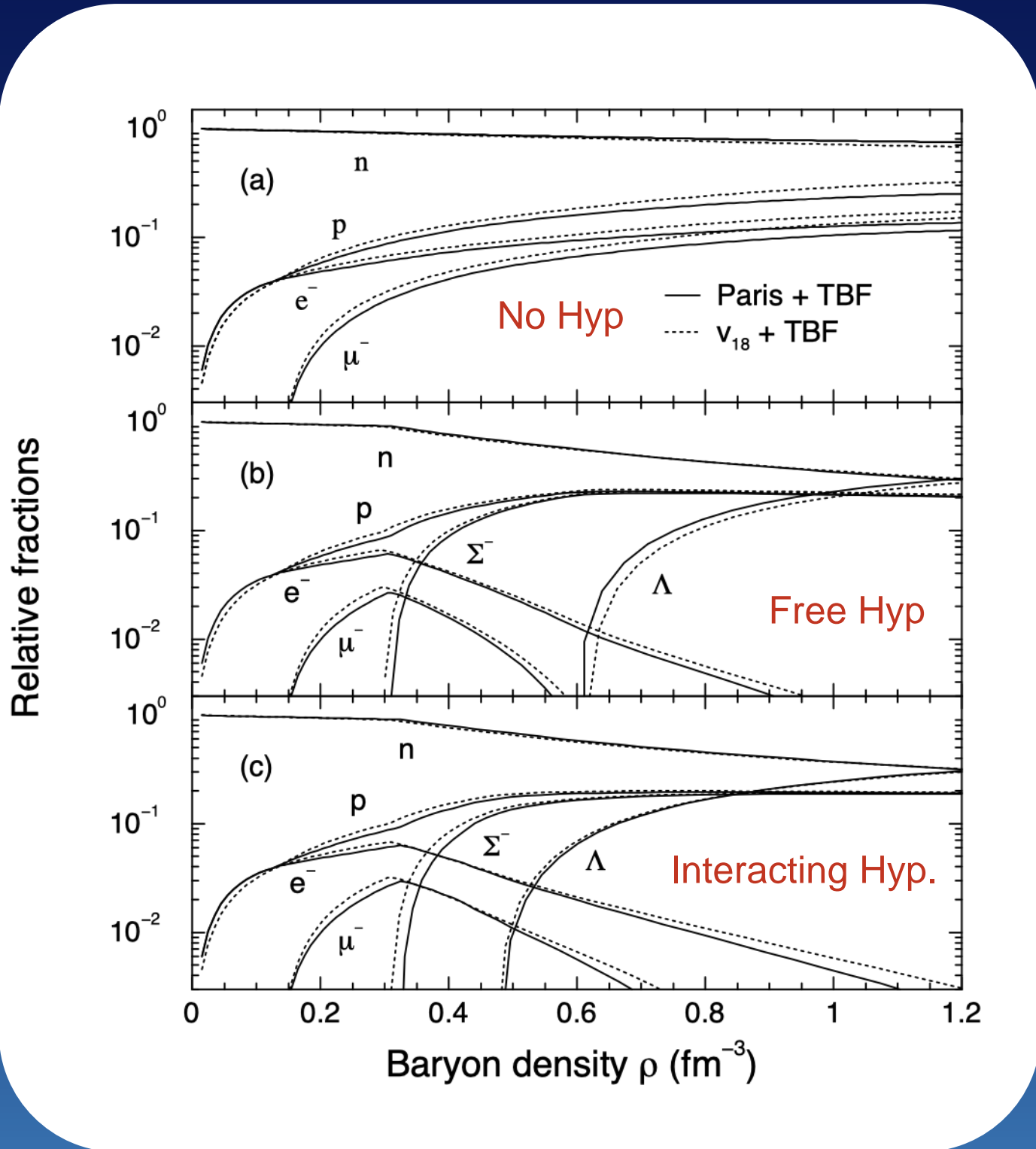


## Microscopic approaches

- ✧ **Brueckner-Hartree-Fock theory:** Baldo et al. 2000; I. V. et al. 2000, Schulze et al. 2006, I.V. et al. 2011, Burgio et al. 2011, Schulze & Rijken 2011
- ✧ **DBHF:** Sammarruca (2009), Katayama & Saito (2014)
- ✧  **$V_{\text{low } k}$ :** Djapo, Schaefer & Wambach, 2010
- ✧ **Quantum Monte Carlo:** Lonardonì et al., (2014)



# Including hyperons in BHF approach : The composition of hypernuclear matter



Maximum mass independent of potentials !  
Maximum mass too low ( $< 1.4 M_{\odot}$ ) !



## Hyperon puzzle

Hyperons  $\longrightarrow$  in microscopic approaches  
a too soft EoS not compatible with measured NS masses.  
CAVEAT : the presence of hyperons in the NS core seems to  
be unavoidable !

Proof for “quark” matter inside neutron stars ?



# Possible solutions

- One excludes hyperons in the nuclear models **by hand**. However, constructing a model of the nuclear interaction by ignoring experimental data from hypernuclei is sweeping the intrinsic failure of the nuclear model under the carpet.
- One pushes up the critical density for the onset of hyperon formation in neutron star matter beyond the maximum density in neutron stars. There is an additional repulsion between hyperons at high densities so that the fraction of hyperons is suppressed. However, this repulsion has to compensate the weaker repulsion between nucleons and hyperons.

The hyperon puzzle is a real puzzle.

At present, there is no accepted solution to the problem. One solution, however, is a particular striking one: Hyperons appear but before they can destabilize the neutron star a new phase appears at high density with a stiff EOS supporting a  $2M_{\odot}$  compact star. That new phase would be not based on hadronic degrees of freedom, nucleons, and hyperons, but on a new degree of freedom in the form of the constituents of hadrons, that is, quarks, forming a quark matter core.

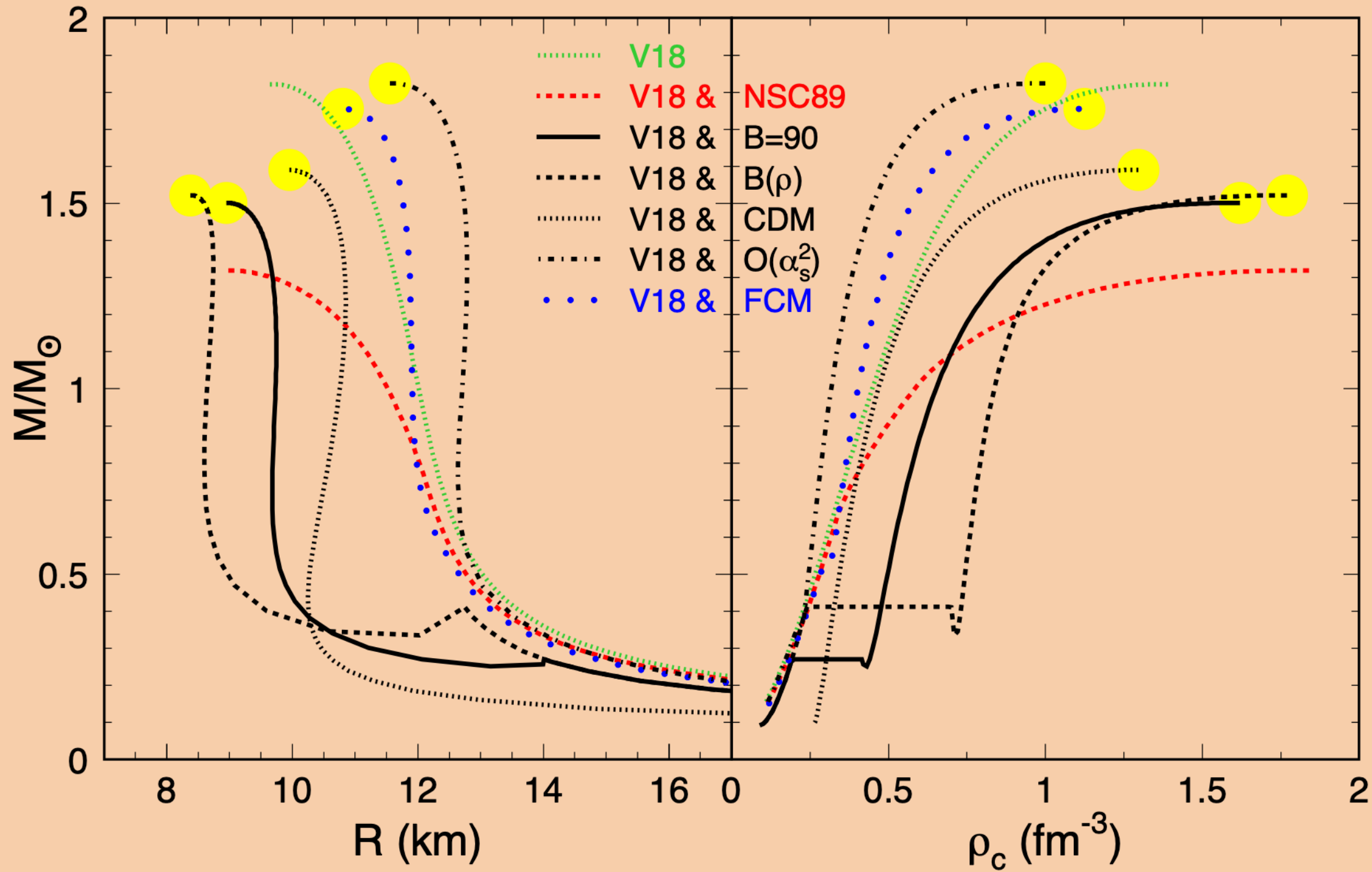
# Quark Matter EOS of Dense Matter:

- Problem: No “exact” results from QCD:  
Large theoretical uncertainties, limited predictive power
- Current strategy:  
Use available eff. quark models (MIT, NJL, CDM, DSM, ...) in combination with the hadronic EOS
- An important constraint (from heavy ion collisions):  
In symmetric matter phase transition not below  $\approx 3\rho_0$
- ↪ E.g., the simplest (MIT) quark model requires a density-dependent bag “constant”:

$$\epsilon_Q = B + \epsilon_{\text{kin}} + \alpha_s \times \dots$$

$$B(\rho) = B_\infty + (B_0 - B_\infty) \exp\left[-\beta\left(\rho/\rho_0\right)^2\right]$$

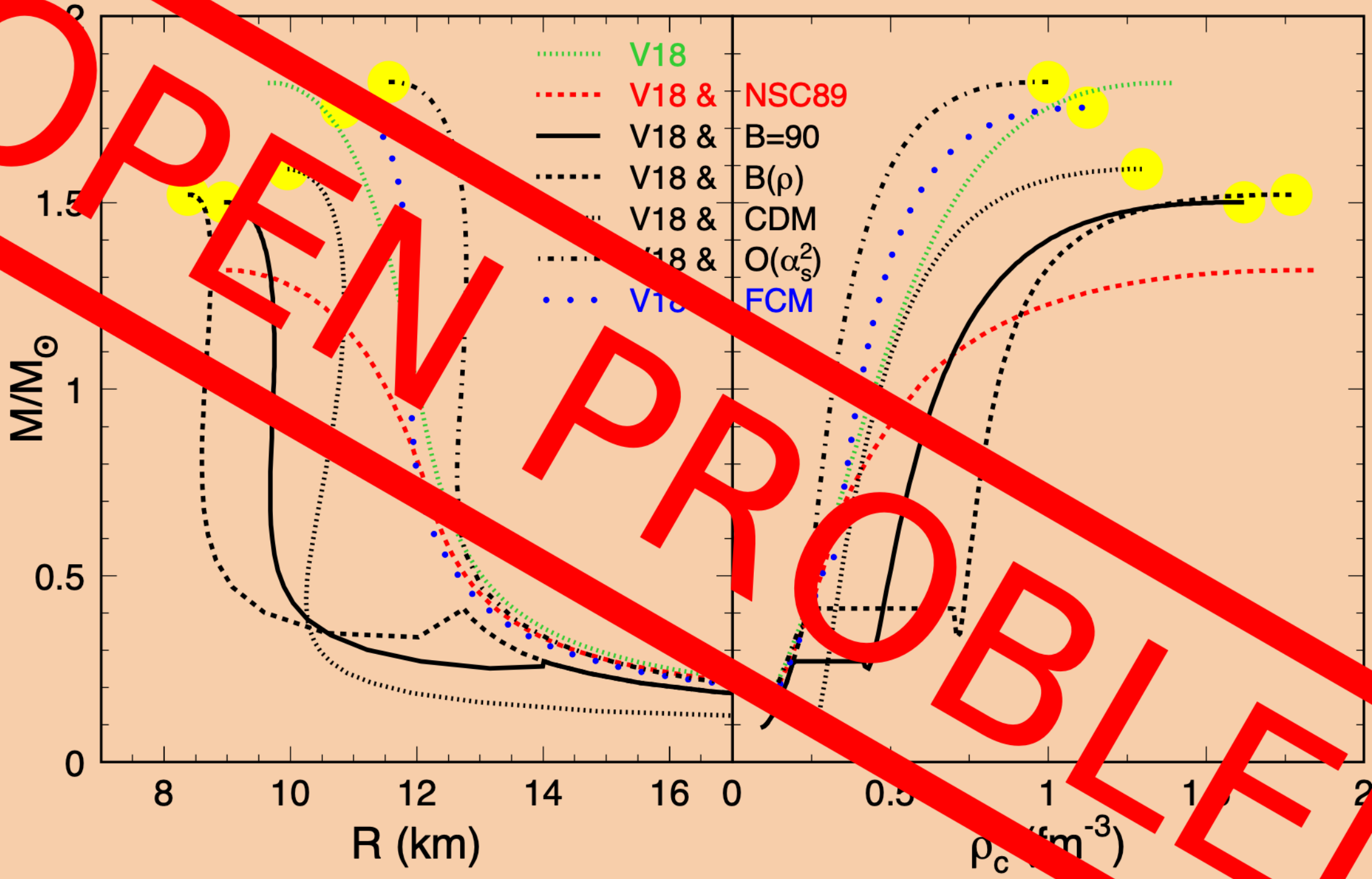
● Different quark EOS's: bag models, color dielectric model:



NJL, FCM, Dyson-Schwinger models: hyperons prevent phase transition

➡ Maximum masses:  $1.5 \dots 1.9 M_{\odot}$ , Radii are different !

Different quark EOS's: bag models, color dielectric model:



NJL, FCM, Dyson-Schwinger models: hyperons prevent phase transition

↪ Maximum masses:  $1.5 \dots 1.9 M_{\odot}$ , Radii are different !

## “Recipe” for neutron star structure calculations

Brueckner results :

$$\epsilon(\rho_i); i = n, p, e, \mu, \Lambda, \Sigma, u, d, s, \dots$$

Chemical potentials :

$$\mu_i = \frac{\partial \epsilon}{\partial \rho_i}$$

Beta-equilibrium :

$$\mu_i = b_i \mu_n - q_i \mu_e$$

$$\sum_i x_i q_i = 0$$

Charge neutrality :

Composition :  
Equation of State :

$$x_i(\rho)$$

$$p(\rho) = \rho^2 \frac{d(\epsilon/\rho)}{d\rho}(\rho, x_i(\rho))$$

TOV equations :

$$\frac{dP}{dr} = -\frac{Gm}{r^2} \frac{(\epsilon + P)(1 + 4\pi r^3 P/m)}{1 - \frac{2Gm}{r}}$$

$$\frac{dm}{dr} = 4\pi r^2 \epsilon(r)$$

Structure of the star :  $\rho(r)$ ,  $M(R)$  etc.

$$\begin{aligned} \mu_e &= \mu_\mu = \mu_n - \mu_p \\ \mu_{\Sigma^-} &= 2\mu_n - \mu_p \\ \mu_{\Sigma^0} &= \mu_\Lambda = \mu_n \\ \mu_{\Sigma^+} &= \mu_p \end{aligned}$$

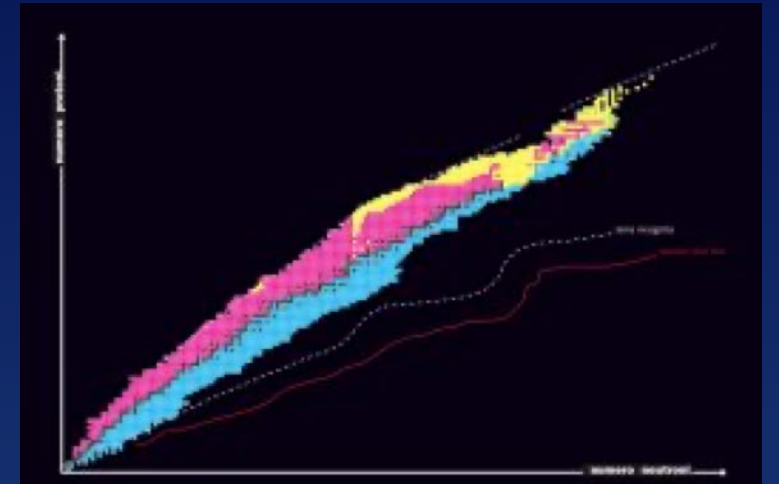


Vela pulsar

# Data ?

# The EoS : where do we stand ?

- Structure properties known for about 3400 nuclides
- Binding energy in the Liquid Drop Model
- Extrapolating the mass formula for  $A \rightarrow \infty$  in the symmetric case, the binding energy close to saturation is usually expanded as



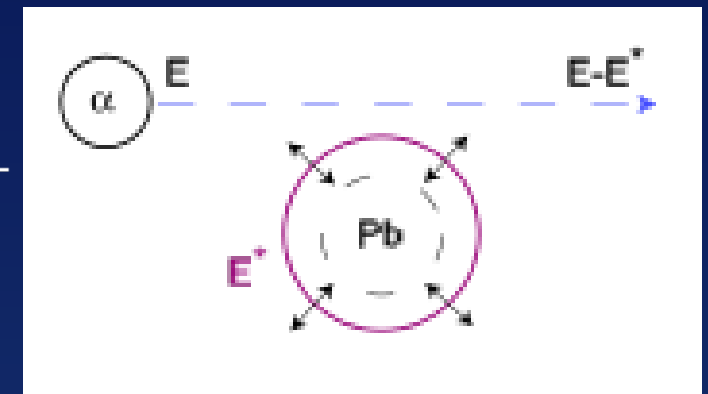
$$\frac{E}{A}(\rho, \beta) = E_0 + \frac{1}{18}K_0\epsilon^2 + \left[ S_0 - \frac{1}{3}L\epsilon + \frac{1}{8}K_{sym}\epsilon^2 \right] \beta^2$$
$$\beta = \frac{\rho_n - \rho_p}{\rho}, \quad \epsilon = \frac{\rho - \rho_0}{\rho_0}$$

# Nuclear Incompressibility for symmetric matter $K$

$$K = 9\rho_0^2 \frac{d^2}{d\rho^2} \left( \frac{E}{A} \right)_{\rho=\rho_0} = R^2 \frac{d^2}{dR^2} \left( \frac{E}{A} \right)_{\rho=\rho_0}$$

In radial oscillations induced by  $\alpha$ -particles scattering :

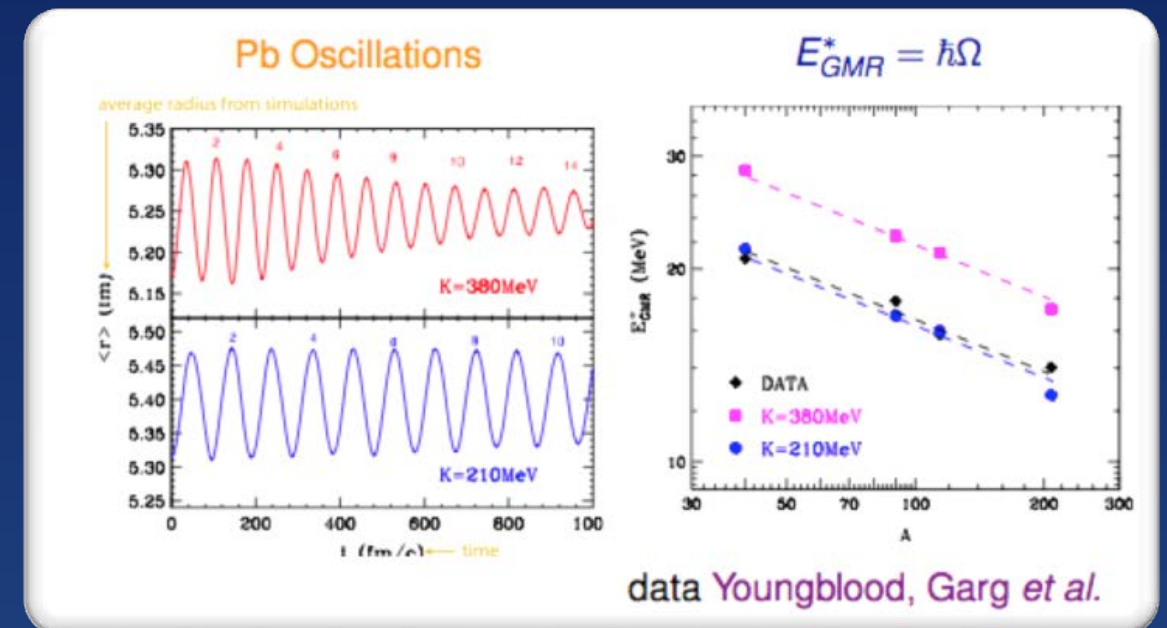
$$E^* = \hbar \sqrt{\frac{K}{m_N \langle r^2 \rangle_A}}$$



$$K = 240 \pm 10 \text{ MeV} \quad (\text{Colo}', 2004)$$

$$= 248 \pm 8 \text{ MeV} \quad (\text{Piekarewicz}, 2004)$$

A soft EoS is favourite close to saturation density

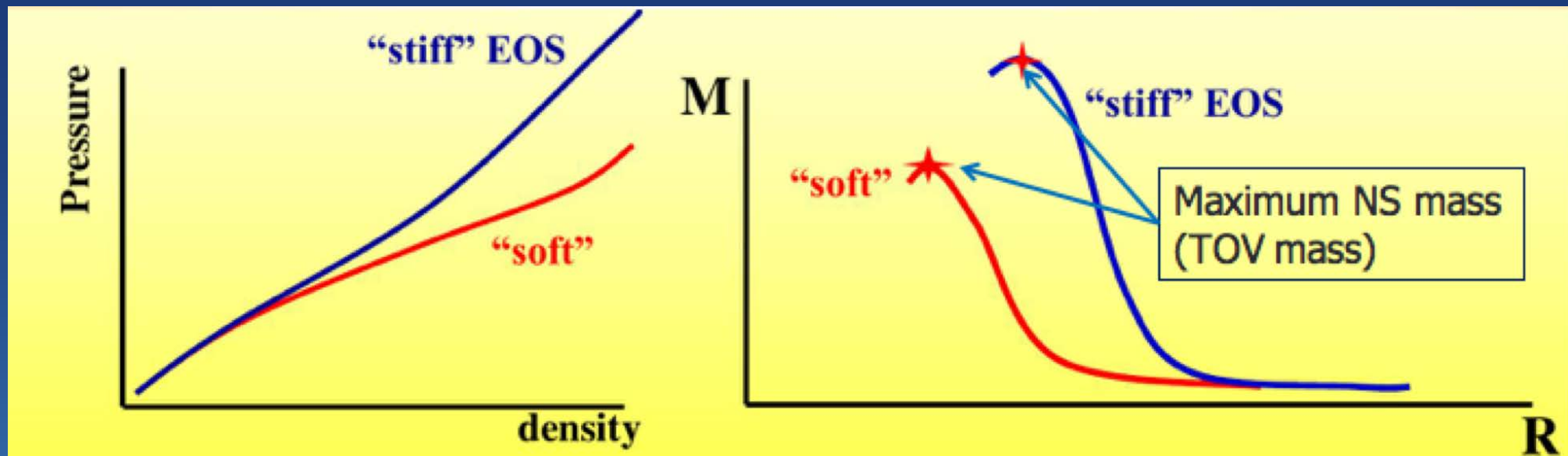




Soft or Stiff ?

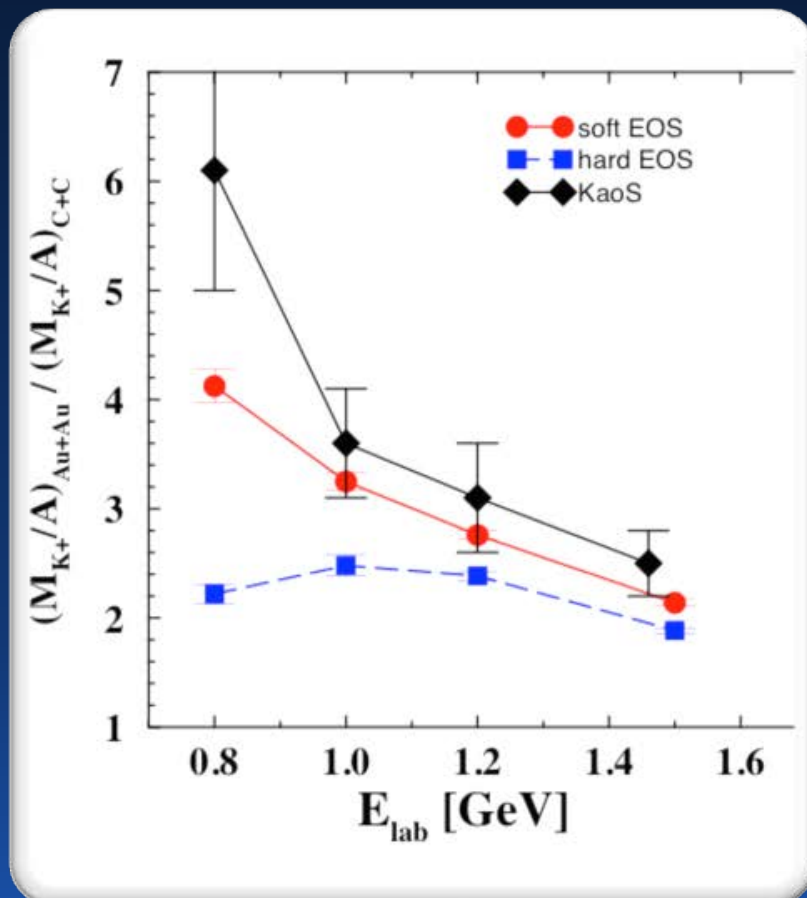


Given an EoS, compute the sequence of equilibrium models :  
The Mass-Radius relation



# Kaon production in heavy ion collisions

ral part of the participant zone. near threshold strange particles are produced in the high-density region and interact weakly with matter, because of strange



- K-N interaction is not well known  $NN \rightarrow N\Delta \rightarrow N\Lambda K^+$
- $K^+$  produced by :
- Simulations must include nucleon excitations and must be relativistic.
- Production rate dependent on the maximal density -----> compressibility.

Experimental data by the KaoS and FOPi Collaborations :

Double ratio : multiplicity per mass number for C+C collisions and Au+Au collisions at 0.8 AGeV and 1.0 AGeV .

Largest density explored :  $\rho \approx 2-3 \rho_0$

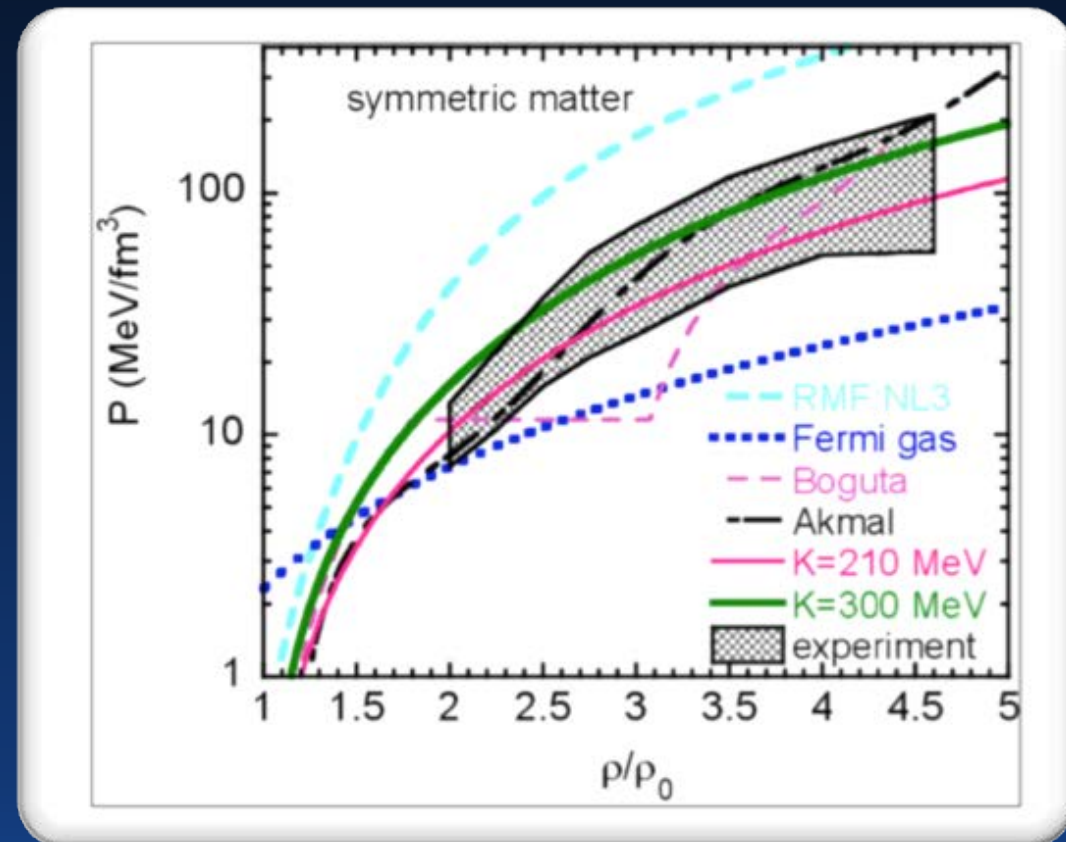
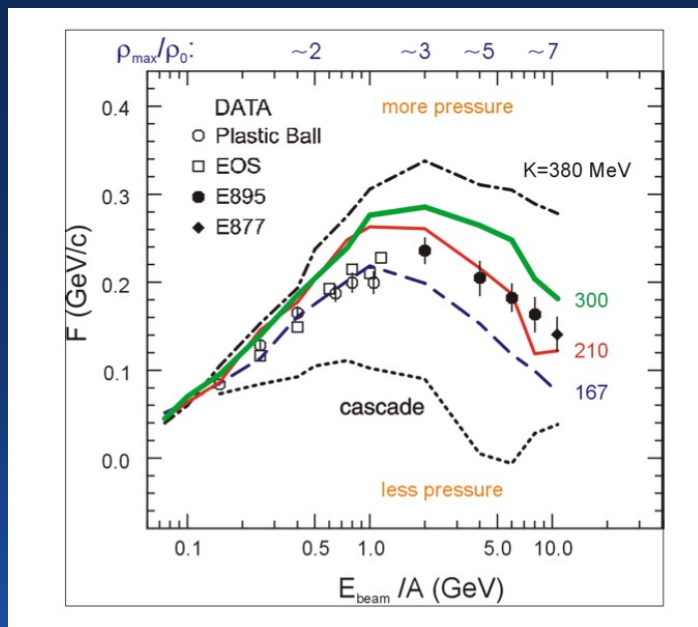
Only calculations with a compression  $180 \leq KN \leq 250$  MeV can describe the data (Fuchs, 2001)

The nuclear equation of state up to  $2-3\rho_0$  is SOFT!

# Determination of the Equation of State of Dense Matter

P. Danielewicz, R. Lacey and W. Lynch  
 Science 298, 1592 (2002)

- Transverse flow measurements in Au + Au collisions at  $E/A=0.5$  to  $10$  GeV
- Pressure determined from simulations based on the Boltzmann-Uehling Uhlenbeck transport theory



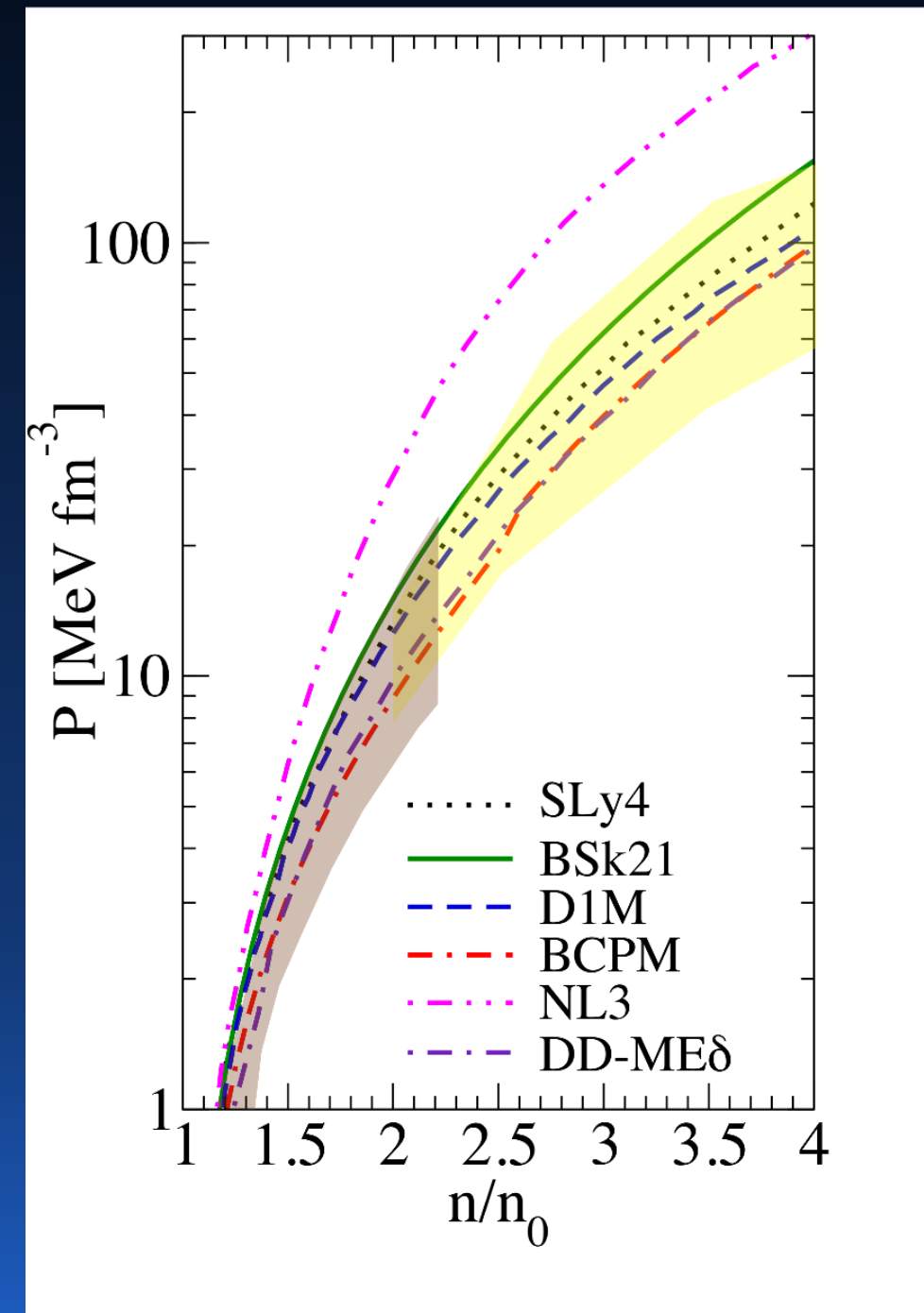
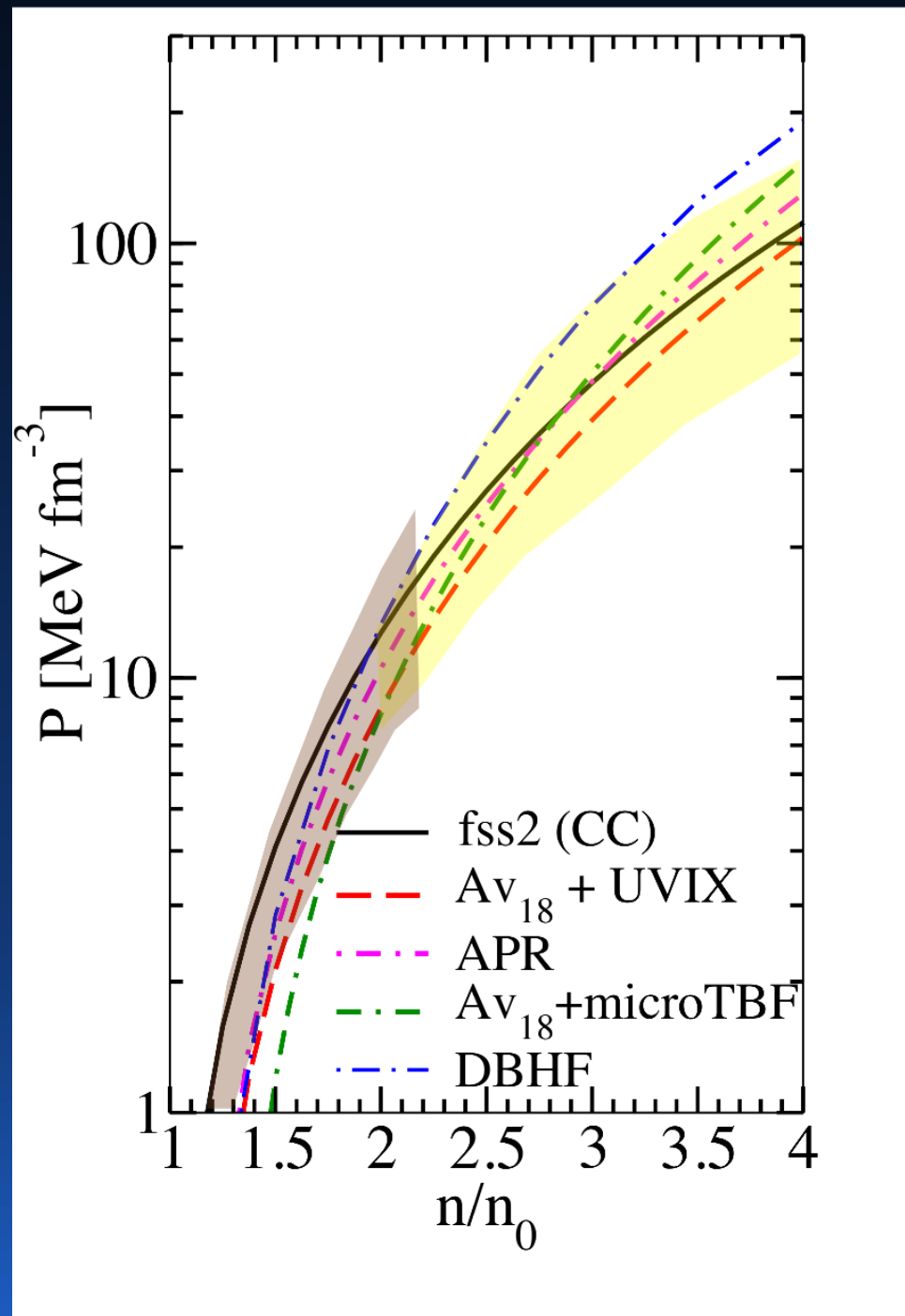
Flow data exclude very repulsive equations of state, but confirm very soft EoS at  $\rho < 3\rho_0$

# Flow data : do the EoS fit the data ? YES !

Microscopic

vs.

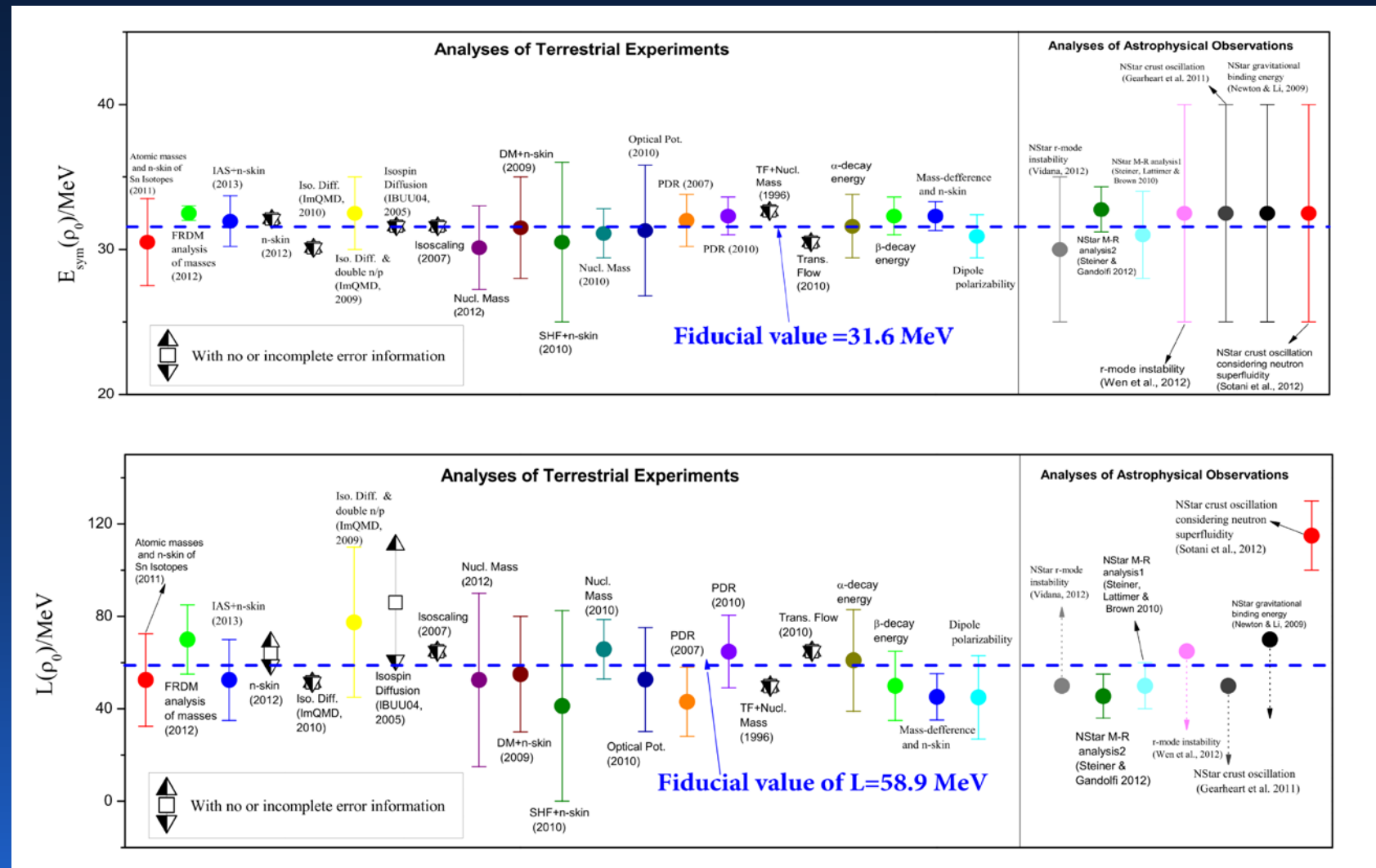
Phenomenological



# The Symmetry Energy $S(\rho)$ and the slope parameter $L$

- ✓ Composition of neutron star matter
- ✓ Expected neutrino signal from the PNS.
- ✓ Neutrino processes responsible of cooling.
- ✓ Core-crust transition density => important for pulsar glitches.

$$S(\rho) = \frac{E(\rho)}{A} \Big|_{PNM} - \frac{E(\rho)}{A} \Big|_{SNM}$$



## A few experimental data at density above saturation

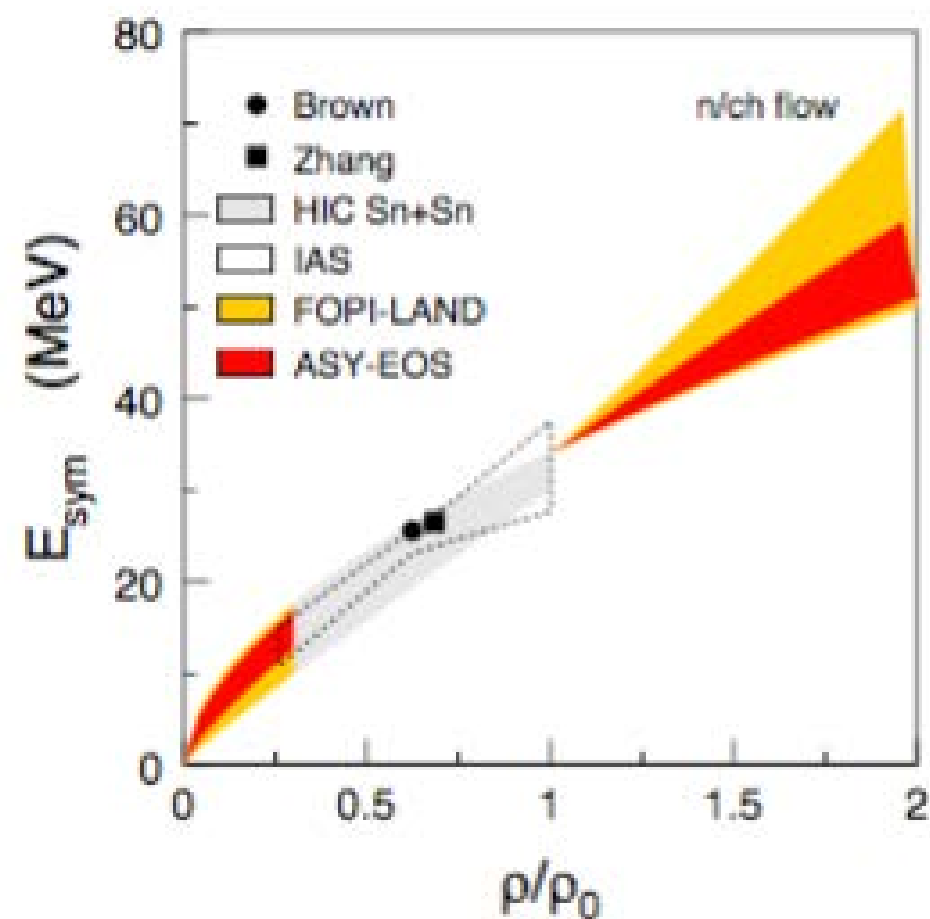


**Figure 1:** (Color online) Constraints deduced for the density dependence of the symmetry energy from the ASY-EOS data [28] in comparison with the FOPI-LAND result of Ref. [18] as a function of the reduced density  $\rho/\rho_0$ . The low-density results of Refs. [7, 8, 9, 10] as reported in Ref. [11] are given by the symbols, the grey area (HIC), and the dashed contour (IAS). For clarity, the FOPI-LAND and ASY-EOS results are not displayed in the interval  $0.3 < \rho/\rho_0 < 1.0$  (from Ref. [28]; Copyright (2016) by the American Physical Society).

# Check wrt nuclear physics constraints

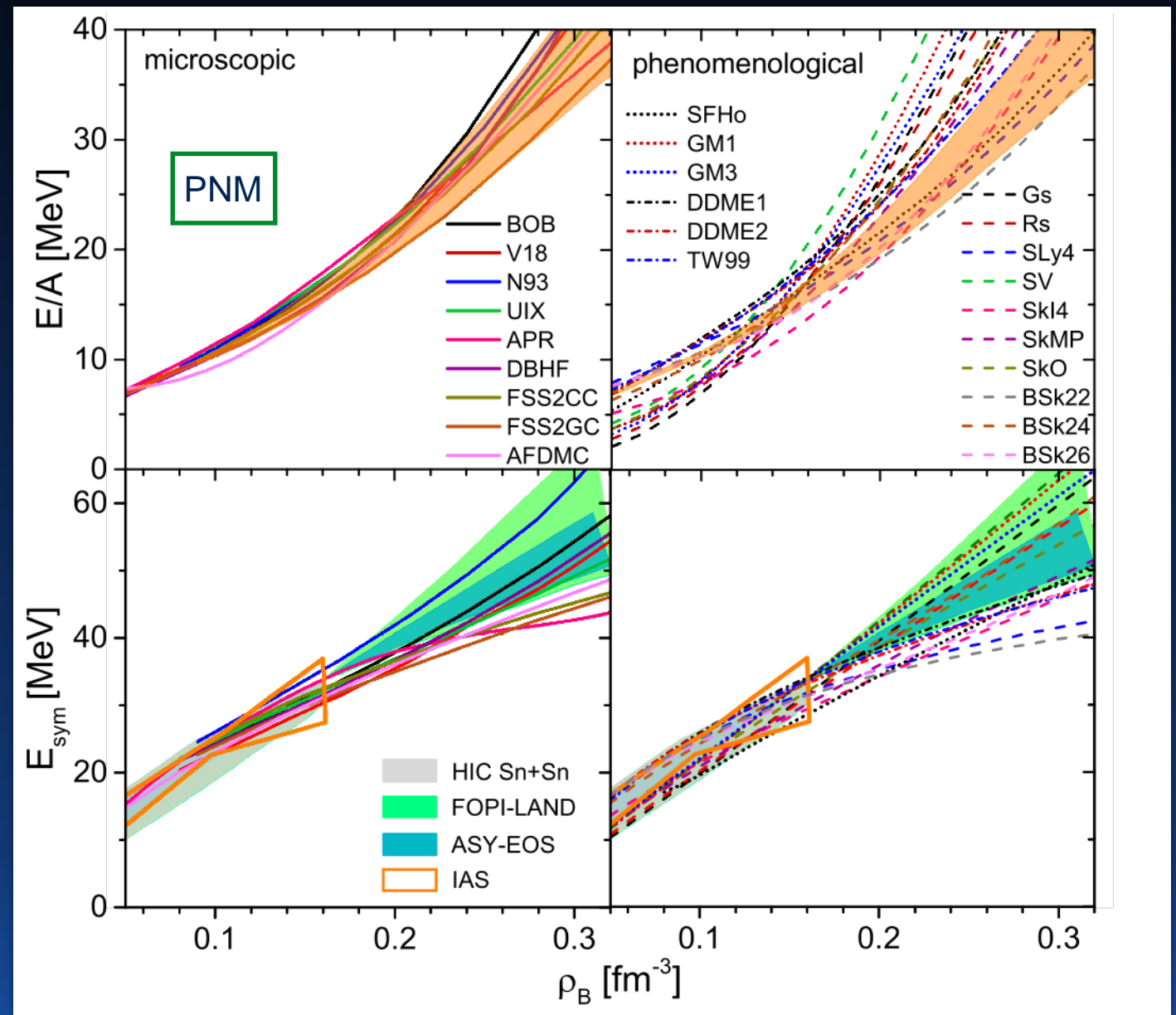
Orange : predictions from the  $\chi$ EFT up to N3LO order  
C. Drischler et al., PRL 125, (2020) 202702

## Microscopic EoS

- BHF with Argonne V18 or Nijmegen 93 2NF and microscopic 3NF (BOB, V18, N93, UIX)
- BHF with FSS2 NN interaction (quark d.o.f. explicitly taken into account)
- Variational APR with Argonne V18 and 3NF of Urbana UIX type
- Relativistic DBHF (Bonn A)
- AFDMC with modified V18

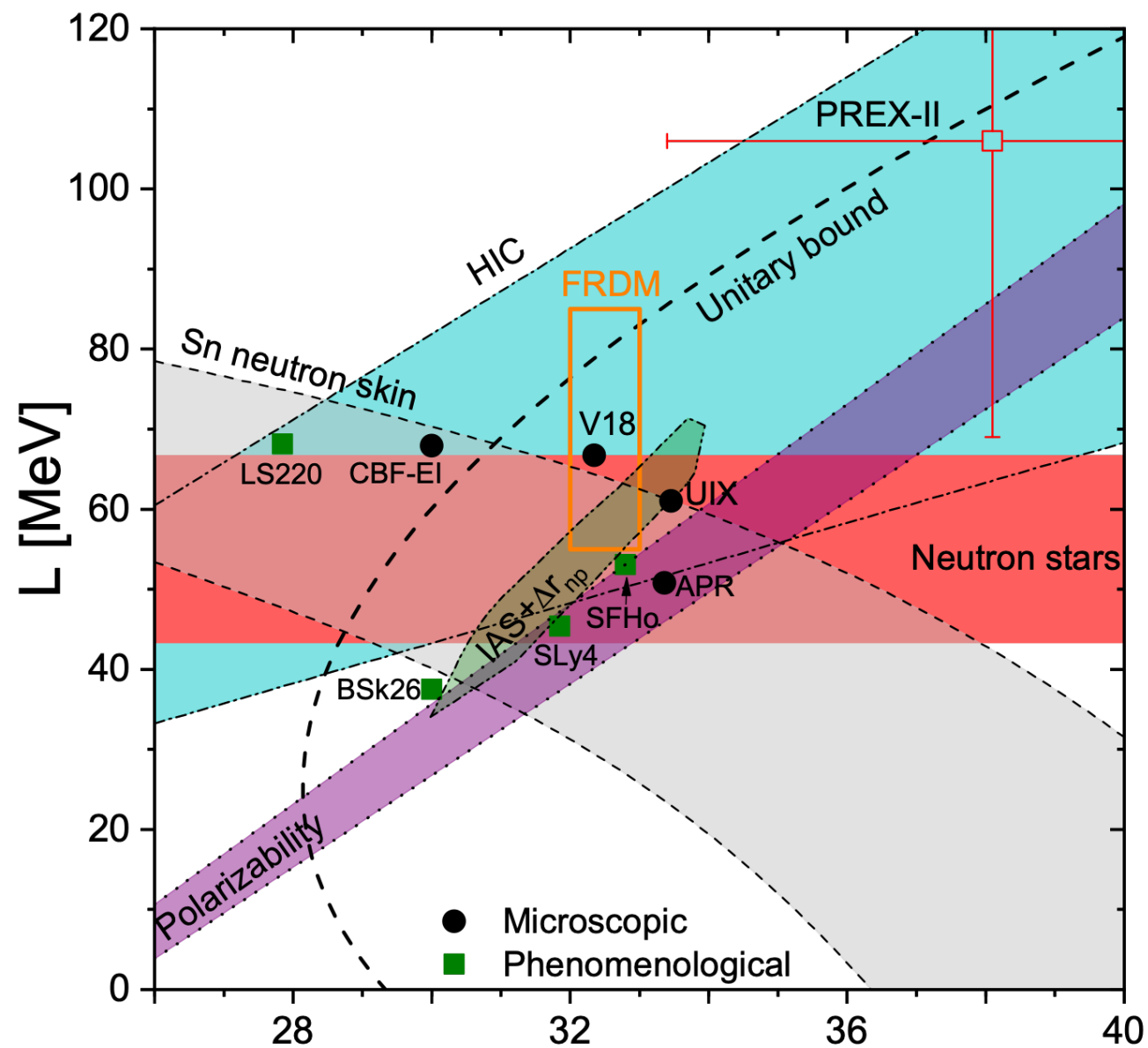
## Phenomenological EoS

- Skyrme forces (Gs, Rs, SLy4, SV etc...)
- Brussels-Montreal group BSk22,24,26
- NLWM (SFHo, GM1,3), RMF models with different parameterizations.
- DDM, RMF model with density dependent coupling constants.



PNM and Symmetry energy behave better for the microscopic approaches.

$$L \equiv 3\rho_0 \frac{dE_{\text{sym}}}{d\rho}(\rho_0)$$



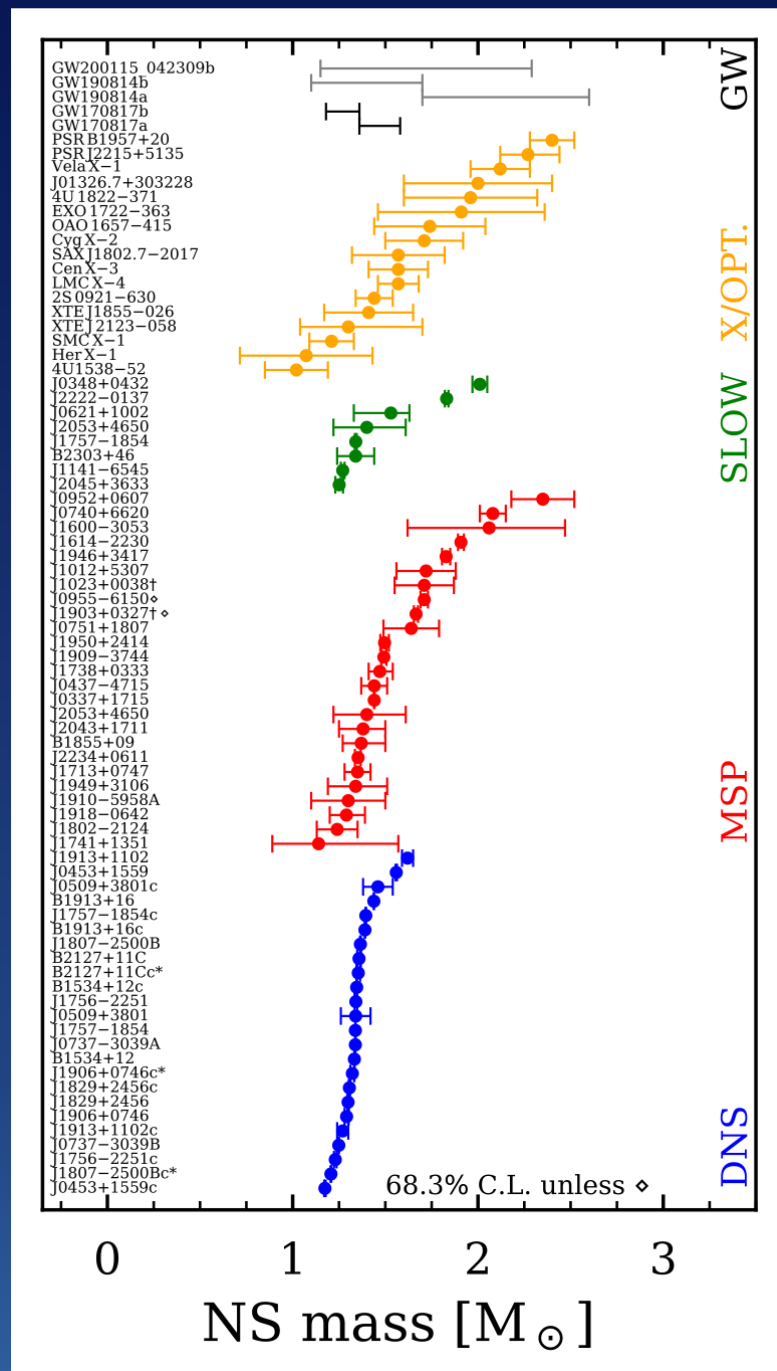
**L parameter** does not exclude any of the microscopic EoS, but several phenomenological models predict too large values.

- HIC : heavy ion collisions. Isospin diffusion
- Sn neutron skin : Sn isotopes neutron thickness
- Polarizability : giant dipole resonance
- FRDM : Finite Range Droplet Model. Masses fit.
- IAS + ... : binding energies of Isobaric nuclei
- Neutron stars : analysis of M-R measurement

No overlap region !  
Too many uncertainties in the experimental measurements and in the models used for the data interpretation.

No theoretical model can be ruled out a priori.

# Observational facts : the Mass



Lami Suleiman,  
PhD thesis, OBSPM-CAMK,  
2022

Observation of  $\sim 2 M_{\odot}$  neutron stars



Dense matter EoS stiff enough is required such that

$$M_{\max} [EoS] > 2M_{\odot}$$

A natural question arises:

Can hyperons, or strangeness in general, still be present in the interior of neutron stars in view of this constraint ?

# Observational facts : the Radius

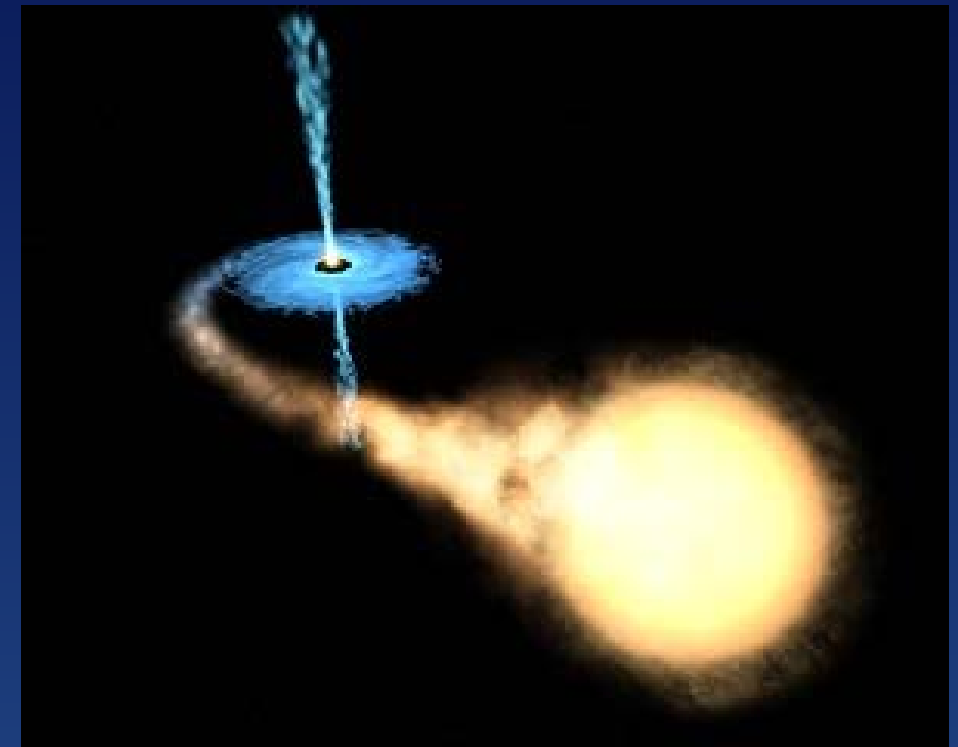
NS radii are very difficult to measure because

- ❖ NS are very small objects
- ❖ are very far away from us, the closest NS being at about 400 light-years from the Earth.

*A possible to measure it is through the thermal emission of low-mass X-ray binaries.*

The observed X-ray flux  $F$  and estimated surface temperature  $T$ , together with the distance  $D$  and  $M$  the mass of the NS, can be used to obtain the radius of the NS through the relation

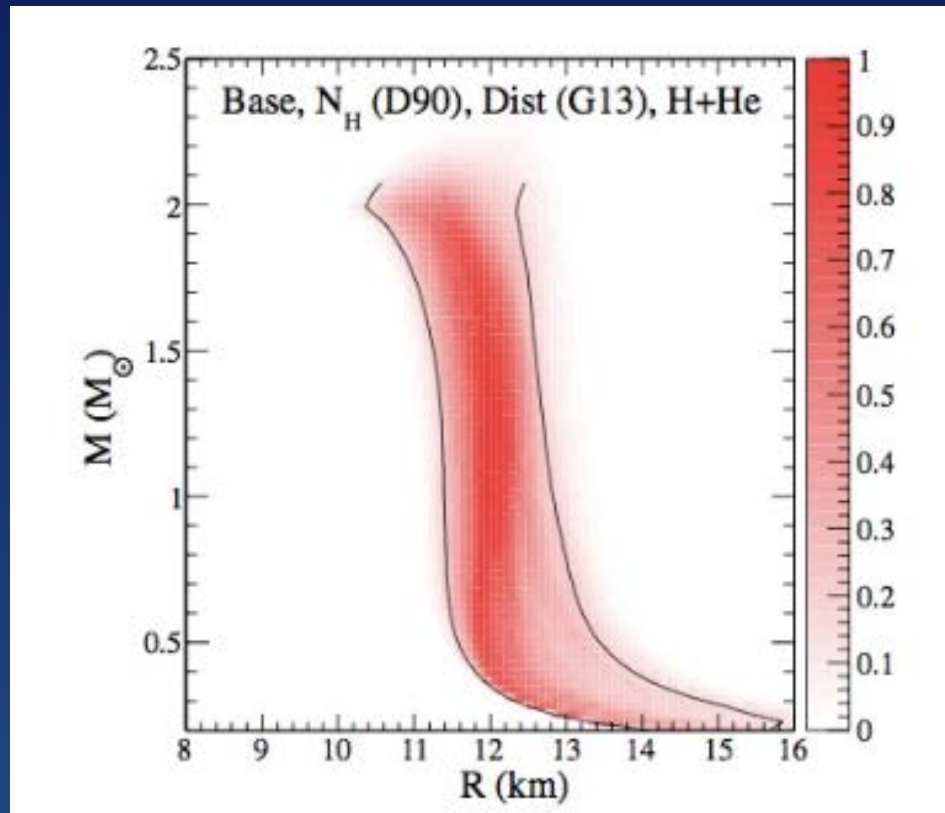
$$R_{\infty} = \sqrt{\frac{FD^2}{\sigma T^4}} \rightarrow R_{NS} = \frac{R_{\infty}}{1+z} = R_{\infty} \sqrt{1 - \frac{2GM}{Rc^2}}$$



The major uncertainties come from the determination of the temperature, which requires the assumption of an atmospheric model, and the estimation of the distance of the star.

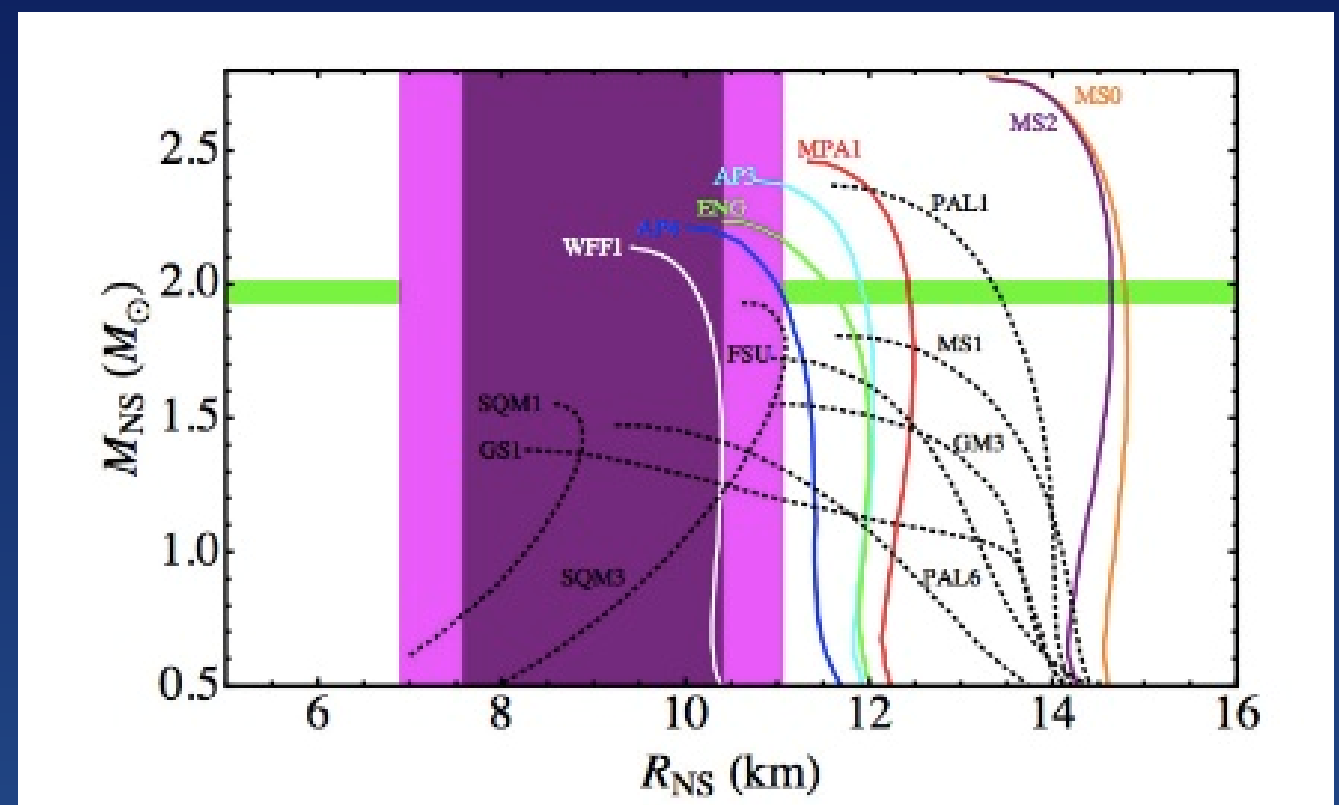
# Past estimations of the radius

Analysis of the thermal spectrum of 5 quiescent LMXB :  
different conclusions !



Steiner et al., (2013, 2014)

$$R = 12.0 \pm 1.4 \text{ km}$$



Guillot et al., (2013,2014)

$$R = 9.1^{+1.3}_{-1.5} \text{ km} \quad (2013)$$

$$R = 9.4 \pm 1.2 \text{ km} \quad (2014)$$

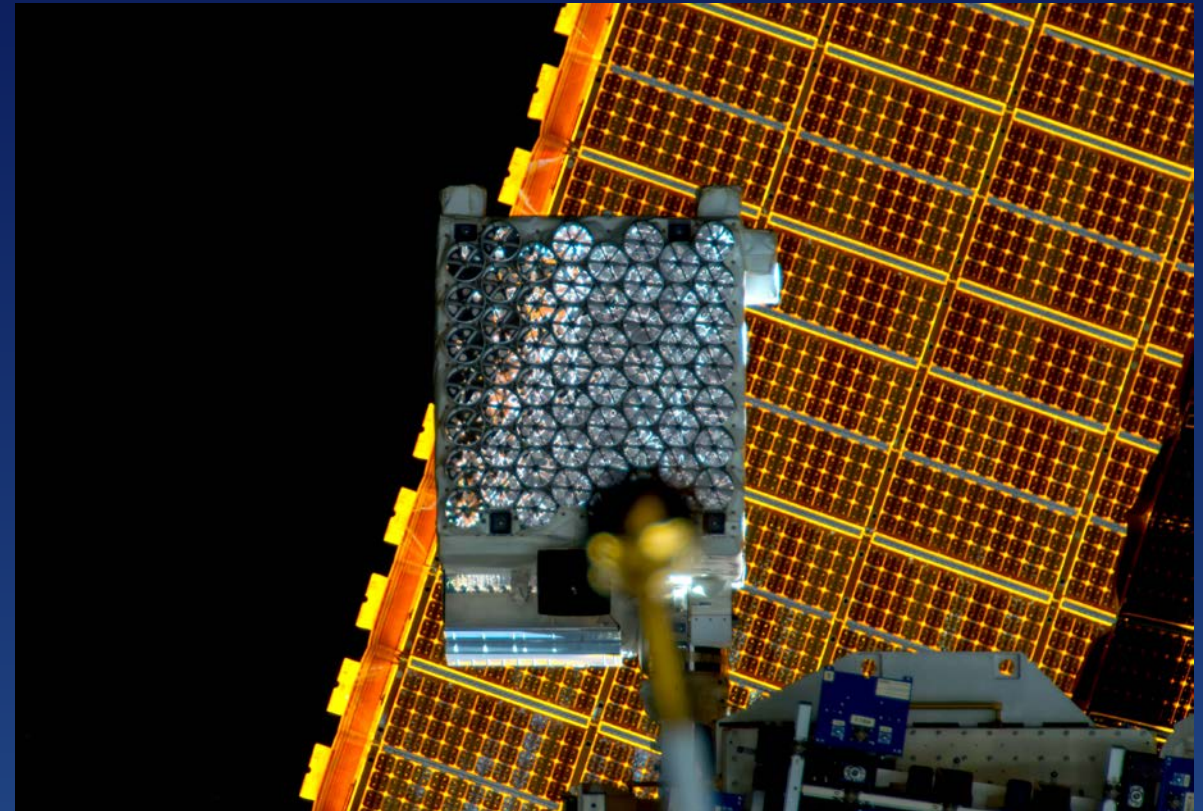
# NICER

## Neutron Star Interior Composition Explorer

<https://heasarc.gsfc.nasa.gov/docs/nicer>

The simultaneous measurement of both mass and radius of the same NS would provide the most definite observational constraint on the nuclear composition.

NICER : a new technique to measure **M & R** from rapidly spinning compact stars with a hot spot, based on Doppler effect (R) and GR corrections of the signal (M/R)



Inferred values for

PSR J0030+0451

$$M/R = 0.156^{+0.008}_{-0.010}$$

$$R = 13.02^{+1.24}_{-1.06} \text{ km}$$

$$R = 12.71^{+1.14}_{-1.19} \text{ km}$$

PSR J0740+6620

$$M = 2.072^{+0.067}_{-0.066} M_{\odot}$$

$$R = 13.7^{+2.6}_{-1.5} \text{ km}$$

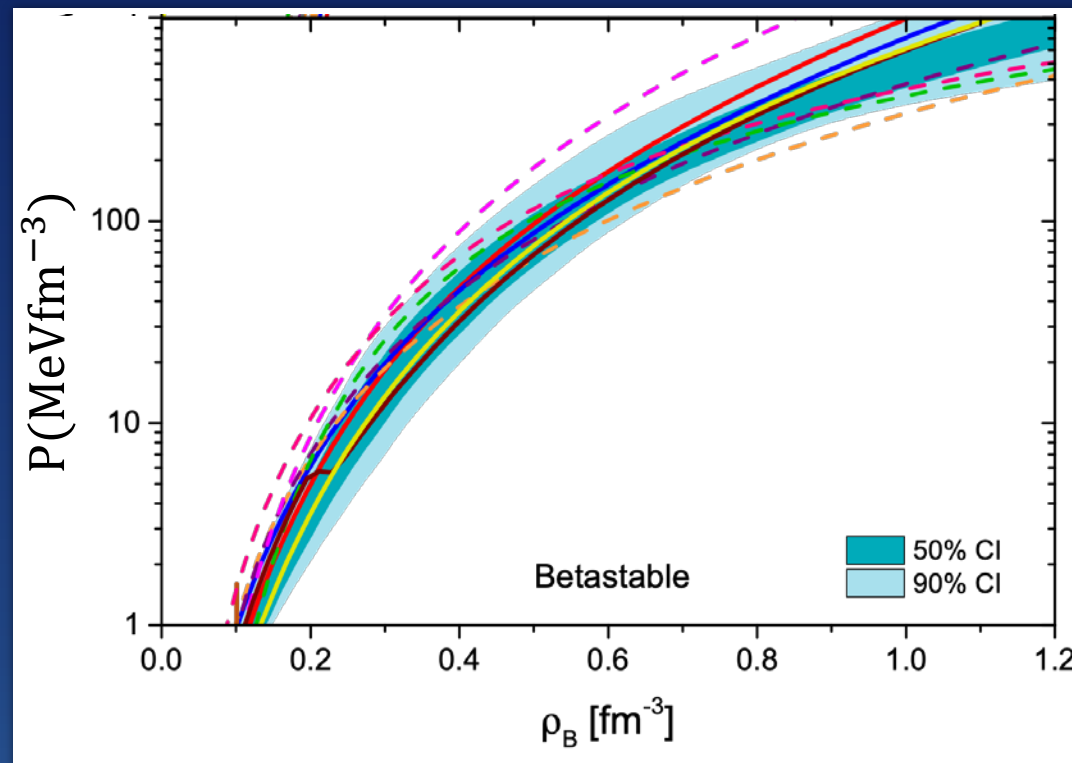
$$R = 12.39^{+1.30}_{-0.98} \text{ km}$$

Miller, Riley, 2019, 2021

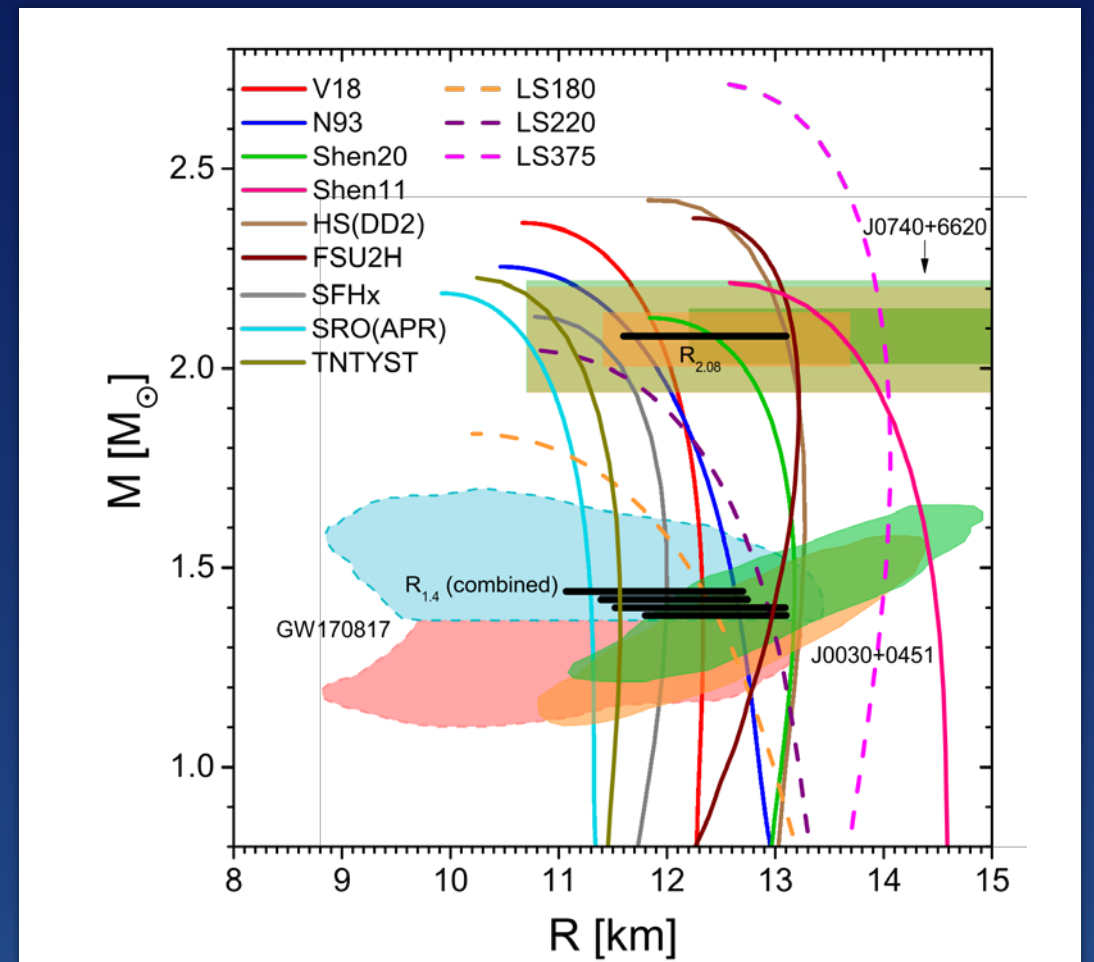
# Composition : beta-stable and charge neutral matter with nucleons and leptons

GW170817 → Abbott et al., PRL119 (2017) 161101

For a given density value, the value of the pressure has a 50% chance to lie within the darker blue area and a 90% chance to lie within the lighter blue band.



Most of the EoS are compatible with the data, except LS180 and LS375.



Mass-radius relations obtained with different EOSs. The mass of the most heavy pulsar PSR J0740+6620 observed until now is also shown, together with the constraints from the GW170817 event and the mass-radius constraints on the pulsars J0030+0451 and J0740+6620 of the NICER mission. The black bars indicate the limits on  $R_{2.08}$  and  $R_{1.4}$  obtained in combined data analyses.

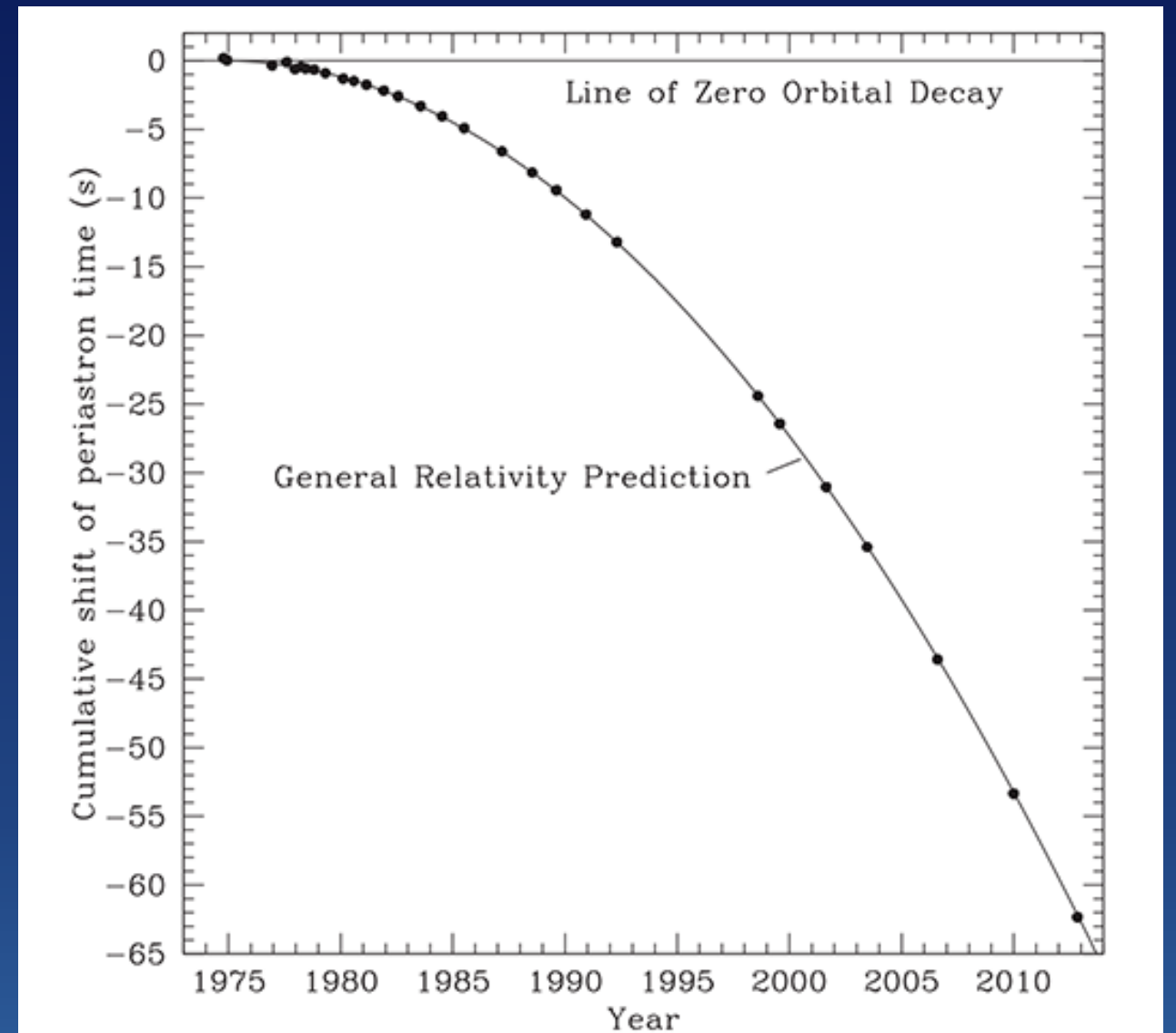
GW : a new way of  
observing NS

# Gravitational waves : indirect detection

Gravitational waves : ripples in space-time, a solution of the Einstein equations in vacuum in linearized theory. Among the first predictions of general relativity made by Einstein himself in 1916.

Keplerian orbits are stable, orbits in general relativity are not. Binary systems spiraling around each other emit gravitational waves, thereby losing energy. The loss of energy leads to a decrease of the orbital period, the binary stars are getting closer in time, eventually merging with each other.

The orbital decay for binary pulsars confirmed by observing the Hulse–Taylor pulsar for several decades. The ratio of the observed value to the predicted one is  $0.9983 \pm 0.0016$ .

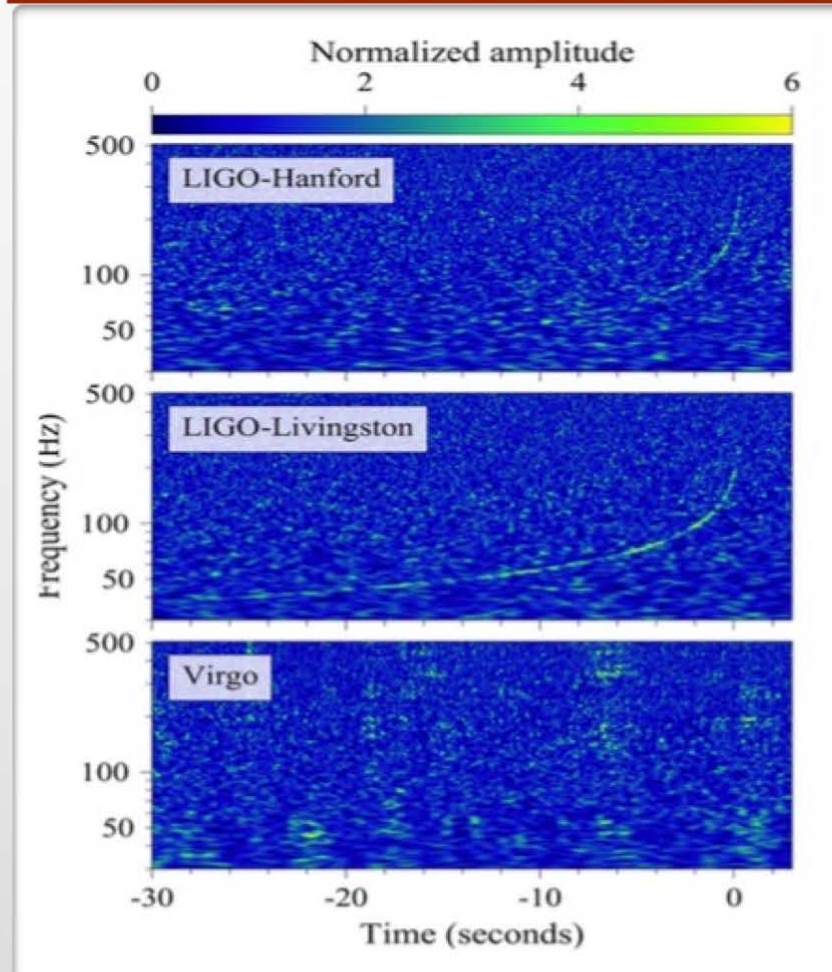


Change of the orbital period from 1974 until 2016. The prediction of general relativity shown by a solid line goes right through the data points.

# Gravitational waves : direct detection

## The dawn of multi-messenger astronomy

On August 17, 2017, the LIGO-VIRGO detector network observed a gravitational-wave signal from the inspiral of two low-mass compact objects consistent with a binary neutron star (BNS) merger.



PRL 119, 161101 (2017) Selected for a Viewpoint in *Physics* week ending 20 OCTOBER 2017  
PHYSICAL REVIEW LETTERS

**GW170817: Observation of Gravitational Waves from a Binary Neutron Star Inspiral**  
B. P. Abbott *et al.*<sup>\*</sup>  
(LIGO Scientific Collaboration and Virgo Collaboration)  
(Received 26 September 2017; revised manuscript received 2 October 2017; published 16 October 2017)

On August 17, 2017 at 12:41:04 UTC the Advanced LIGO and Advanced Virgo gravitational-wave detectors made their first observation of a binary neutron star inspiral. The signal, GW170817, was detected with a combined signal-to-noise ratio of 32.4 and a false-alarm-rate estimate of less than one per  $8.0 \times 10^5$  years. We infer the component masses of the binary to be between  $0.86$  and  $2.26 M_{\odot}$ , in agreement with masses of known neutron stars. Restricting the component spins to the range inferred in binary neutron stars, we find the component masses to be in the range  $1.17$ – $1.60 M_{\odot}$ , with the total mass of the system  $2.74^{+0.04}_{-0.01} M_{\odot}$ . The source was localized within a sky region of  $28 \text{ deg}^2$  (90% probability) and had a luminosity distance of  $40^{+8}_{-4} \text{ Mpc}$ , the closest and most precisely localized gravitational-wave signal yet. The association with the  $\gamma$ -ray burst GRB 170817A, detected by Fermi-GBM 1.7 s after the coalescence, corroborates the hypothesis of a neutron star merger and provides the first direct evidence of a link between these mergers and short  $\gamma$ -ray bursts. Subsequent identification of transient counterparts across the electromagnetic spectrum in the same location further supports the interpretation of this event as a neutron star merger. This unprecedented joint gravitational and electromagnetic observation provides insight into astrophysics, dense matter, gravitation, and cosmology.

DOI: 10.1103/PhysRevLett.119.161101

About 60 groups/collaborations participated to the investigations of GW170817, GRB170817A, AT2017fgo

# GW170817 : Timeline of a collision

- ◆ For compact star physics, a milestone was the observation of the gravitational wave event GW170817 with the near-simultaneous detection of the gamma-ray burst GRB170817A by the satellite missions Fermi and INTEGRAL followed by an astronomical transient called AT2017gfo.
- ◆ The measurement of an astronomical event over the entire range of electromagnetic spectrum from radio to gamma-rays including the measurement of gravitational waves constitutes a prime example of multi-messenger astronomy.

**0 sec** The two neutron stars merge.

**2 sec** The Fermi satellite detects a gamma-ray burst.

**14 sec** The Fermi satellite sends out an automated message of detection.

**6 min** LIGO–Virgo software identifies a GW signal.

**40 min** Astronomy community is notified of gravitational-wave detection.

**1 hr** First neutrino results come in from the IceCube observatory – none were seen.

**5 hr** LIGO and Virgo gravitational-wave data are combined to make accurate map of source direction.

**11 hr** First optical detection reported by Swope Telescope, also identifying the host galaxy. Five other observatories take independent optical image of the event within an hour of Swope.

**15 hr** Swift satellite detects bright, ultraviolet emission.

**17 hr** Optical spectrum of the event is first measured by the 6.5 m Magellan Telescope.

**9 days** Chandra satellite reports observation of X-rays from the event.

**15 days** Radio emission is detected by the Very Large Array observatory.



X-axis : time, Y-axis : frequency content of the data.

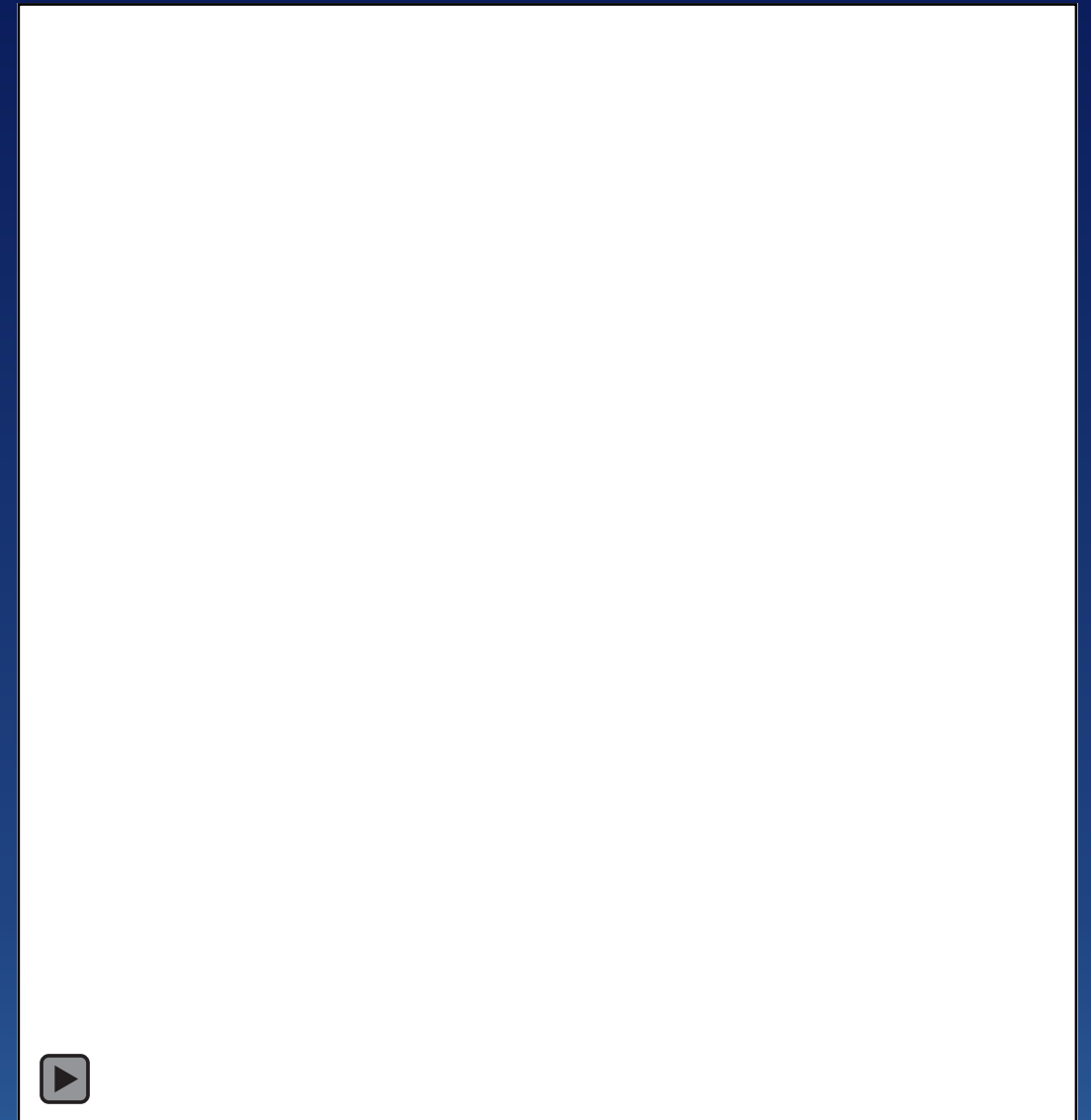
In color code : strength of the signal as a function of time and frequency. The signal is so strong that we see the track of GW170817 for nearly 30 seconds. An audible chirp can also be heard at [0:29](#) just before the merger time.

Inspiring binary systems emit characteristic GW of amplitude increasing with time and frequency, called the **chirp signal**.

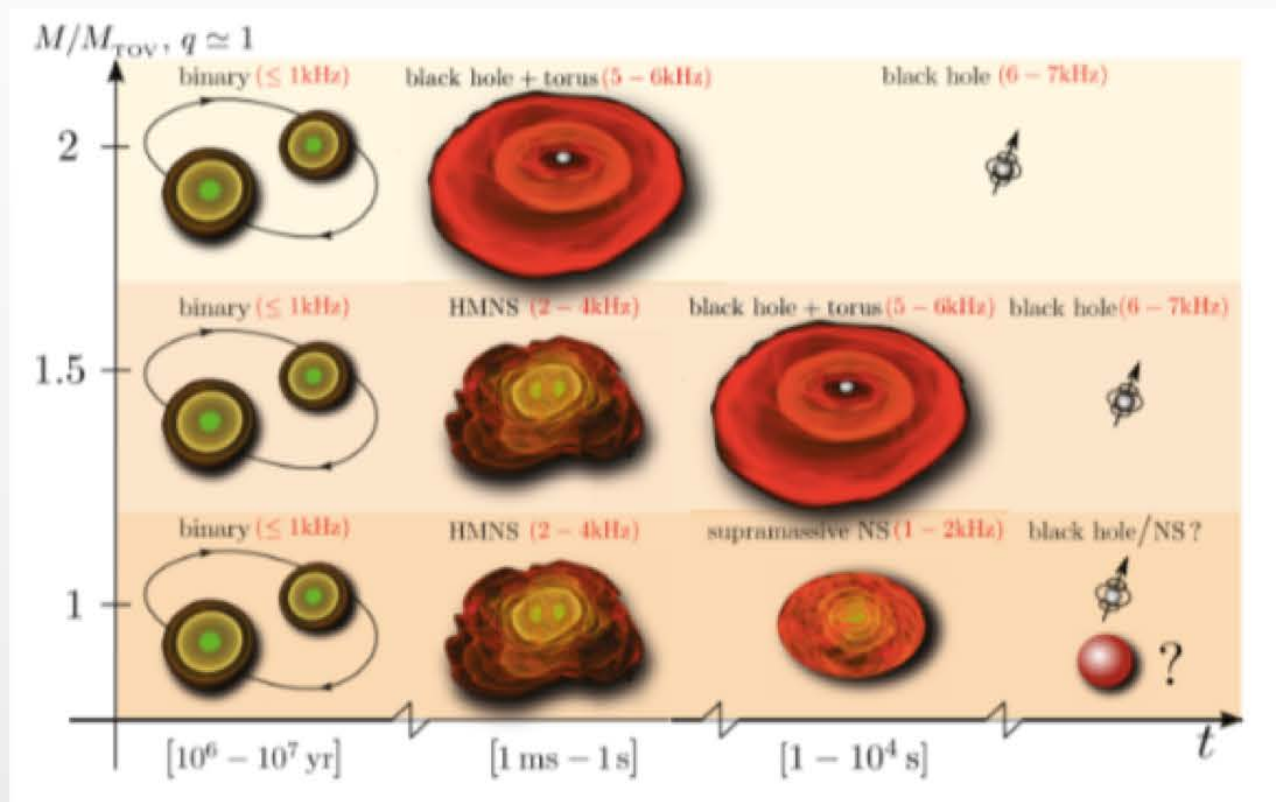
The waveform changes because the bodies approach to each other due to the GW emission. The inspiral phase is sufficiently well understood —> **masses of the components**.

Chirp ends abruptly after the components merge into one hot neutron star that afterwards collapses and forms a black hole. Gigantic electromagnetic explosion – **a short gamma ray burst**.

The details of the merger waveform depend on largely unknown microphysical details of the hot and dense neutron-star matter (composition, transport properties, viscosities).



# Role of the EoS during NS-NS merger



- **Inspiral** decay of the orbital separation with progressive reduction of the orbit. GW emission. Strong tidal forces depending on the compactness  $M/R$ , i.e. EoS.
- **Merger** Duration and fate depend on EoS and total mass. Stiffer EoS  $\rightarrow$  larger supported mass  $\rightarrow$  collapse to BH delayed or avoided.
- **Post-merger** Remnant size and frequency of the dominant oscillation mode dependent on the EoS.

👉 NS mergers as valuable probe for testing the EoS !!!!



L. Baiotti and L. Rezzolla, Rep. Prog. Phys. (2017), arXiv:1607.03540

# Inspiral phase of GW170817 : Tidal deformability $\lambda$ and Love numbers

## The Newtonian Theory of Tides :

They are a set of dimensionless parameters which measure the rigidity of a planetary body and

These numbers can be generalized for stars in General Relativity.

In particular, we are interested in one of these numbers, which connects the tidal field with the quadrupolar deformation of the star.

# The Love number $k_2$

Solve in GR together with the TOV eqs. for the pressure  $p$  and the enclosed mass  $m$

$$k_2 = \frac{8}{5} \frac{\beta^5 z}{6\beta(2 - y_R) + 6\beta^2(5y_R - 8) + 4\beta^3(13 - 11y_R) + 4\beta^4(3y_R - 2) + 8\beta^5(1 + y_R) + 3z \log(1 - 2\beta)}$$

$$z \equiv (1 - 2\beta^2)[2 - y_R + 2\beta(y_R - 1)]$$

$$\frac{dp}{dr} = -\frac{m\epsilon(1 + p/\epsilon)(1 + 4\pi r^3 p/m)}{r^2(1 - m/r)},$$

$$\frac{dm}{dr} = 4\pi r^2 \epsilon,$$

$\epsilon$  being the mass-energy density

$$\frac{dy}{dr} = -\frac{y^2}{r} - \frac{y - 6}{r - 2m} - rQ,$$

$$Q \equiv 4\pi \frac{(5 - y)\epsilon + (9 + y)p + (\epsilon + p)/c_s^2}{1 - 2m/r} - \left[ \frac{2(m + 4\pi r^3 p)}{r(r - 2m)} \right]^2,$$

$$k_2 = \frac{3G}{2R^5} \lambda$$

with  $c_s^2 = d\epsilon/dp$  and the EOS  $\epsilon(p)$  as input.

The Love number  $k_2$

depends crucially on the compactness  $\beta=M/R$ , hence on the EoS.



Abbott et al., PRL 119, 161101 (2017)

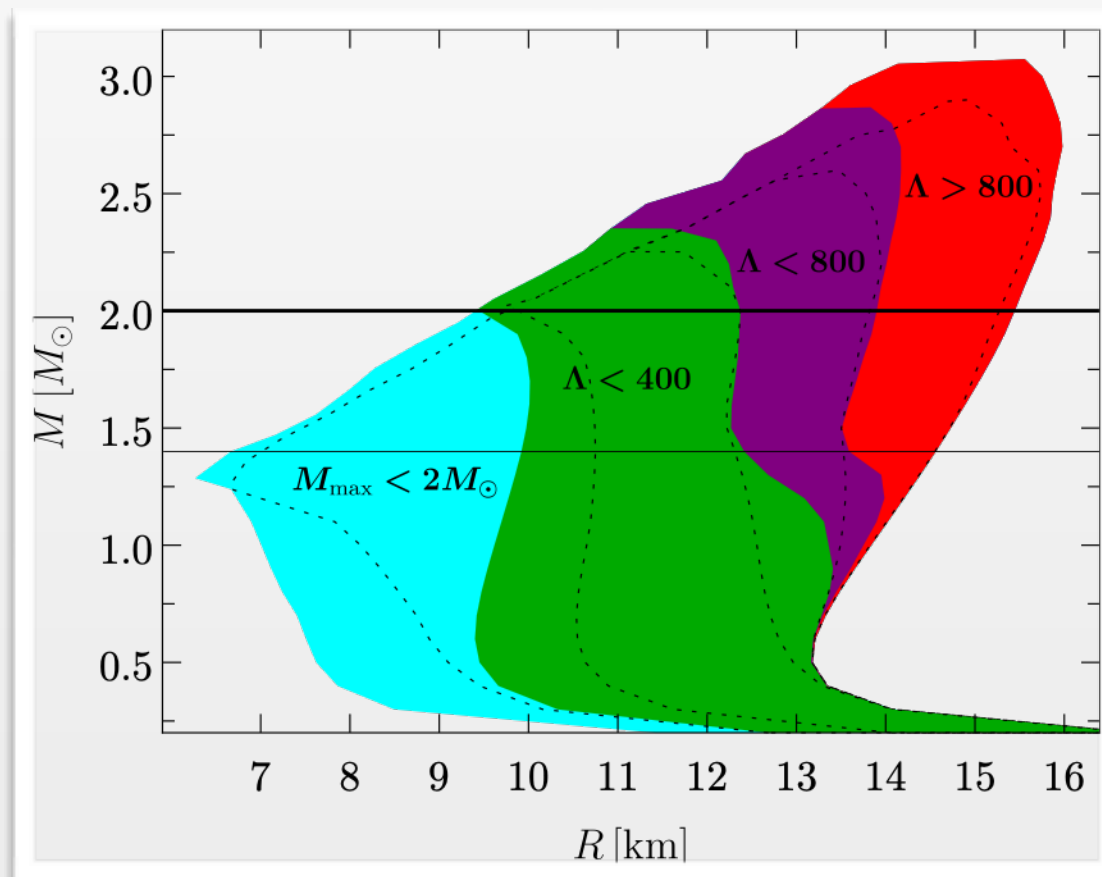
**Constraints from GW170817 and the kilonova signal AT2017gfo:  
The tidal deformability  $\Lambda = \lambda/M^5$**

$\Lambda_{1.4} < 800$  at 90% confidence level

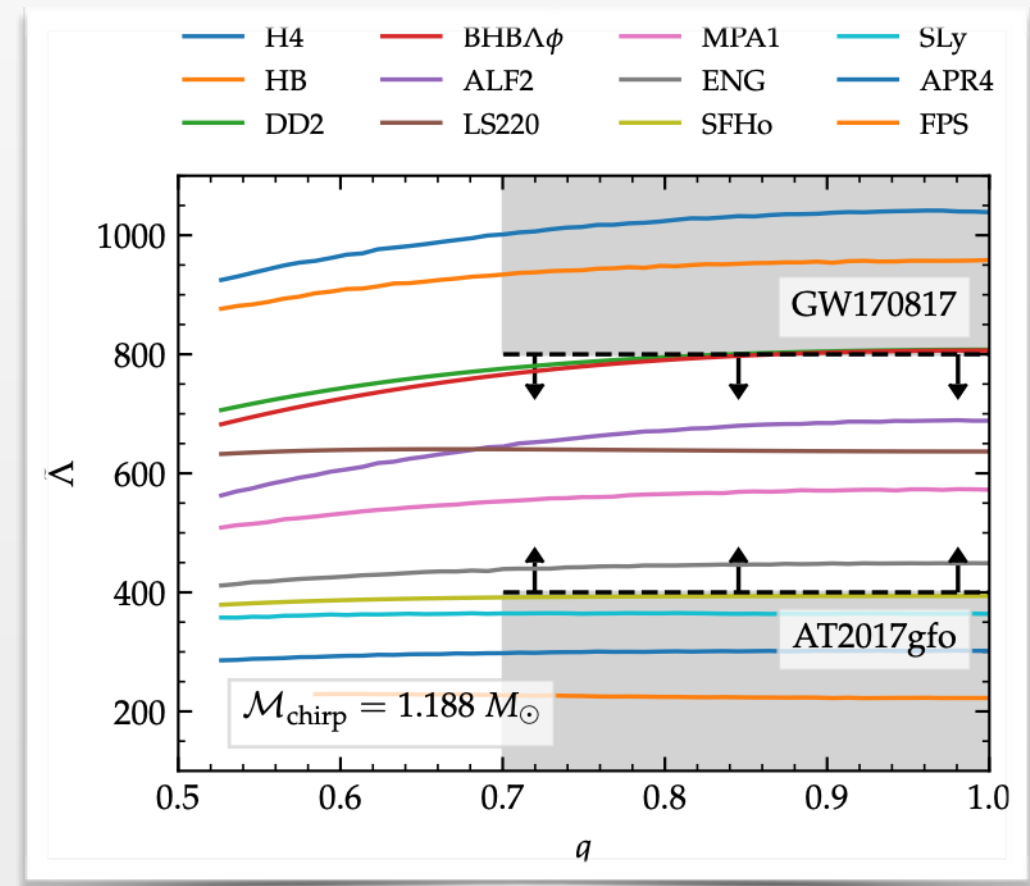
$$\tilde{\Lambda} = \frac{16}{13} \left\{ \frac{(M_1 + 12M_2)M_1^4}{(M_1 + M_2)^5} \Lambda_1 + (1 \leftrightarrow 2) \right\} > 400$$



Annala et al., PRL 120, 172703 (2018)



Radice et al., ApJ 852, L29 (2018)



- Very stiff EoS are excluded (large radii)
- Limit for the radius  $R_{1.4} < 13.6$  km

Most et al., arXiv:1803.00549

Lim et al., arXiv:1803.02803

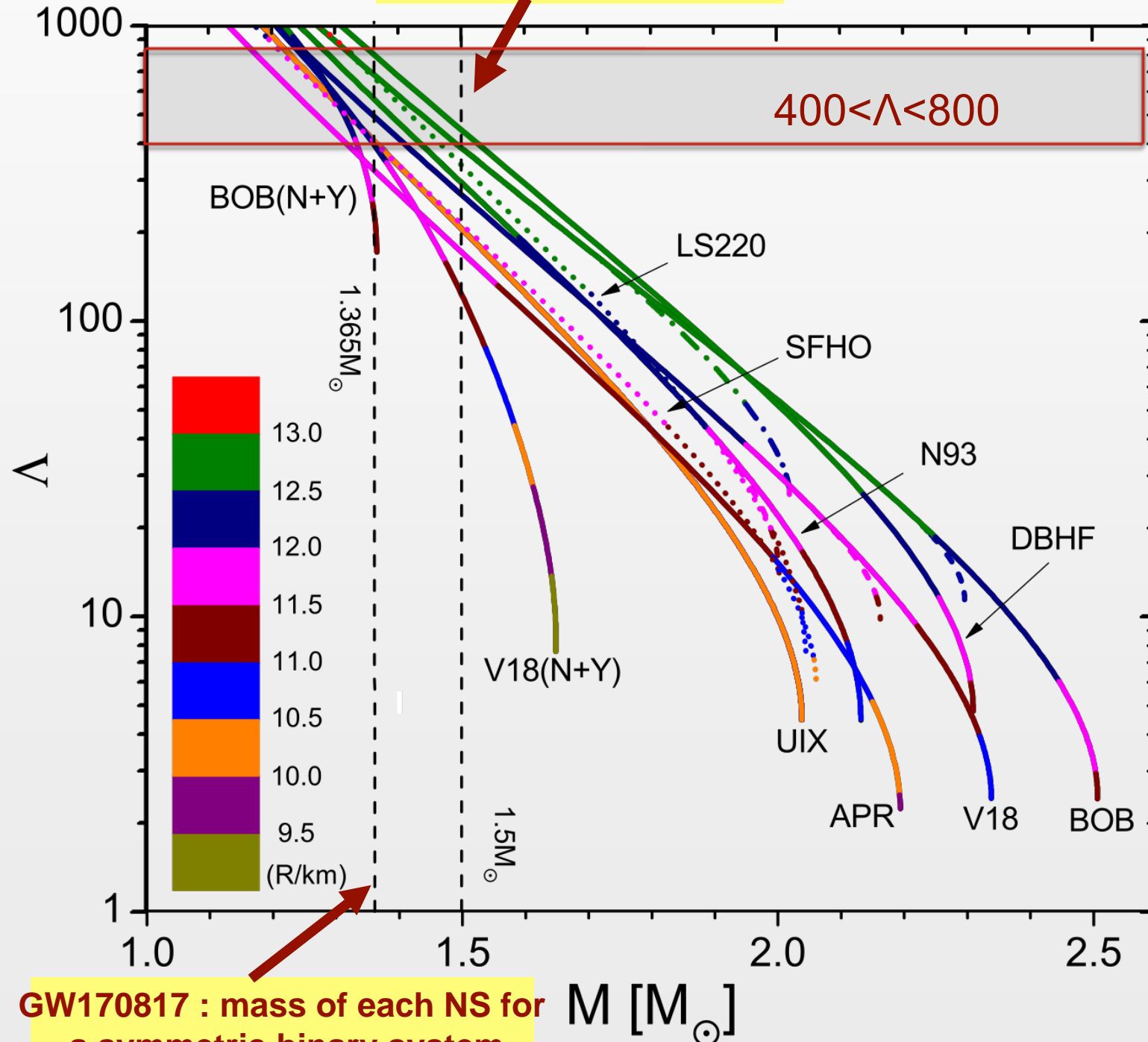
**$R_{1.4} \gtrsim 12$  km**

Fattoyev, PREX experiment (neutron skin),  
PRL 108, 112502 (2012)

# Constraining the EoS

## Correlations between $M$ , $R$ and $\Lambda$

GW170817 : limit derived in Annala et al



GW170817 : mass of each NS for a symmetric binary system

Fixed chirp mass

$$\mathcal{M}_c = \frac{(M_1 M_2)^{3/5}}{(M_1 + M_2)^{1/5}} = 1.188 M_\odot$$

$$q = \frac{M_2}{M_1} = 0.7 - 1$$

The conditions  $M_1=M_2=1.365 M_\odot$  and  $400 < \Lambda < 800$  imply  **$12 < R < 13$  km**

Compatible EoS : V18(N+Y), UIX, V18, N93, BOB(N), DBHF, LS220, DS1, DS2.

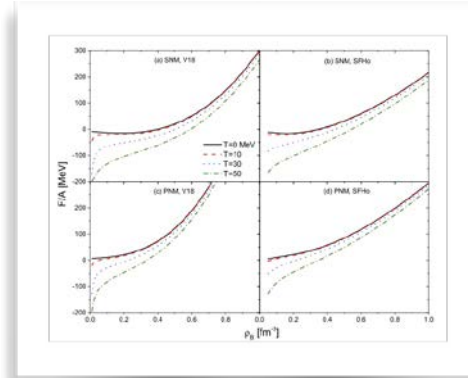
Not compatible : APR, BOB(N+Y), and SFHO (marginally).

**Selection of the EoS !**

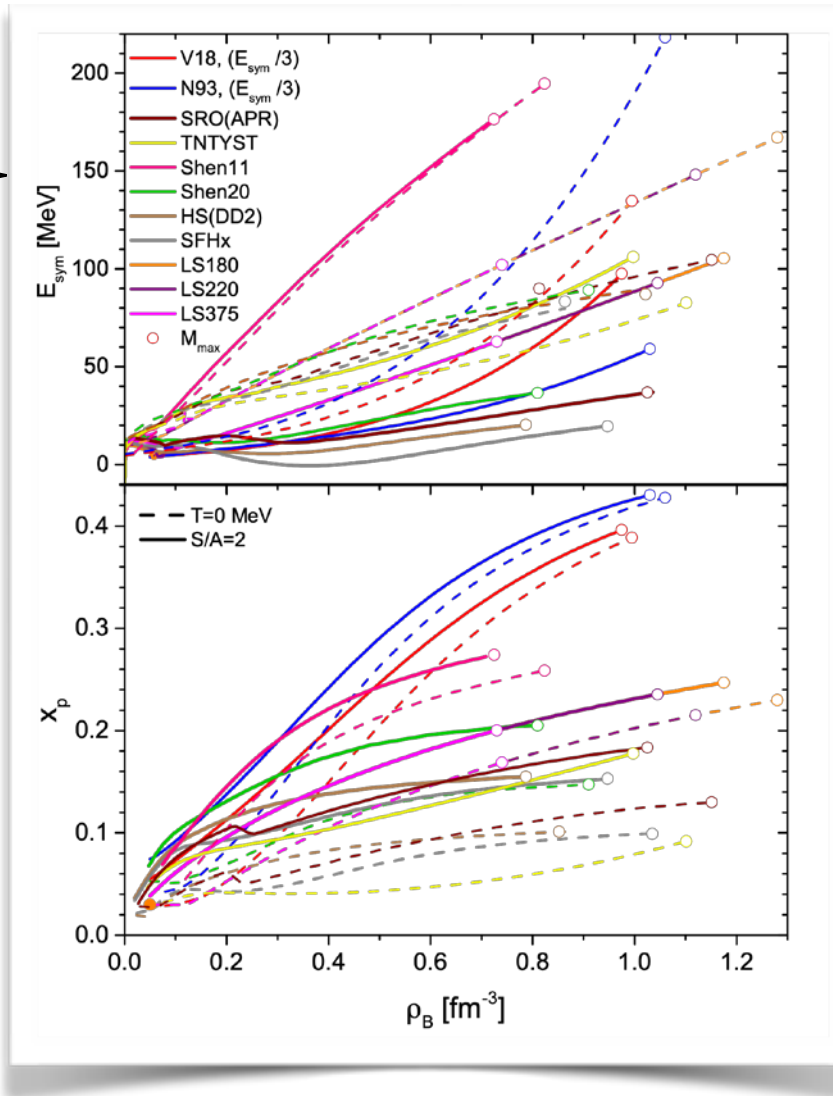
# EoS models

## Extension at finite Temperature

Isothermal curves for BHF and SFHo



Free energy per particle for symmetric and pure neutron matter vs. nucleon density for different  $T$  values. The typical Van Der Waals behaviour is evident.



Easy increases monotonically from the outer layers to the core. Large dispersion at high densities.  
 Highest values for BHF V18 and N93 because of the strong repulsive character of 3NF.  
 Lowest temperatures obtained for the two BHF EOSs and the three LS EOSs.  
 Intermediate values for RMF models.

Proton fraction of hot and cold  $\beta$ -stable matter correlated to the symmetry energy.

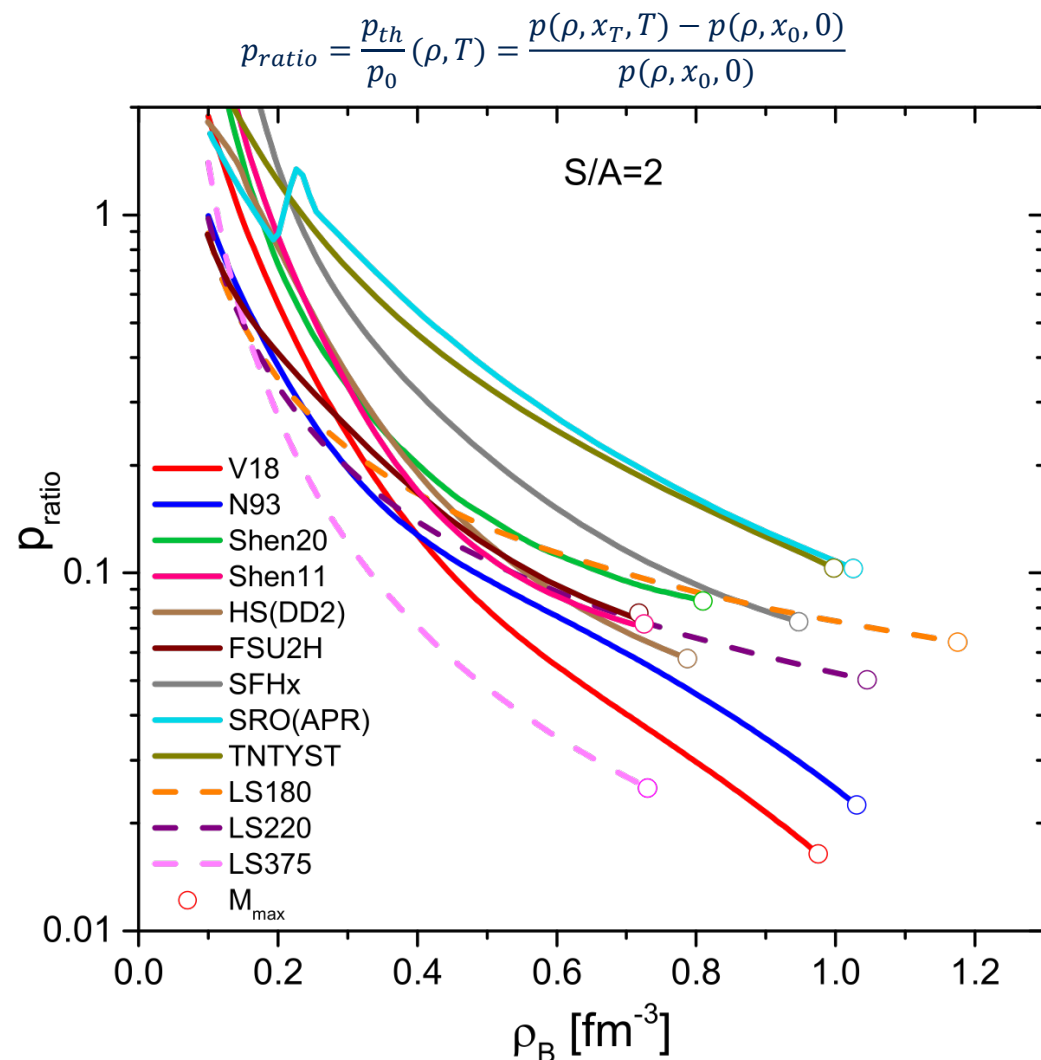
Finite  $T/S$  increases the proton fraction due to the increased lepton fraction as a result of Fermi distributions at finite temperature because of the charge-neutrality condition.

The final EoS is a complicated interplay between the increased lepton thermal pressure, and the increased nucleonic thermal pressure which is limited by the increased symmetry.

# Thermal effects on the EoS : the thermal pressure

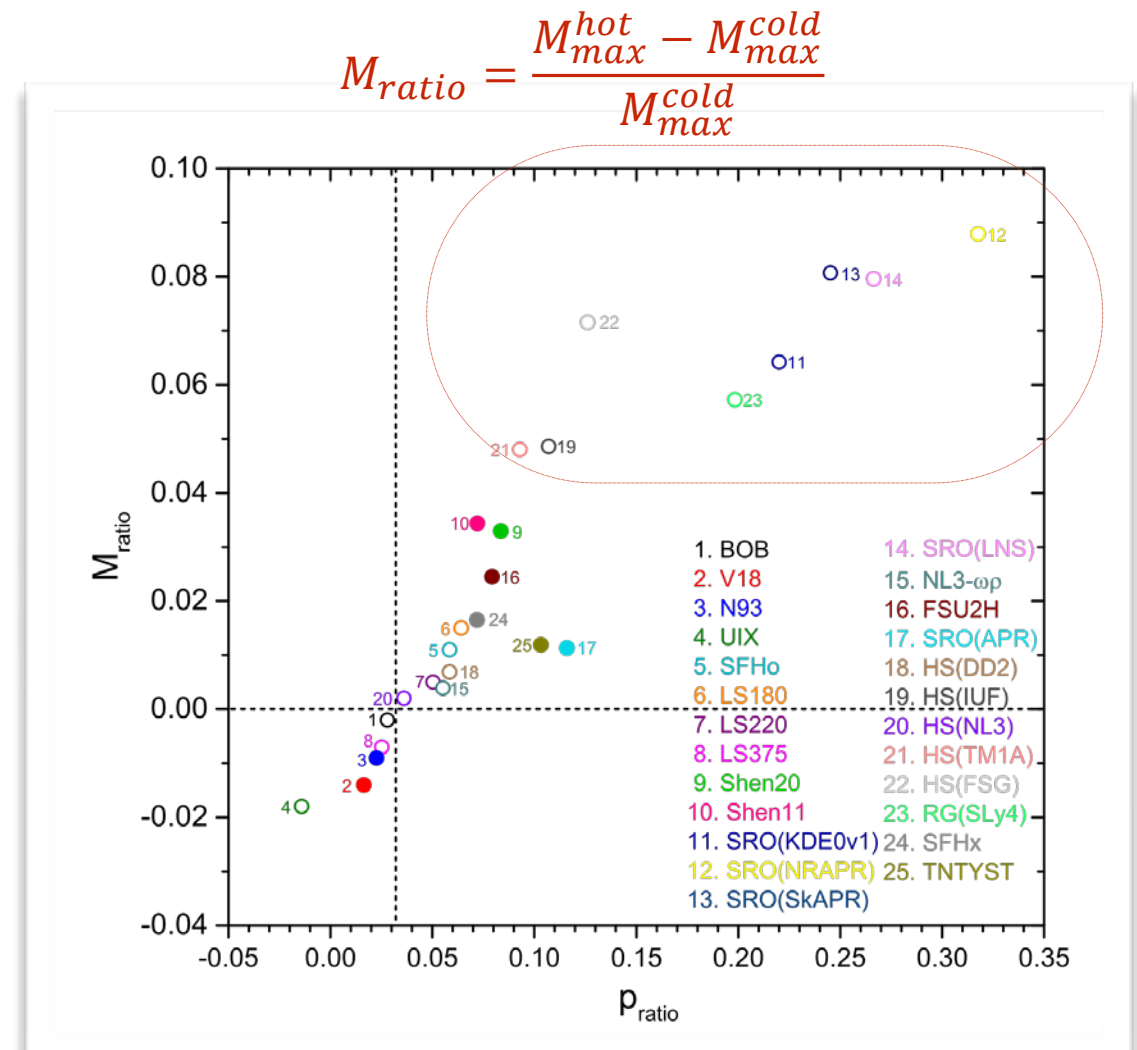
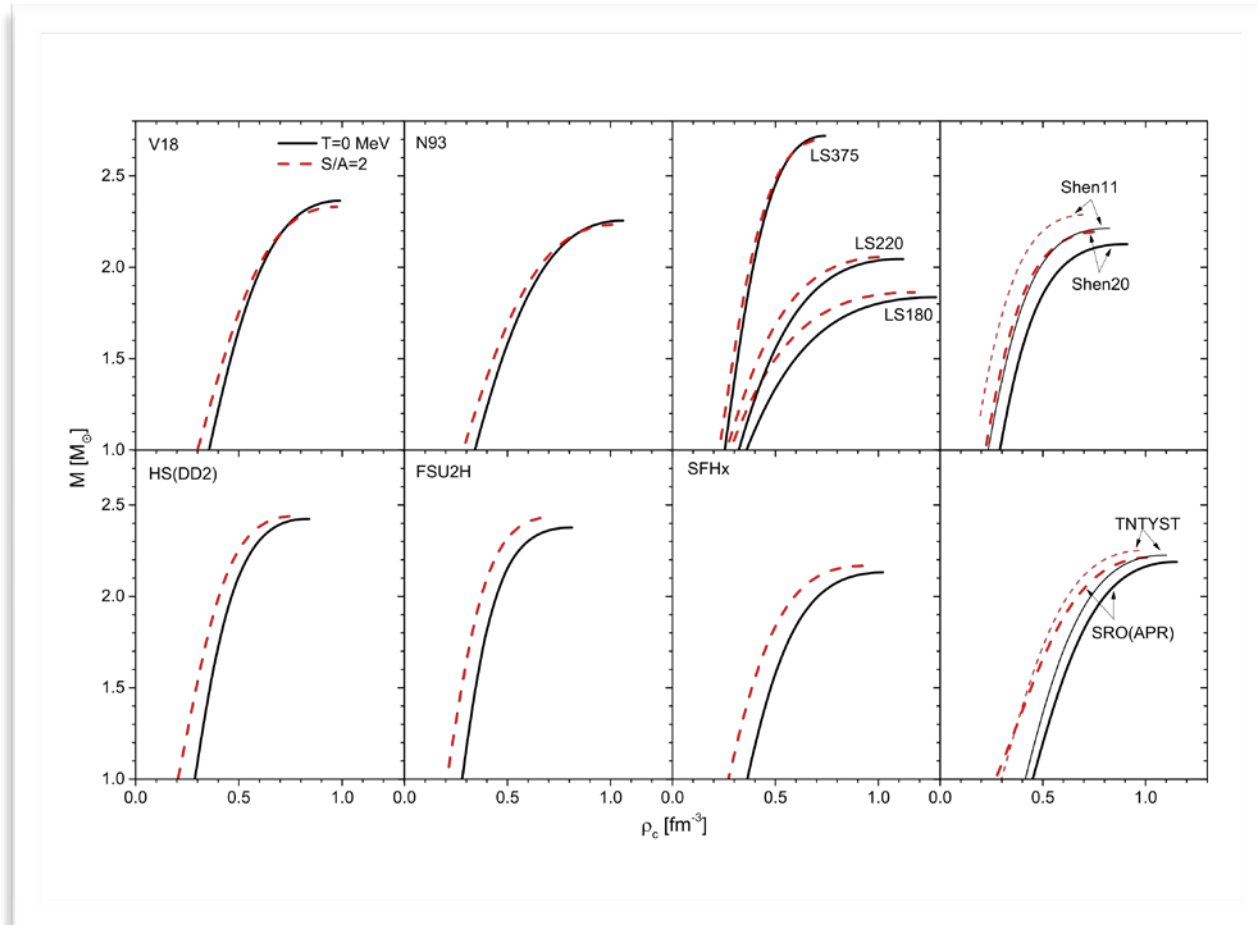
*Crucial for the stability of the star against collapse !*

$$p_{th}(\rho, T) = p(\rho, x_T, T) - p(\rho, x_0, 0)$$



- $p_{ratio}$  decreases with increasing density and reaches a few percent at the maximum-mass configurations.
- The V18, N93, and LS375 ratios are below 3 percent, while the others are up to 10 percent for the SRO(APR) and TNTYST.
- For LS EOSs the thermal pressure is identical for all three models, and the different ratios are caused solely by different Fermi pressures of cold matter, related to the different incompressibility values.

# Mass-central density relation



Thermal effects on the maximum mass are very small !  
 Change of the maximum masse is just a few percent, and can be both positive or negative.

A clear correlation does exist for all of them!  
 For the subset of realistic EoS the relative increase of  $M_{max}$  is limited to *less than 4 percent*.

# Application to BNS merger

A. Figura et al., PRD **102**, 043006 (2020)  
PhD Thesis 2021, Catania Univ.

Simulations performed in full general relativity  
Mathematical and numerical setup as in  
Papenfort, Gold & Rezzolla, PRD **98**, 104028 (2018)

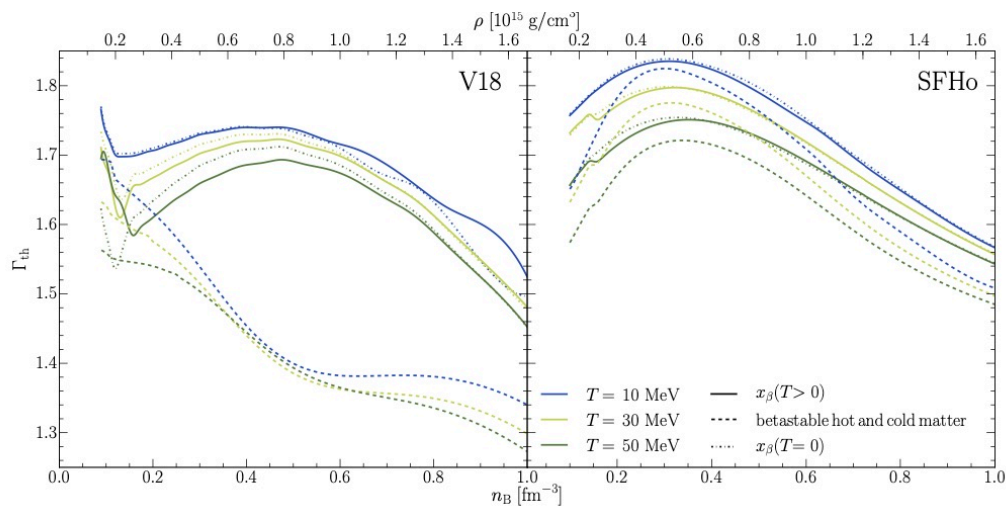
- a) FT approach : a fully temperature dependent EoS
- b) Hybrid EoS approach : **a cold EoS plus a thermal contribution** obeying the ideal-fluid EoS

$$p_{th}(\rho, T) = e_{th}(\Gamma_{th} - 1)$$

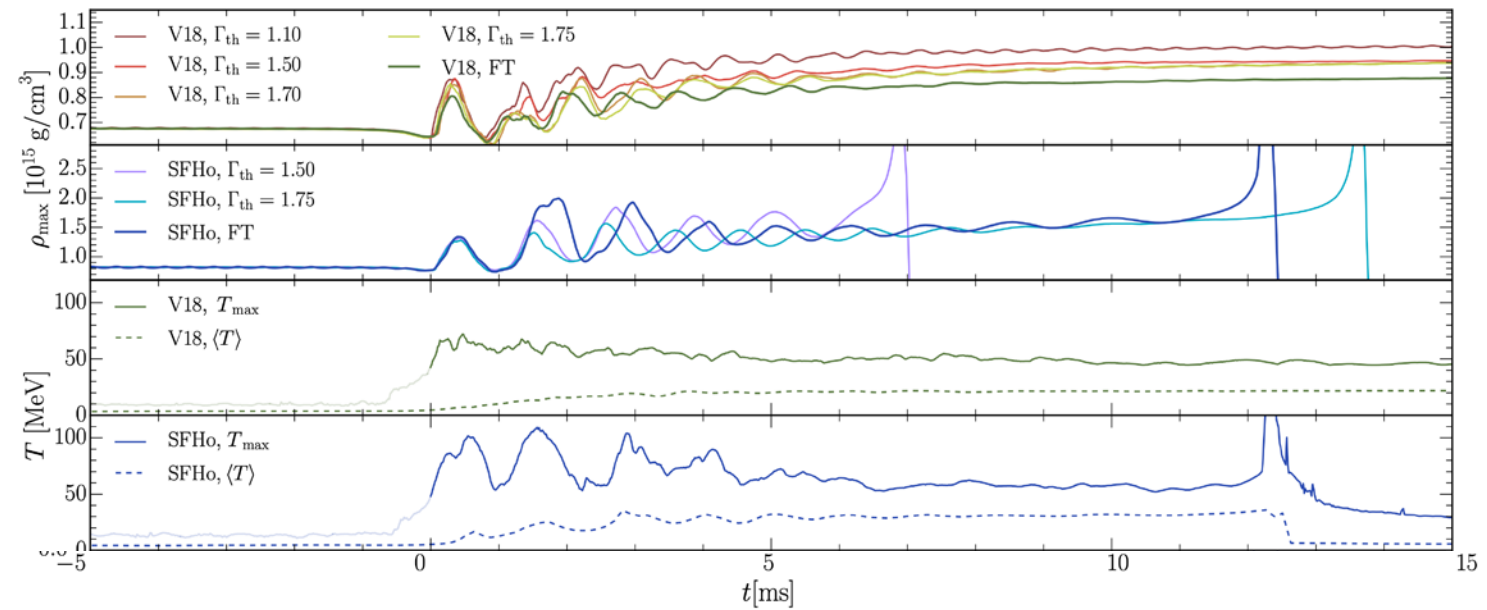
Usually  $\Gamma_{th} = \text{const}$

Bauswein, Janka and Oechslin, PRD **82**, 084043 (2010)

Strong impact on the stability of the merger remnant  
hence on its lifetime before collapsing to BH.



Simulation of equal-mass binaries with  $M_G = 1.35 M_\odot$ ,  
and initial separation 45 km.



## Evolution of the maximum rest-mass density $\rho_{max}$

Increasing  $\Gamma_{th}$  leads to a less dense remnant. FT EoS leads to a remnant with even smaller maximum rest-mass density than the hybrid-EoS case.

V18 produces a metastable HMNS up to the largest time. SFHo leads to a collapse into a BH, in a time which is dependent on  $\Gamma_{th}$ .

## Maximum and density-weighted aver. temperature, $T_{max}$ and $\langle T \rangle$

Temperature fluctuations during the metastable phase before collapse, stronger for SFHo. In the post merger phase  $T_{max}$  peak around 70 (110) MeV for V18 (SFHo).

# Final remarks